
Progress in Development of a Methodology for Geochemical Sensitivity Analysis for Performance Assessment

Parametric Calculations, Preliminary
Databases, and Computer Code Evaluation

Edited by M. D. Siegel, C. D. Leigh

Sandia National Laboratories

Prepared for
U.S. Nuclear Regulatory
Commission

HYDROLOGY DOCUMENT NUMBER 542

8909110389

AVAILABILITY NOTICE

Availability of Reference Materials Cited in NRC Publications

Most documents cited in NRC publications will be available from one of the following sources:

1. The NRC Public Document Room, 2120 L Street, NW, Lower Level, Washington, DC 20555
2. The Superintendent of Documents, U.S. Government Printing Office, P.O. Box 37082, Washington, DC 20013-7082
3. The National Technical Information Service, Springfield, VA 22161

Although the listing that follows represents the majority of documents cited in NRC publications, it is not intended to be exhaustive.

Referenced documents available for inspection and copying for a fee from the NRC Public Document Room include NRC correspondence and internal NRC memoranda; NRC Office of Inspection and Enforcement bulletins, circulars, information notices, inspection and investigation notices; Licensee Event Reports; vendor reports and correspondence; Commission papers; and applicant and licensee documents and correspondence.

The following documents in the NUREG series are available for purchase from the GPO Sales Program: formal NRC staff and contractor reports, NRC-sponsored conference proceedings, and NRC booklets and brochures. Also available are Regulatory Guides, NRC regulations in the *Code of Federal Regulations*, and *Nuclear Regulatory Commission Issuances*.

Documents available from the National Technical Information Service include NUREG series reports and technical reports prepared by other federal agencies and reports prepared by the Atomic Energy Commission, forerunner agency to the Nuclear Regulatory Commission.

Documents available from public and special technical libraries include all open literature items, such as books, journal and periodical articles, and transactions. *Federal Register* notices, federal and state legislation, and congressional reports can usually be obtained from these libraries.

Documents such as theses, dissertations, foreign reports and translations, and non-NRC conference proceedings are available for purchase from the organization sponsoring the publication cited.

Single copies of NRC draft reports are available free, to the extent of supply, upon written request to the Office of Information Resources Management, Distribution Section, U.S. Nuclear Regulatory Commission, Washington, DC 20555.

Copies of industry codes and standards used in a substantive manner in the NRC regulatory process are maintained at the NRC Library, 7920 Norfolk Avenue, Bethesda, Maryland, and are available there for reference use by the public. Codes and standards are usually copyrighted and may be purchased from the originating organization or, if they are American National Standards, from the American National Standards Institute, 1430 Broadway, New York, NY 10018.

"This document was prepared under U.S. Nuclear Regulatory Commission (NRC) Contract No. A-1756. The opinions, findings, conclusions, and recommendations expressed herein are those of the authors and do not necessarily reflect the views of the NRC. The technical contents do not necessarily represent methods and procedures acceptable to the NRC staff for demonstrating compliance with rules, regulations, and staff positions."

DISCLAIMER NOTICE

This report was prepared as an account of work sponsored by an agency of the United States Government. Neither the United States Government nor any agency thereof, or any of their employees, makes any warranty, expressed or implied, or assumes any legal liability of responsibility for any third party's use, or the results of such use, of any information, apparatus, product or process disclosed in this report, or represents that its use by such third party would not infringe privately owned rights.

Progress in Development of a Methodology for Geochemical Sensitivity Analysis for Performance Assessment

Parametric Calculations, Preliminary
Databases, and Computer Code Evaluation

Manuscript Completed: May 1989
Date Published: August 1989

Edited by
M. D. Siegel, C. D. Leigh

Contributing Authors
M. D. Siegel, K. L. Erickson, M. S. Chu, E. J. Bonario,
S. L. Phillips, L. Silvester, V. Tripathi, J. O. Leckie,
H. E. Nuttall, J. Catasca, A. T. Trujillo, S. Bayley

Sandia National Laboratories
Albuquerque, NM 87185

Prepared for
Division of High-Level Waste Management
Office of Nuclear Material Safety and Safeguards
U.S. Nuclear Regulatory Commission
Washington, DC 20555
NRC FIN A1756

ABSTRACT

The purpose of the Geochemical Sensitivity Analysis Project is to develop a methodology to identify physicochemical and hydrogeological conditions wherein use of a simple retardation factor will lead to underestimation or overly conservative estimation of the cumulative radionuclide discharge over the 10,000-year regulatory period. This report describes activities from the initiation of the Geochemical Sensitivity Analysis project in April 1984 to September 30, 1985. During this first phase of the project, compilation of necessary geochemical data was started, radionuclide transport codes were evaluated and parametric methods to assess the significance of matrix diffusion, colloidal transport and reaction kinetics on integrated radionuclide discharge from high-level waste repositories were developed. Although available data are inadequate to support final conclusions for site specific conditions, the method of sensitivity analysis being developed in this project can be used to guide future data collection.

CONTENTS

	<u>Page</u>
Executive Summary	1
1 INTRODUCTION	5
2 SITE CONCEPTUAL MODELS	7
2.1 Basalt	7
2.2 Tuff	7
3 CRITICAL EVALUATION OF THERMOCHEMICAL AND SORPTION DATA	13
3.1 The Aqueous Solutions Database	13
3.2 Self-Consistency and Accuracy of the Database	13
3.3 Uncertainty and Propagation of Errors	18
3.4 Data for High Salinities	19
3.5 The Sandia Sorption Data Management System	21
3.6 Theoretical Sorption Calculations	22
4 EFFECT OF HOMOGENEOUS REACTION RATES ON RADIONUCLIDE DISCHARGE	25
4.1 Theory	25
4.2 Application to EPA Standard and NRC Regulations	28
4.3 Application to Experimental Design	30
5 COUPLED TRANSPORT AND CHEMICAL EFFECTS	35
5.1 Description of TRANQL	35
5.2 Feasibility of TRANQL Simulations in Performance Assessment	36
6 APPROXIMATE METHODS FOR CALCULATION OF RADIONUCLIDE DISCHARGES IN FRACTURED ROCK	39
6.1 Derivation of Criteria for Application of Three Approximate Methods	39
6.2 Semi-Infinite Solid Approximation Including Radioactive Decay	41
7 POTENTIAL TRANSPORT OF RADIONUCLIDES BY COLLOIDS	44
7.1 Migration and Retention of Colloids in a Single Fracture	47
7.2 Adsorption of Radionuclides by Natural Ground-Water Colloids (Pseudocolloids)	51
7.3 Production of Colloids by Homogeneous and Heterogeneous Nucleation	58

CONTENTS

	<u>Page</u>
8 CONCLUSIONS	61
References	63
Appendix A Annotated Bibliography of Available Compilations of Thermochemical Data for Actinides and Fission Products	A-1
Appendix B Analysis of Data from Batch Sorption Experiments When Radionuclides Undergo Chemical Speciation Reactions	B-1
Appendix C Computer Code for Calculating Adsorption of Radionuclides by Natural Ground-Water Colloids	C-1

FIGURES

<u>Figure</u>		<u>Page</u>
1	Simplified Outline of Performance Assessment Calculations	6
2	Conceptual Model of Ground Water Flow Paths Used in Basalt Site Sensitivity Analysis	8
3	Conceptual Model for Tuff Site Sensitivity Analysis	10
4	A Scenario for Geochemical Sensitivity Analysis	27
5	Effect of Retardation Factor of Sorbing Species A on EPA Compliance Curves	29
6	Media-Specific Chemical Stability $1/k_m$ Required to Ensure that Integrated Discharge of ^{243}Am is Less than the EPA Release Limit	32
7a	Conversion of Hypothetical Sorbing Species A to a Nonsorbing Species During a Batch Sorption Experiment Considered in Equation 4.4	34
7b	Solution to Equation 4.4 and Relationship Between Analytical Precision ϵ_1 and Experimental Run Time t_1 Required to Observe Disequilibrium Due to Irreversible Conversion of A to B	34
8	Application of Criteria to Representative Site-Specific Data for Granite and Tuff	41
9	Concentration Profile of Diffusion of Radionuclides into a Semi-infinite Rock Matrix Adjoining a Fracture After 10,000 Years for Different Radionuclide Retardation Factors	44
10	Colloid Release Scenario	48
11	Colloid Concentration Profiles for Single Fractures as a Function of Position Along Channel	50
12	Sherwood Number as a Function of Position for Different Sizes	50
13a	Colloid Radiation Levels for ^{241}Am	55
13b	Colloid Radiation Levels for ^{237}Np	55

FIGURES

<u>Figure</u>		<u>Page</u>
13c	Colloid Radiation Levels for ^{239}Pu	56
13d	Colloid Radiation Levels for ^{226}Ra	56
13e	Colloid Radiation Levels for ^{99}Tc	57
13f	Colloid Radiation Levels for ^{230}Th	57
13g	Colloid Radiation Levels for ^{235}U	58
B-1	Values of A/A^0 Versus Time t for a Hypothetical Batch Sorption Experiment	B-7
B-2	Values of A/A^0 Versus Time t for a Hypothetical Batch Sorption Experiment	B-8
C-1	Configuration Assumed for Calculation of the Number of Radionuclide Atoms Sorbed onto a Colloid	C-3

TABLES

<u>Table</u>		<u>Page</u>
1	Summary of Hydrogeologic Data for Preliminary Scenarios for Basalt Repository Site	9
2	Summary of Sorption Data for Stratigraphic Sorption Intervals for Yucca Mountain, Nevada	11
3	Current Status of Data in Aqueous Solutions Data-Base, November 1985	14
4	Example ASD Element Chart	16
5	Example ASD Reaction Chart	17
6	Technical Advisory Committee for HLW Database	20
7	Variables in Sorption Database	23
8	Retardation Factors Assumed for Sorbing Species ²⁴³ Am	31
9	Comparisons of TRANQL Simulation Run Times	37
10	Comparison of Benchmark Code Run Times	37
11	Results of Semi-Infinite Basalt Matrix Calculations Including Radioactive Decay	42
12	Colloid Concentration and Size Effects	54
13	Cation Exchange Capacities for Clays and Zeolites	59

FOREWORD

This report describes progress in the Geochemical Sensitivity Analysis project during FY84 and FY85. Much of the information presented here has been previously reported in monthly and annual progress reports to the Nuclear Regulatory Commission. As discussed in later sections of this report, details of the results of several subtasks also have been published in the proceedings of technical conferences and other SAND and NUREG reports. The results of activities carried out in FY86 and FY87 are described in a letter report entitled Progress in Development of a Methodology for Geochemical Sensitivity Analysis for Performance Assessment: Sorption and Transport in Fractured Media. These two reports plus a final letter report, which will be published in FY89, will serve as a guide to the results of the Geochemical Sensitivity Analysis Project.

The original objectives of this report included analysis of processes occurring in the saturated zone below the water table at repository sites in basalt, tuff, and salt formations. This report contains descriptions of sites in tuff and basalt formations that provide the hydrogeological framework for sensitivity studies. Calculations for a hypothetical basalt site were initiated in FY87 and completed in FY88; this work is reported in a separate letter report to the NRC. In 1988, DOE work related to candidate HLW repositories in salt and basalt was curtailed. Current DOE investigations are focused on the proposed repository site on Yucca Mountain in Nevada. The results and methodology presented in this and subsequent reports can be applied directly to repository sites in salt and basalt formations and to the saturated zone of a tuff site; however, a complete analysis of the repository site in tuff would require additional studies of processes occurring in the unsaturated zone.

ACKNOWLEDGMENTS

This report integrates the work of many people. The authors wish to acknowledge the contributions of the following coworkers: C. D. Updegraph (GRAM, Inc.) assisted in the benchmark calculations for TRANQL runtimes on the CRAY and CDC computer systems discussed in Chapter 5; D. Vopicka (SNLA) wrote the program to solve the analytical expressions discussed in Chapter 4; D. Kent and D. Freyberg (Stanford University) assisted in the evaluation of the TRANQL code; F. Hale (Lawrence Berkeley Laboratory) helped to design and compile the data in the Aqueous Solutions Database. The careful reviews of J. Sprung and L. Paul of SNLA are appreciated. Finally, the support and encouragement of W. Kelly and Julia Corrado of the U.S. Nuclear Regulatory Commission are gratefully acknowledged.

EXECUTIVE SUMMARY

Geochemical interactions between radionuclides and rocks are one of the barriers to the transport of radionuclides from proposed high-level waste (HLW) repositories. These interactions are usually characterized by a retardation factor in performance assessment calculations. A simple retardation factor may be useful in describing transport in systems in which reversible sorption is the only important chemical process; however, the extent to which a particular radionuclide is retarded by rocks in natural systems will be determined by many factors including sorption equilibria, chemical kinetics, and the rates of mass transfer between flowing fluids and the rock matrix. Under contract to the U.S. Nuclear Regulatory Commission, Sandia National Laboratories; Albuquerque (SNLA) undertook the Geochemical Sensitivity Analysis project to investigate the possible significance of chemical effects that are overlooked by the use of a simple retardation factor in transport calculations.

This report describes progress in the project from May 1984 to October 1985. During this first phase of the study, compilation of necessary geochemical data was started, radionuclide transport codes were evaluated and parametric methods to assess the significance of matrix diffusion, colloidal transport and reaction kinetics on integrated radionuclide discharge from high-level waste repositories were developed. Although available data are inadequate to support final conclusions for site specific conditions, the method of sensitivity analysis being developed in this project can be used to guide data collection in the future.

Conceptual models for repositories in tuff, basalt and bedded salt will be used in the parametric calculations of integrated radionuclide discharge to the environment. These model sites will provide a framework within for evaluating the importance of uncertainties in geochemical data relative to uncertainties in hydrological and geological information. Preliminary conceptual models for basalt and tuff media have been formulated and are described in this report.

As part of this work, critical reviews of both thermochemical data for radioelements and sorption data relevant to rocks and ground waters at HLW sites have been conducted. The results of the data reviews are contained in two computerized data management systems: the Aqueous Solutions Database (ASD) and the Sandia Sorption Data Management System (SSDMS). The ASD contains basic thermochemical data that can be used to calculate chemical speciation and the extent of sorption in model systems. Two computer codes, MINEQL (Westall and others, 1976), and PHREEQE (Parkhurst and others, 1980) will be used in these calculations. In the future, interfaces between these codes and the Aqueous Solutions Database will be written. The ASD is located on the central VAX 8600 cluster computer at Lawrence Berkeley Laboratory and is accessible via telecommunication networks such as MILNET or on commercial phone lines. An annotated bibliography of thermochemical data compilations available as of 1985 is included as an appendix to this report. The SSDMS contains descriptions of batch sorption (K_d or R_d) experiments. It is designed for use with personal computers and uses the dBASE III system (Ashton-Tate, 1984). K_d values for particular rock-water

combinations can be selected from the database and ranges or averages can be computed for use in performance assessment calculations.

The possibility of including the combined effects of chemical speciation and transport in performance assessment calculations was addressed in this study by an examination of the TRANQL code. TRANQL is an equilibrium geochemical transport code that couples MICROQL (Westall, 1979), a condensed subset of the speciation code MINEQL, with the transport code ISOQUAD (Pinder and Gray, 1977). Calculations of run times suggest a single 10,000-year, 10-km TRANQL simulation with a grid size of 10 meters for a geochemically simple system (14 complexes) would require approximately 40 hours of CPU time on the SNLA CRAY-1. It is possible that TRANQL's potential efficiency on the CRAY was seriously underestimated, and with proper vectorization the code could run faster. However, substantial improvements in efficiency would be required before TRANQL could be used to run even simple long-term simulations at an affordable cost (1 hour of CPU time on the SNLA CRAY-1 costs \$1,000). Although this type of model is clearly useful in providing basic mechanistic insights and identifying key chemical parameters in radionuclide transport, the routine use of this code in performance assessment appears to be impractical based on this investigation.

Parametric calculations that examine the effect of the rates of speciation reactions on calculations of integrated radionuclide discharge are described in this report. Reactions involving the conversion of a radionuclide from a strongly sorbing (immobile) species to a nonsorbing (mobile) species are considered. In these calculations, a general transport equation describing convection, dispersion, radioactive decay, sorption and a first-order speciation reaction was solved to estimate the integrated discharge over the 10,000-year regulatory period. Site-specific combinations of retardation factors, initial radionuclide concentrations, and ground-water travel times were assumed in the calculations. When the integrated radionuclide discharge was set equal to the release limit in the EPA Standard 40 CFR Part 191.13, the values of the other parameters could be used to calculate the corresponding chemical reaction rates. From this analysis, a measure of the chemical stability of radionuclide species in laboratory studies or under natural conditions needed to comply with the EPA Standard was obtained. The required stability can be compared to values of the reaction rates obtained in laboratory studies or predicted for natural systems. The method could be used to determine the criteria for experiments designed to quantitatively observe the effect of important chemical speciation reactions on transport. Analyses like this could be used by regulatory agencies to prioritize research needs and to evaluate published or ongoing radionuclide transport studies.

Approximate methods to calculate the discharge of radionuclides from fractured media are also examined in this report. The general transport equations for a solute in a fractured porous rock were solved using three approximations: an equivalent porous medium approximation, a linear-driving-force approximation, and a semi-infinite medium approximation. With an equivalent porous medium approximation, it is assumed that the concentration of radionuclide in the rock matrix and in the fracture are

the same. In the linear-driving-force approximation, the concentration of radionuclide is uniform in the rock matrix and differs from that of the fracture fluid. With the semi-infinite medium approximation, it is assumed that the concentration of radionuclide at the center of the rock matrix block is zero. In all three cases, criteria for the types of flow systems where each approximation can be accurately applied were derived.

Site-specific data for tuff and granite were used with the above criteria. Results indicate that for tuff, the porous-medium approximation should be valid even for relatively thin beds (about 30 m in thickness), and that the linear-driving force or semi-infinite medium approaches are necessary only for extremely high flow rates or very impermeable tuff layers. For granite, the semi-infinite medium or linear-driving-force approaches may be required, while the porous-medium approximation may be applicable only to relatively large granitic bodies.

Equations for matrix diffusion using the semi-infinite medium approximation were also solved to determine the sensitivity of these criteria to radioactive decay. These calculations suggested that except for the very short-lived radionuclides (Pu-241, Pu-238 and Am-241) and the highly retarded radionuclides (e.g., Thorium), the semi-infinite approximation was not required for calculations of transport in fractured basaltic rock.

An approach to estimate the potential effect of colloids on radionuclide transport is examined in this report. Calculations focused on three aspects of colloid migration in the far field at repository sites: (1) migration and retention of colloids and particulates in a single fracture, (2) adsorption of radionuclides by natural colloids in ground water (pseudocolloids), and (3) production of radiocolloids by homogeneous nucleation. The migration and retention of colloids in a single fracture was examined by calculating the balance of the gravitational, London-Van der Waals and electric double layer forces on the colloids. The results of the analysis show the conditions under which the net force will cause the colloid to deposit on the fracture wall as it travels along the fracture. When the required site-specific hydrological and geochemical data become available, the method of analysis developed in this work could be used to determine if colloids released from the repository will reach to the accessible environment.

Several bounds on the capacity of natural colloidal suspensions to transport adsorbed radionuclides were calculated based on estimated colloid surface area, suspension concentration, and cation exchange. The colloid-associated radionuclide concentrations were compared to the Maximum Permissible Concentration (MPC) in drinking water. Th-230 and Pu-239 concentrations exceed the MPC for colloid diameters of 10 and 100 nm and for 1000 nm, if the colloid concentration is 25 ppb or higher. Np-237, Tc-99, and U-235 show the least hazard. Am-241 and Ra-226 concentrations exceed the MPC for all colloid diameters and concentrations. Thus, naturally occurring colloids cannot be easily ruled out as a transport factor in geologic repositories using the available data.

Finally, the production of homogeneous colloids by nucleation was examined. It was concluded that available data on nucleation rates gathered from

Continuous Mixed Suspension Product Removal Crystallizer experiments could not be directly applied to performance assessment calculations and might not represent an upper bound on colloid formation due to nucleation.

1. INTRODUCTION

Geochemical interactions between radionuclides and rocks are but one of the barriers to the transport of radioactive waste from proposed high-level waste (HLW) repositories. Performance assessment calculations consider the roles of the waste package, the engineered facility, and the hydrogeochemistry of the repository site in limiting potential releases of radioactivity. The overall objective of a geochemical sensitivity analysis is to assess the relative contribution of the uncertainty in geochemical data and models to the overall uncertainty in the predicted performance of candidate HLW repositories.

At Sandia National Laboratories, calculations have been carried out to assess the compliance of hypothetical HLW sites with the NRC Rule 10 CFR Part 60 and EPA Standard 40 CFR Part 191. Figure 1 illustrates the general structure of these calculations. Typically, the assessment process involves statistical sampling of required input parameters (hydrogeologic and geochemical) from a probability density function over the range of their uncertainty followed by a large number of calculations to predict the uncertainty in the radionuclide discharge at the candidate HLW sites. The calculations predict the discharge of radionuclides to the accessible environment (typically at a 5 km distance) over a 10,000-year period. In the past, such performance assessment calculations have used simple models to represent complex geochemical processes. In particular, solute-water-rock interactions have been represented by retardation factors calculated from empirical sorption ratios (K_d) obtained under conditions which simulate the range of environments predicted to prevail at specific repository sites. The use of simple algorithms to represent geochemical processes is necessitated in part by the complexity of the calculation of integrated solute discharge which include radioactive decay and production.

The adequacy of the use of retardation factors derived from sorption ratios in calculations of radionuclide discharge has been questioned by a number of researchers (Apps and others, 1983). In general, the speciation of the radioelements in the sorption experiments are not known and sorption behavior cannot be confidently predicted for conditions that differ from those of the experiments. Radionuclides are not introduced into the experimental solutions in the forms that would be released from the nuclear waste, and the relatively short duration of the experiments may preclude detection of any slow speciation reactions that could change sorption behavior and lead to increased radionuclide discharge.

Coupled reaction-transport codes that explicitly model geochemical reactions have been proposed as an alternative to currently available performance assessment models. These codes are clearly useful in providing basic mechanistic insights and identifying key chemical parameters in radionuclide transport; however, the routine use of such codes in performance assessment is impractical. The use of coupled reaction-transport models is hampered in part by the lack of fundamental thermochemical data describing surface-complexation reactions. In addition, it is difficult to extrapolate theoretical models of the sorption of trace metals by simple oxides and aluminosilicates to the behavior of natural materials. Finally, the high computing costs associated with realistic calculations of

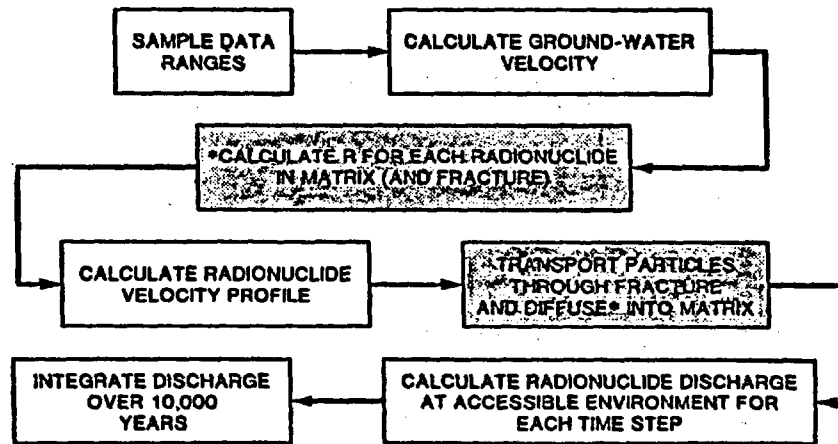


Figure 1. Simplified Outline of Performance Assessment Calculations. Shaded areas indicate steps in which geochemical processes are considered. R is a radionuclide retardation factor.

radionuclide discharge over a 5 km distance and a 10,000-year period, at present, preclude the use of coupled reaction-transport models in repository performance assessment. An important objective of the work presented in this report is to identify physicochemical conditions under which the use of such complex codes is truly required in order to assess compliance of candidate HLW repositories with the EPA Standard 40 CFR Part 191.

The results of preliminary, scoping parametric calculations that were performed to identify geochemical and hydrological conditions wherein chemical speciation and colloidal transport can significantly affect radionuclide discharges are presented in this report. These types of calculations can be used to obtain criteria for the design of experiments to ensure that important speciation effects are not overlooked in sorption studies. In addition, the results of a critical evaluation of available thermodynamic data, and empirical sorption data (K_d 's) are presented. Reliable data in these areas would be required for the calculations involved in an assessment of the releases from potential HLW repositories. The thermodynamic and sorption data were compiled in two computerized data management systems: the Aqueous Solutions Database (ASD) and the Sandia Sorption Data Management System (SSDMS). A description of the status of these databases at the time of writing is given in this report. These databases will be updated on a regular basis and subject to stringent quality assurance.

2. SITE CONCEPTUAL MODELS

Conceptual models for repositories in tuff, basalt and bedded salt are needed in order to perform parametric calculations for these HLW sites. These model sites will provide a framework within which to evaluate the importance of uncertainties in geochemical data relative to uncertainties in hydrological and geological information. This chapter gives a brief description of the preliminary scenarios proposed for the basalt and tuff sites.

2.1 Basalt

Two alternative flow scenarios are proposed for basalt. These two scenarios are described in Figure 2 and Table 1. In these scenarios, radionuclides flow vertically from the HLW repository in the candidate horizon to the Cohasset flow top and then horizontally to the accessible environment. The hydrologic parameters for the two scenarios are listed in Table 1. Scenario 1 is based on information given in Demonstration of a Performance Assessment Methodology for High-Level Radioactive Waste Disposal in Basalt Formations (Bonano and others, 1988). Scenario 2 is based on the analysis contained in the Draft Environmental Assessment for the BWIP Site (DOE, 1984). These scenarios are only preliminary versions and may not appear in the final analysis of the BWIP site. Geochemical data for the basalt site are still needed to complete these scenarios.

2.2 Tuff

The conceptual model for the tuff repository site is based on the data and site stratigraphy described in Bryant and Vaniman (1984) and Tien and others (1985). Figure 3 illustrates the sorptive stratigraphy that will be assumed in the initial system calculations of radionuclide discharge. Sorption data for samples from Yucca Mountain are compiled in a dBASE III (Ashton-Tate, 1984) data management system. [Tien and others (1985) describe the contents of the tuff sorption database.] Table 2 summarizes descriptive statistics for sorption ratios for each stratigraphic sorption interval. Hydrogeological data and models for the unsaturated zone at Yucca Mountain are still needed in order to complete the conceptual model for this medium.

In initial calculations, the ranges for parameter values will be set wide enough to conservatively bracket current uncertainties in geochemical data for the parametric calculations. These calculations help to identify parameters and scenarios for which current data are insufficient to allow assessment of compliance with the EPA Standard 40 CFR Part 191. The tools and databases described in this report will be used to examine the conservatism of the assumed parameter ranges. Then, detailed geochemical analyses can allow a more sophisticated set of system calculations to be carried out and help identify the important geochemical research objectives in support of repository performance assessments.

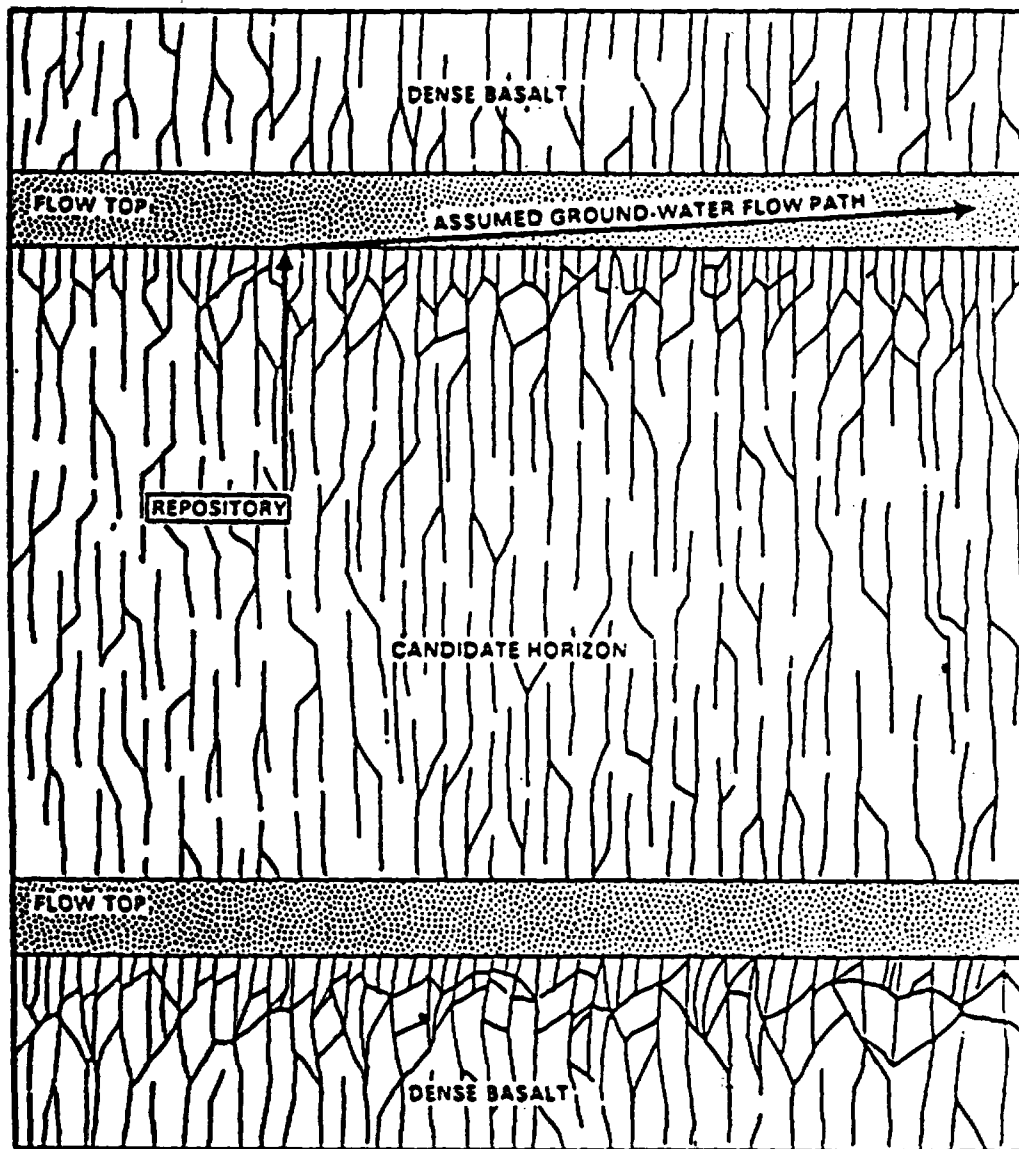


Figure 2. Conceptual Model of Ground Water Flow Paths Used in Basalt Site Sensitivity Analysis (DOE, 1984)

Table 1

Summary of Hydrogeologic Data for Preliminary Scenarios
for Basalt Repository Site

Scenario 1* (Flow direction SE → NW)

<u>Unit of Flow Leg</u>	<u>Length (ft)</u>	<u>Hydraulic Conductivity (ft/d)</u>	<u>Hydraulic Gradient</u>	<u>Porosity</u>	<u>Dispersivity (ft)</u>	<u>Cross Sectional Thickness (ft²)</u>
Cohasset Flow Top	55,000	5.2	0.0014	0.001	0	30
Cohasset Interior	22	1.1×10^{-6}	0.18	0.001	0	NA
Repository	16.4	1.1×10^{-5}	0.18	0.01	0	8000 x 6000

Scenario 2** (Flow direction NW → SE)

Cohasset Flow Top	32,800	6.3×10^{-2}	0.001	0.005 ⁺	0 ⁺	26
Repository	16.4	6.3×10^{-2}	0.003	0.005	0	8000 x 6000

*Source: Data gathered under Bonano and others (1988).

**Source: Data for Cohasset were taken from DOE (1984) except where indicated by +

+Source: Values assumed for initial parametric sensitivity calculations.

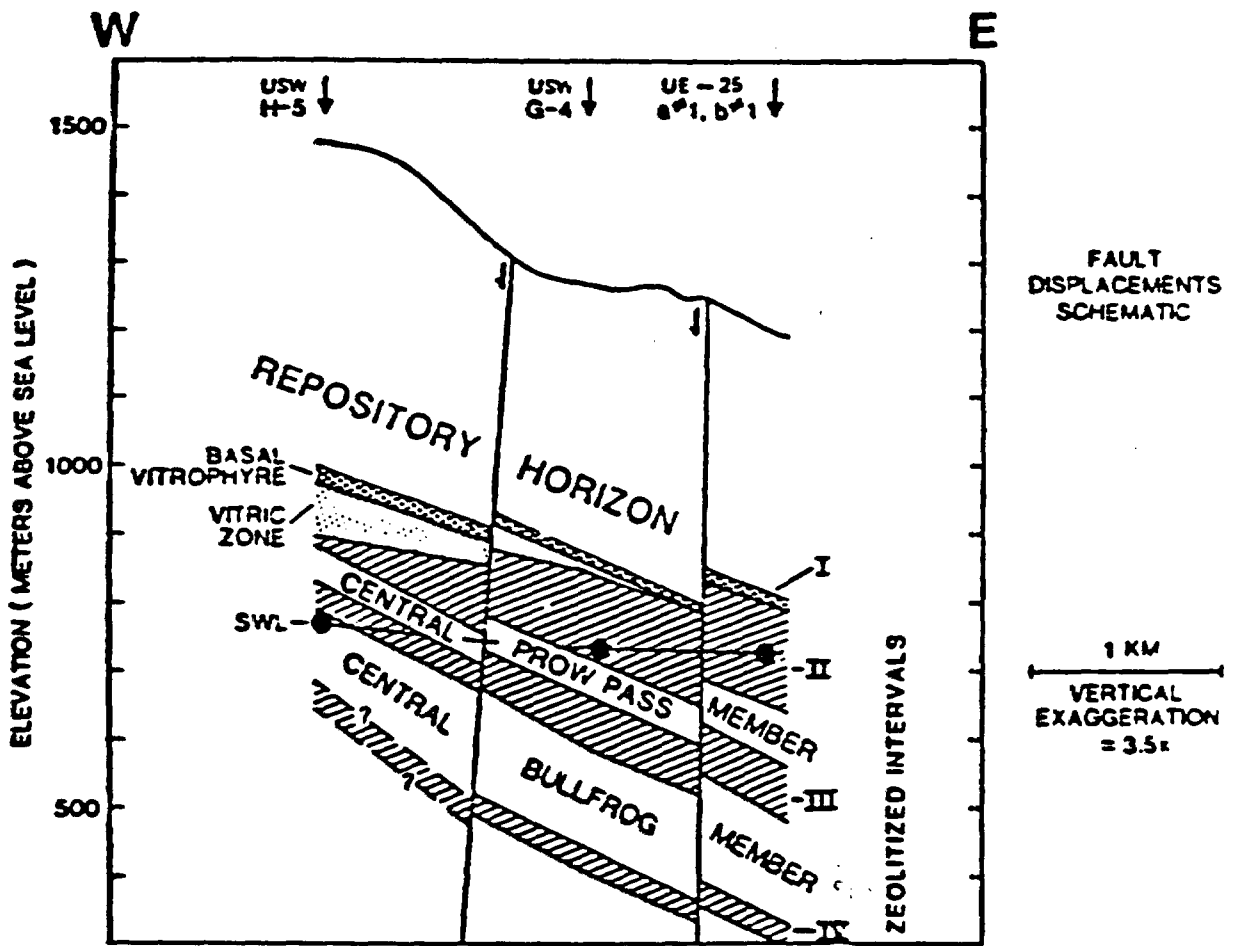


Figure 3. Conceptual Model for Tuff Site Sensitivity Analysis. Roman numerals refer to zeolite intervals (Bryant and Vaniman, 1984).

Table 2

Summary of Sorption Data for Stratigraphic Sorption
Intervals for Yucca Mountain, Nevada

Sorption Interval	Element			
	Am	Ba. Ra	Cs	Eu
Host Rock	3350±354 2, N 3100:3600	575±332 2, N 340:810	515±163 2, N 400:630	84±23 2, N 68:100
Zeolite I		3400	855	160000
Basal Vitrophyre	1110±269 2, N 920:1300	1585±690 4, N 640:2100	390±57 2, N 350:430	165±35 2, N 140:190
Vitric Zone	1750±354 2, N 1500:2000	357±250 3, N 82:570	108±58 3, N 45:160	[2.56±1.45] 3, L 38:17000
Zeolite II	[3.18±0.32] 10, L 490:5500	[4.66±0.43] 23, L 6180:150000	[3.9±0.2] 19, L 3660:17000	[3.74±0.43] 21, L 1340:100000
Central Prow Pass	4700	[2.92±0.64] 11, L 162:1400	[2.81±0.41] 11, L 184:3650	878±598 9, N 110:1900
Zeolite III	4300	[4.46±0.71] 15, L 1170:250000	[4.02±0.59] 12, L 1160:42000	[3.17±0.27] 12, L 779:5600
Central Bull Frog	372±309 2, N 153:590	[2.70±0.37] 16, L 140:3040	[2.75±0.36] 15, L 120:2020	[2.99±0.43] 12, L 340:5500
Zeolite IV		63000	7700	200
Deep Zone		7427±5685 10, N 1000:15000	[3.52±0.39] 10, L 1080:16000	[3.22±0.54] 9, L 440:15000

Table 2

Summary of Sorption Data for Stratigraphic Sorption Intervals
for Yucca Mountain, Nevada
(Concluded)

Sorption Interval	Element				
	Np	Pu	Sr	Tc	Y
Host Rock	5.1±0.3 4, N 4.9:5.4	287±84 4, N 240:420	46±22 2, N 30:61	0.44±0.38 4, N 0:0.81	5.0±7.1 2, N 0:10
Zeolite I			260		0 2 0:0
Basal Vitrophyre		365±64 2, N 320:418	121±112 2, N 42:200		0 2 0:0
Vitric Zone	2.1±0.1 4, N 2.0:2.2	285±106 2, N 210:360	22±11 3, N 10:32	0.03±0.02 5, N 0:0.04	10±14 2, N 0:20
Zeolite II	6.5±3.5 6, N 4:11	[1.66±0.32] 12, L 19:250	[3.86±0.52] 24, L 1760:81000	0.01±0.01 3, N 0:0.02	7.2±3.3 3, N 5.3:11.0
Central Prow Pass	6.4	77	[1.73±0.34] 10, L 22:194		28±36 2, N 2.4:54
Zeolite III	9	230	[3.5±0.88] 12, L 148:56000	0.18±0.04 2, N 0.15:0.21	6.0±3.8 3, N 2.5:10
Central Bull Frog		85±7 2, N 80:90	[1.94±0.29] 13, L 41:280		1.0±0.9 3, N 0:1.7
Zeolite IV		42000			
Deep Zone		[2.93±1.02] 11, L 68:13200		2.15±2.33 2, N 0.5:2.33	

3. CRITICAL EVALUATION OF THERMOCHEMICAL AND SORPTION DATA

3.1 The Aqueous Solutions Database

One of the main objectives of the present work is to demonstrate the potential importance of radionuclide speciation relevant for the models used for calculation of integrated discharge for basalt, salt, and tuff media. In support of this objective, a thermochemical database has been assembled with the assistance of staff at Lawrence Berkeley Laboratory (LBL). This database is not a rote compilation of existing data, but rather is a critical evaluation of currently available data, and includes new values. The Aqueous Solutions Database (ASD) has been under development at LBL since 1980. It has been expanded and adapted for the purposes of this project.

A report describing other relevant databases has recently been published. The report, Thermodynamic Data for Nuclear Waste Disposal. Overview of (Phillips, 1984) provides an annotated bibliography of critical compilations and a summary of thermodynamic property values for Cs, Cm, Pb, Sn, Se, Ra, and Th selected from the research literature. Values of Gibbs energy of formation, ΔG°_f , enthalpy of formation, ΔH°_f , entropy, S° , and heat capacity, C_p , are tabulated for solids and aqueous substances such as carbonate and hydroxy complexes of the metals. Suggested criteria for the critical evaluation of thermodynamic data included in the thermochemical database and for quality assurance are also discussed. That report complements the information contained in LBL-14996: Hydrolysis, Formation and Ionization Constants at 25°C, and at High Temperature-High Ionic Strength (Phillips and others, 1985).

At present the database includes the elements listed in Table 3. These elements include those contained in the inventory of Light Water Reactor (LWR) processed waste, spent fuel, and associated cladding. The data is compiled from Salter and Jacob (1983) and Wolfsberg and others (1983). The database currently resides on the central LBL VAX 8600 Cluster computer and uses the DATATRIEVE (DEC, 1984) data management system. Several revised formats are available. For example, the user may ask for a particular element (e.g., from Table 4) or a specific reaction (e.g., from Table 5) and obtain reaction equilibrium stoichiometries, values of thermochemical constants, estimates of uncertainties, and sources of data. The database provides clear identification of calculated-versus-tabulated values, clear referencing of sources for each datum, a "comments" section to document new data in the database, and index tables of selected reactions for each element. The data are available via a telecommunications net such as MILNET. Future modifications to the database that have been planned include input files in formats compatible with MINEQL (Westall and others, 1976) and PHREEQE (Parkhurst and others, 1980). These codes are used to calculate the equilibrium speciation of chemical aqueous ions involved in aqueous and/or surface complexation reactions.

3.2 Self-Consistency and Accuracy of the Database

Every effort is being made to ensure that the database is a self-consistent compilation of the best values based on expert, critical evaluation of currently available data. To avoid unnecessary duplication of effort, the

Table 3

Current Status of Data in Aqueous Solutions Database, November 1985

<u>Element</u>	<u>Number of Species</u>	<u>Number of Solids</u>	<u>Status of Data*</u>
Aluminum	11	4	2
Americium	30	14	1
Arsenic	28	11	1
Bromine	1	1	1
Calcium	21	12	2
Carbon	22	1	2
Cesium	20	11	2
Chlorine	1	--	1
Chromium	63	21	2
Copper	--	--	3
Curium	24	11	2
Electron	1	--	1
Europium	40	22	2
Fluorine	3	--	1
Hydrogen	3	--	1
Iodine	29	9	1
Iron	13	5	2
Lead	48	27	2
Magnesium	12	9	3
Manganese	12	10	2
Molybdenum	35	3	1
Neptunium	67	21	1
Nickel	9	8	3
Nitrogen	7	--	1
Oxygen	5	--	1
Phosphorus	5	1	1
Plutonium	38	12	1
Potassium	9	6	3
Protactinium	13	11	3
Radium	69	51	2
Ruthenium	43	12	2
Selenium	92	70	2
Silicon	16	8	1
Sodium	14	8	2
Strontium	20	12	1

Table 3

Current Status of Data in Aqueous Solutions Database, November 1985
(Concluded)

<u>Element</u>	<u>Number of Species</u>	<u>Number of Solids</u>	<u>Status of Data*</u>
Sulfur	12	1	1
Technetium	27	13	2
Thorium	82	34	3
Tin	34	15	3
Uranium	106	63	1
Zinc	13	8	3

- *Key: 1. Data critically evaluated and internally consistent.
2. Data critically evaluated but may not be consistent with other data in ASD.
3. Data tabulated.

ASD project compiles data evaluated by others. These sources include National Bureau of Standards (NBS), Committee on Data for Science and Technology (CODATA), International Atomic Energy Agency (IAEA), Joint Army, Navy, Air Force Thermochemical Tables (JANAF), United States Geological Survey (USGS), Naumov and others (1974), Baes and Mesmer (1976), Lemire (1984), Lemire and Tremaine (1980); and Smith and Martell (1976). Problems associated with inconsistencies between data from different sources are minimized by assigning a hierarchy to available data and calculating any missing theoretical constants from the best experimental values. The hierarchy assumed in the database, in order of decreasing importance is:

1. Critically reviewed experimental data for actinides and fission products.
2. CODATA compilations.
3. NBS compilations.
4. IAEA compilations.
5. USGS compilations.
6. Other recognized authoritative compilations such as those by Baes and Mesmer (1976), Lemire and Tremaine (1980), and JANAF (Joint Army, Navy, Air Force) Thermochemical Tables (1971).

The criteria for selection of experimental data from research publications for inclusion in the database include:

Table 4

Example ASD Element Chart

Aqueous Solutions Database	Lawrence Berkeley Laboratory	NEPTUNIUM Solids: Aqueous Species September 1984
----------------------------------	------------------------------	---

PROPERTIES OF ELEMENTAL NEPTUNIUM:

Atomic Number: 93

Formula Mass: 237.05

Electronic Configuration: 5f5 7s2

Electronegativity: 1.1

Hydration Number:

Ionic Radius: 1.012 angstrom (Np⁻⁻⁻⁺); 0.91 angstrom (Np⁻⁻⁻⁻)

Selected Average for Soils:

Concentration in Natural Waters:

THERMODYNAMIC PROPERTIES OF SUBSTANCES: 25 °C; I=0

Substance	$\Delta_f G^\circ$ kJ mol ⁻¹	$\Delta_f H^\circ$ kJ mol ⁻¹	S° J mol ⁻¹ K ⁻¹	C_p° J mol ⁻¹ K ⁻¹	Ref.
Np(s)	0.000	0.000	50.46	29.62	0011
			1.00	0.6	
Np ₂ O ₅ (s)	-2013.000	-2148.250	163.00	129.00	1111
	14.0	15.0	23.00		
NpO ₂ (s)	-1021.800	-1074.000	80.30	66.21	1111
	2.5	2.5	0.40		
NpO ₃ ·H ₂ O(s)	-1247.000	-1379.000	146.00	112.00	3339
	8.0	4.6	33.00		
NpO ₂ (OH) ₂ (s)	-1236.000	-1377.010	118.00	112.00	1111
	12.0	12.0	20.00		
NpO ₂ (OH)(am)	-1128.000	-1224.580	101.00	86.00	1111
	5.5	6.0	8.00		
Np(OH) ₄ (s)	-1447.000	-1621.365	139.00	131.00	1111
	20.0	20.0	25.00		
NpF ₄ (s)	-1783.630	-1874.000	152.72	116.06	2222
		13.0	4.10		
NpF ₃ (s)	-1460.310	-1528.830	124.68	98.32	2222
		5.0	4.00		
NpCl ₄ (s)	-896.208	-984.100	201.67	120.46	2222
		1.7	4.10		
NpCl ₃ (s)	-831.699	-898.500	161.50	104.39	2222
		2.5	8.40		

Table 5

Example ASD Reaction Chart

 * Aqueous *
 * Solutions *
 * Database *

NEPTUNIUM
 HYDROXIDES
 rc = NP1
 September 1984

EQUILIBRIUM REACTION: $\text{NpO}_2^{++} + \text{H}_2\text{O} = \text{NpO}_2\text{OH}^+ + \text{H}^+$

THERMOCHEMICAL PROPERTIES:

$^{-r}H_o$, J mol⁻¹ : 43439
 $^{-S}_o$, J mol⁻¹ K⁻¹ : 46.99
 $^{-C}_{p_o}$, J mol⁻¹ K⁻¹ : - 21.29
 $A_{y^{-z}z}$, (kg mol⁻¹)^{1/2} : - 1.02
 b, kg mol⁻¹ : 1.74
 log K_o : - 5.15

EQUILIBRIUM QUOTIENTS: I=ionic strength, mol kg⁻¹

I/T	log Q							
	25 C	50 C	75 C	100 C	150 C	200 C	250 C	300 C
0.00	- 5.15	- 4.57	- 4.07	- 3.65	- 2.97	- 2.44	- 2.03	- 1.69
0.01	- 5.23							
0.10	- 5.22							
0.20	- 5.12							
0.50	- 4.70							
1.00	- 3.92							
2.00	- 2.27							
3.00	- 0.58							

REFERENCES: 3;6;7

COMMENTS:

1. Purity of materials and use of standard reference materials for calibration.
2. Details given on experimental procedure including instrumentation, calibration procedures, and theoretical expectations.
3. Uncertainty assigned by researcher.
4. Number of replicate measurements and the magnitude of deviation of replicate results from the calculated average value.
5. Publication in refereed journal.
6. Previous publications by researcher.
7. Temperature, pressure, and concentration range covered.

The internal consistency of ΔG°_f , ΔH°_f , and S° data in the database is ensured by checking the relationship $\Delta G = \Delta H - T\Delta S$ for all reactions. The measure of agreement between values of an equilibrium constant calculated by two or more procedures is also checked. Tabulated values of the chemical thermodynamic properties are related so that the equilibrium constant ($\log K$) calculated in any number of ways will yield the same result. Methods of computing $\log K$ include: net change in Gibbs energy of reaction, enthalpy and entropy of reaction, and addition of two or more chemical reactions which yield the desired reaction. Examples of these comparisons are given in Phillips and others (1988).

The networks of interrelated calculations and the possible interdependence of measured formation constants and tabulated G, H, and S data are reexamined as new values are added to the database. A change in the recommended value of ΔG°_f , ΔH°_f , or S° for a key substance that results in a change in $\log K$ greater than 0.05 units is propagated throughout the database. This is done with the dual purpose of compiling the best data in the database, and to ensure consistency in calculated values of $\log K$. Key substances include ground-water species as well as metal ions such as UO_2^{2+} and Am^{3+} .

3.3 Uncertainty and Propagation of Errors

Uncertainty is the estimated deviation of a thermodynamic property such as ΔG from the "true value." For the ASD, uncertainty is defined as the upper and lower bounds about the selected best value. These bounds are given as a \pm , for example -502.90 ± 7.5 which gives values of -510.4 and -495.4 . As a general rule, uncertainties assigned by a researcher or by an evaluator are accepted for the ASD compilation. The uncertainties of parameter values calculated for the ASD are obtained from both computation of the propagation of error and subjective criteria based on evaluation of the quality of experimental work. The role of personal appraisal in the overall uncertainty has been recognized in other standard compilations (Parker, 1965); therefore, a strictly mathematical evaluation cannot be made. In the ASD, subjective evaluations lead to assignment of conservative (i.e., overestimated) uncertainties.

The uncertainties in thermomechanical data will lead to uncertainties in calculated equilibrium constants. Currently, an evaluation of methods to propagate this uncertainty in speciation and solubility calculations is underway. This is discussed more fully in Phillips and others (1988).

The accuracy of the data is checked in several ways. Values of calculated thermodynamic properties are compared to published experimental data whenever possible. Prior to publication, each value of a thermodynamic property has been recalculated an average of three to five times. The calculated value of $\log K$ is compared with existing experimental or smoothed data to arrive at recommended values at high temperatures and high ionic strength.

Data are also reviewed by recognized experts, such as those at laboratories which published the data. The review has included members of a technical advisory committee and by additional experts in the fields of thermochemistry and database compilation. A list of the members of the technical advisory committee is given in Table 6. The technical advisory committee provides guidance and review in the following areas:

1. Evaluation of the status of the current database.
2. Proper role and limitations of theoretical calculations using the current database.
3. Selection of appropriate geochemical codes and database format for performance assessment calculations.
4. Program plan for data-base compilation.
5. Quality assurance procedures for selection of data.
6. Reasonable expectations for generation of new data for actinides and other waste elements before 1990.
7. Defensible homologs for actinides.

Copies of the database are routinely sent to the experts for review and evaluation in these areas.

3.4 Data for High Salinities

Equilibrium constants for reactions at high salinities are calculated from the ΔG°_f , ΔH°_f , and S° data compiled for standard conditions (25°C, 1 atm). Salinity corrections for ionic strength of up to 3.0 M are made with the extended Debye-Huckel equation (Stumm and Morgan, 1981; Phillips and others, 1985) for activity coefficients. It has been suggested (Stumm and Morgan, 1981) that Pitzer-type equations should be used to calculate solubilities at ionic strengths above 3.0 M.

Data for the coefficients of Pitzer-type equations, however, are sparse and are nearly nonexistent for actinides. Thus, although considerable uncertainty results from a fit to the extended Debye-Huckel equation up to ionic strength of 3.0 M, this approach is the best available at this time.

Table 6

Technical Advisory Committee for HLW Database
December 1984*

Gregory R. Choppin
Department of Chemistry
Florida State University
Tallahassee, FL 32306

Howard J. White
Office of Standard Reference Data
National Bureau of Standards
Washington, DC 20234

Gary K. Jacobs
P. O. Box X
Oak Ridge National Laboratory
Oak Ridge, TN 37830

Kenneth M. Krupka (observer)
Pacific Northwest Laboratories
Battelle Boulevard
Richland, WA 99352

Malcolm Siegel
Waste Management Systems
Division 6431
Sandia National Laboratories
Albuquerque, NM 87185

William Dam
U.S. Nuclear Regulatory Comm.
M.S. 697-SS
Office of Nuclear Material Safety and Safeguards
Washington, DC 20555

Vivian B. Parker
Center for Thermodynamics
National Bureau of Standards
Washington, DC 20234

Table 6

Technical Advisory Committee for HLW Database
December 1984*
(Concluded)

Vijay Tripathi
Department of Applied Earth Sciences
Stanford University
Stanford, CA 94305

Sidney Phillips
Computing Division
Lawrence Berkeley Laboratory
Berkeley, CA 94720

*affiliations of members as of December 1984 are listed.

Some techniques for calculation of equilibrium constants for reactions involving major and minor components of brine do exist and can possibly be applied to salt repository sites. For such applications, the methods needed will have to be useful for ionic strengths ranging from 4 to 6 molar where the dominant electrolyte is NaCl. Some possible techniques that fit this criterion include hydration theory, trace activity coefficients, mean salt methods, and polynomial type (i.e., "extended") Debye-Huckel equations. Many of these techniques are described by Pytkowicz (1979).

3.5 The Sandia Sorption Data Management System

Two computerized data management systems currently being used to store and manipulate sorption data were examined as part of this work. These systems are the International Sorption Information Retrieval System (ISIRS), installed at Pacific Northwest Laboratories (PNL) and the System 2000 used by the Nevada Nuclear Waste Site Investigations (NNWSI) and maintained by DOE at Sandia Laboratories. The NNWSI database contains sorption data compiled from LA-9328-MS (CODATA, 1978) and some mineralogical and hydrogeologic data relevant to geochemistry. The data subsetting and statistics capabilities of the database are limited, however, and there are no subroutines for data manipulation or isotherm generation. Therefore, a system similar to System 2000 would not be suitable for this application. The other option, ISIRS, has very few data for basalt or tuff. It contains 250 entries for sediments associated with salt, 450 entries for granite, and 170 entries for clay minerals. The standard coding form used for data entry is very detailed and includes spaces for information on rock, ground water, nuclide characteristics, and experimental methodology. However, it is likely that values for many of the parameters listed in the form needed by ISIRS are not currently available in the literature. Based on this information, it was decided that a new

database for sorption data should be developed particularly for this application. The new database is called the Sandia Sorption Data Management System (SSDMS).

dBASE III (Ashton-Tate, 1984) was chosen as a suitable database for the sorption measurements and ancillary data. dBASE III allows the building of small modular files which contain a few parameters for a large number of samples. These small files can be linked together to form very complete, complex descriptions of samples. The input and screen prompts can be formatted specifically to a particular source of data (e.g., a table from a report) yet additional parameters for any sample can be added later without any need for reformatting any files. Thus, dBASE III offers very simple data entry procedures yet allows the user to build very comprehensive master data files as new types of data become available.

Table 7 lists the variables that are included in the tuff sorption database system. All of the experimental data for tuff published as of May 1985 by Los Alamos National Laboratories (LANL) have been entered into the dBASE III system and have been checked for accuracy and redundancy. Programs to calculate descriptive statistics (mean, standard deviation, kurtosis, skewness, frequency distributions, and log transformation) for any subset of the data have been incorporated into the data management system.

A simple quality assurance procedure for data entered into the dBASE III system has been implemented. Under this procedure, a notebook containing copies of data tables from the original sources of data (e.g., LANL reports) and printouts of the data from the data-base system is prepared. The "FORMAT" and "REPORT" capabilities of dBASE III are used to print the data from each table in a format that is similar to that of the original source of information. This allows rapid and accurate checking of the data for typographical errors. The sorption data are described in more detail in Tien and others (1985).

The statistical software described above was used to calculate descriptive statistics for sorption ratios of different tuff lithologic types and stratigraphic sorption intervals. Summary tables have been included in Tien and others (1985). These data can also be used for setting up conceptual models of a tuff site for system-scoping studies. A list of tuff rock samples described in the database are also found in Tien and others (1985).

3.6 Theoretical Sorption Calculations

A review of the state-of-the-art of theoretical modeling of radionuclide sorption was initiated as part of this work. The review is intended to provide an assessment of the error that may result in calculations of integrated discharge due to assumptions regarding sorption and aqueous equilibria in HLW sites. Also, the review will provide an evaluation of the feasibility of using phenomenological models of sorption in performance assessment studies. The investigation centers around the Stanford Generalized Model for Adsorption (SGMA) which can be used to provide a rigorous conceptual framework to estimate the error due to assumptions of linear sorption.

Table 7

Variables in Sorption Database

-
1. Sample Number (e.g., G1-1294)
 2. Element
 3. Batch sorption average
 4. Number of replications for sorption average
 5. Standard deviation of average
 6. Contact time for sorption experiment
 7. Highest pH measured in experiment
 8. Temperature
 9. Batch desorption average
 10. Number of replications
 11. Standard deviation of average
 12. Contact time for desorption experiment
 13. Tracer feed concentration (molar)
 14. Upper particle mesh size
 15. Lower particle mesh size
 16. Lowest pH measured in experiment
 17. Ground-water type (e.g., J-13, G-1, etc.)
 18. Atmospheric conditions (anoxic, oxic, or other)
 19. Solution to solid ratio (volume:mass)
 20. Shaking position (horizontal or vertical)
 21. Rock formation name
 22. Rock formation symbol (e.g., Tpt)
 23. Drill hole number (e.g., J-13)
 24. Sorption category (defined by internal documentation)
 25. Depth interval (ft)
 26. Sorption interval (defined for transport modeling purposes)
 27. Saturation (unsaturated or saturated zone)
 28. Cation exchange capacity of sample (3 methods)
 29. Surface area of sample
 30. Surface site densities
 31. Site-binding constant (calculated value)
 - 32-34. Sources for all data included database
-

A critical review of thermochemical data for use in the theoretical sorption calculations was carried out with the assistance of Drs. J. Leckie, D. Kent and V. Tripathi of Stanford University. Available literature was reviewed and researchers in the field of surface chemistry were contacted to obtain unpublished reports. A planned database includes general sorption reaction stoichiometrics, site-binding constants, and descriptions of experimental conditions for each study that is considered to be acceptable. A summary of the results of the literature and data review, and application of the SGMA to available data is found in Kent and others (1988).

The equilibrium chemistry code MINEQL was installed on the SNLA CDC computing system. MINEQL was modified at Stanford University from the original published version (Westall and others, 1976) by addition of the site-binding triple-layer model to describe sorption. The code has a pre-processor, MININP, which helps the user prepare input decks. MINEQL can be used to examine the potential variation of radionuclide distribution coefficients due to variations in ground-water composition and mineralogy along possible flow paths in the far field.

4. EFFECT OF HOMOGENEOUS REACTION RATES ON RADIONUCLIDE DISCHARGE

The objective of this study is to derive simple analytical expressions for a transport equation which includes terms for speciation reactions. The analytical expression should yield conservative estimates of integrated radionuclide discharge. Parametric calculations intended to examine the dependence of calculated values of radionuclide discharge on the rates of interconversion of immobile radionuclide species and mobile complexes were performed. These expressions could be used to formulate more accurate retardation factors for use in performance assessment calculations. A detailed discussion of the theoretical approach, derivations of analytical expressions used in parametric analyses, a listing of the source program, and the results of computer calculations carried out to date are given in Siegel and others (1984a) and Siegel and Erickson (1986). A brief summary of the methodology and applications to experimental design is given below.

4.1 Theory

In general, transport of radionuclides involved in any number of homogeneous and heterogeneous chemical reactions is described by equations of the form

$$\begin{aligned}
 \left\{ \begin{array}{c} \text{rate} \\ \text{of} \\ \text{accumulation} \end{array} \right\} &= \left\{ \begin{array}{c} \text{net rate of} \\ \text{influx by} \\ \text{convection} \end{array} \right\} + \left\{ \begin{array}{c} \text{net rate of} \\ \text{influx by} \\ \text{dispersion} \end{array} \right\} \\
 &- \left\{ \begin{array}{c} \text{rate of} \\ \text{radioactive} \\ \text{decay} \end{array} \right\} + \left\{ \begin{array}{c} \text{rate of} \\ \text{radioactive} \\ \text{production} \end{array} \right\} \\
 &+ \left\{ \begin{array}{c} \text{net rate of} \\ \text{production} \\ \text{by heterogeneous} \\ \text{reactions} \end{array} \right\} + \left\{ \begin{array}{c} \text{net rate of} \\ \text{production} \\ \text{by homogeneous} \\ \text{reactions} \end{array} \right\}
 \end{aligned}$$

where a separate equation is written for each species of each radionuclide.

The first five terms on the right-hand side of the above expression are normally included in solute transport models. The fifth term is generally used to represent reversible first-order sorption reactions (adsorption and ion exchange). Similar terms also could be used to calculate upper bounds on radionuclide discharge when colloid retention and irreversible sorption must be considered.

The last term in the above expression represents reactions between dissolved constituents. These may include changes in radionuclide speciation, precipitation by homogeneous nucleation, and colloid formation. For the purpose of calculating upper bounds to radionuclide discharge, these reactions can be represented by expressions of the form

$$\left\{ \begin{array}{l} \text{net rate of} \\ \text{production by} \\ \text{homogeneous} \\ \text{reactions} \end{array} \right\} = \sum_m k_m C_i$$

where k_m is the rate constant for the m^{th} reaction involving the i^{th} species of the radionuclide and C_i is the species concentration (see Siegel and others, 1984, and Siegel and Erickson, 1986).

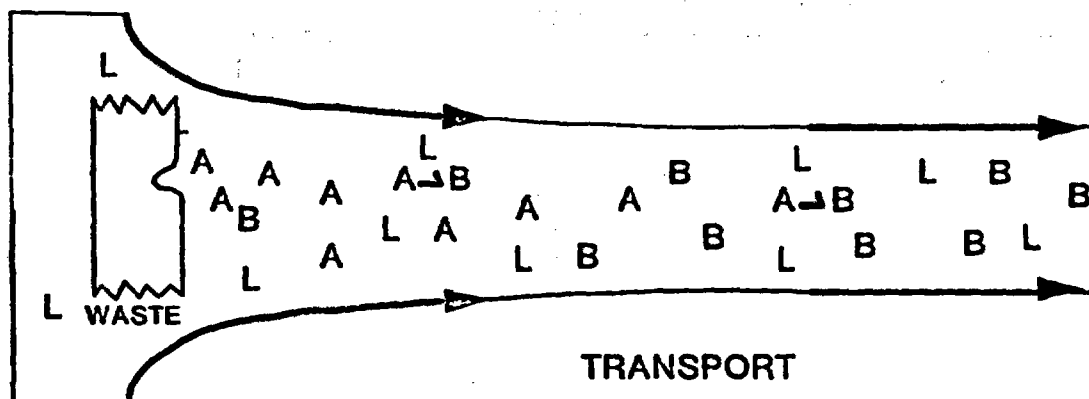
The EPA Standard 40 CFR Part 191 regulates the integrated discharge of radionuclides from a HLW repository to the accessible environment. Critical combinations of values of geochemical and hydrologic parameters which violate the EPA Standard can be identified in the following manner:

1. Terms for both homogeneous and heterogeneous reactions are incorporated into the radionuclide transport equations for each chemical species;
2. The equations are solved and the integrated discharge of each species is calculated for the 10,000-year regulatory period;
3. The equations for discharges of all chemical species of a radionuclide are summed and the resultant expression is set equal to the EPA radionuclide release limit W , $W = f(R_1, R_j, \dots, k_{ij}, \dots, C_i^0, \dots, C_j^0, \lambda_i, Q, x/v)$ where R_1, R_j , etc. are the retardation factors for the chemical species; k_{ij} etc. are the reaction rate constants for speciation reactions; C_i^0, C_j^0 , etc. are the initial concentrations of the chemical species in the engineered facility, λ_i is the radioactive decay constant for the chemical species, Q is the annual volumetric flux of water through the engineered facility; and x/v (distance/velocity) is the ground-water travel time from the engineered facility to the accessible environment;
4. The equation for the radionuclide release limit is solved numerically to determine combinations of the parameters which cause violations of the EPA Standard.

When several radionuclides of an element are present, sorption equilibria and chemical reaction rates are functions of the total concentration of the element. Therefore, the transport equations for each radionuclide are coupled and require simultaneous solution. However, to bound cumulative radionuclide discharges, the transport equations can be uncoupled as shown in Siegel and others (1984a) and solved independently, provided that sorption equilibria and reaction rates do not differ appreciably between nuclides.

This method of sensitivity analysis can best be illustrated by its application to a specific scenario in which radionuclide discharges at 10,000 years would be greater than those predicted by calculations which do not include the effects of speciation reactions. Figure 4 depicts the release of a radionuclide as an unstable sorbing species A which transforms to a mobile species B during transport. Such a transformation could occur due to kinetic constraints (i.e., the metastable species A is released easily

from the waste form due to steric factors but is unstable in the solutions in the repository near-field) or due to changes in the geochemical conditions. Clearly, the total integrated discharge of the radionuclide as species A and B will be greater than predicted by calculations of the discharge which assume that all the nuclide is released as species A. The magnitude of the error will depend upon the relative mobilities of species A and B as well as the rate of the transformation $A \rightarrow B$.



DEFINITIONS

A : SORBING AQUEOUS SPECIES [eg - UO_2^{2+} , $(UO_2)_3(OH)_5^+$]

B : NON-SORBING AQUEOUS SPECIES [eg. $UO_2(CO_3)_3^{4-}$]

L : GROUND-WATER LIGAND [eg HCO_3^-]

k : RATE CONSTANT FOR REACTION $A + L \rightarrow B$

Figure 4. A Scenario for Geochemical Sensitivity Analysis. Species A is a hypothetical sorbing species that has been studied in sorption experiments. The sensitivity of radionuclide discharge to the production of another species B is examined in this study.

The sum of the integrated discharges of species A and B can be set to a specified release limit for the radionuclide of interest.

$$Q \int_{t_0}^{t = 10,000 \text{ yr}} (C_A + C_B) dt = f(x/v, R_A, R_B, k^*, \lambda, t_0, C_A^0, C_B^0, t^*) - W \quad (4.1)$$

where t_0 is the initial containment period; k^* is the reaction rate for the conversion from A to B, $t^* = 10,000 - t_0$; and other terms have been defined above.

For $R_A x/v > R_B x/v > t^*$, both C_A and C_B at the accessible environment should be negligible. For $R_B x/v < t^* < R_A x/v$, $C_A = 0$ at the accessible environment. Siegel and Erickson (1986) show that for this case, the solution to Equation (4.1) is given by

$$W = (QC_B^0 + Q\Gamma)(t^* - R_B x/v) \exp(-\lambda R_B x/v) \quad (4.2)$$

$$+ \frac{Q\Gamma}{\alpha} \left[\exp \frac{(-\lambda t^* - k^*)(t^* - R_B x/v)}{R_A - R_B} - \exp(-\lambda R_B x/v) \right]$$

where

$$\Gamma = \frac{k^* C_A^0}{(R_A - R_B)\lambda + k^*}$$

$$\alpha = \frac{(R_A - R_B)\lambda + k^*}{R_A - R_B}$$

If $t^* > R_A x/v > R_B x/v$, then both C_A and C_B at the accessible environment are nonzero and the solution to Equation (4.1) is (Siegel and Erickson, 1986)

$$W = Q(C_B^0 + \Gamma)(t^* - R_B x/v) \exp(-\lambda R_B x/v)$$

$$+ \frac{Q\Gamma}{\alpha} \left[\exp - \frac{(R_A \lambda + k^*)x}{v} - \exp(-\lambda R_B x/v) \right] \quad (4.3)$$

$$+ Q(C_A^0 - \Gamma)(t^* - R_A x/v) \exp \left[- \frac{(R_A \lambda + k^*)x}{v} \right]$$

The detailed derivations of Equations (4.2) and (4.3) are given in Siegel and others (1984).

4.2 Application to EPA Standard and NRC Rule

Solutions to Equations (4.2) and (4.3) are presented as "EPA Compliance Curves" in Figure 5. These bivariate curves show combinations of the values of retardation factors for the two species and k^* which result in integrated discharges equal to the release limits set by the EPA Standard. Each curve assumes a specific source term and ground-water travel time.

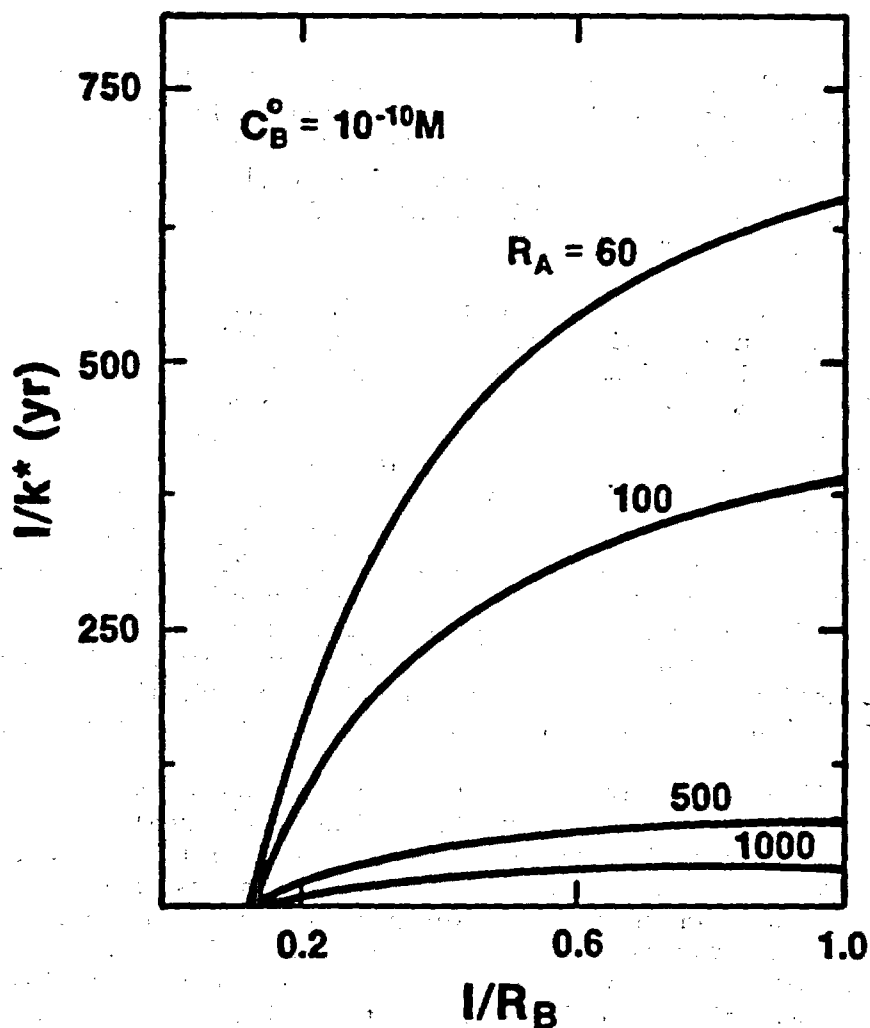


Figure 5. Effect of Retardation of Sorbing Species A on EPA Compliance Curves (release rate = 0.14 moles/yr; $Q = 1.4 \times 10^6$ liter/yr; C_A^0 = initial concentration of species A = 10^{-7} M; $\tau^* = 10,000$ yr; $\tau_0 = 0$ yr; $x/v = 1000$ yr; C_B^0 = initial concentration of species B = 10^{-10} M; $W_{Am-243} = 100$ Ci/1000 metric tons heavy metal (MTHM)).

In previous work (Siegel and others, 1984), this procedure was applied to the discharge of a long-lived radionuclide ^{237}Np ($t_{1/2} > 2 \times 10^6$ yr) in a scenario in which radioactive production was negligible. The conversion of an immobile chemical species A to a mobile species B by irreversible reaction during transport was considered. In this study, the analysis was extended to shorter-lived nuclides such as ^{243}Am , ^{241}Pu , and ^{246}Cm . The relationship between retardation and kinetics for transport scenarios where both sorbing and nonsorbing aqueous species are present was also examined. Calculations for ^{243}Am were carried out in which it was assumed that a nonsorbing species as well as a sorbing species were initially present in the facility. The maximum concentrations of a nonsorbing species consistent with the EPA release limit (100 Ci/1000 MTHM) were calculated for different combinations of flow conditions (ground-water travel time and volumetric flux). Solutions to Equations (4.2) and (4.3) for ^{243}Am are

shown in Figure 5. Release was assumed to start immediately after emplacement and the ground-water travel time to the accessible environment was 1000 years. The fractional release rate listed in the figure captions refers to the inventory at emplacement, 6.6×10^5 Ci (1.41×10^4 moles) for an assumed repository inventory of 46,800 MTHM of BWR and PWR spent fuel assemblies (Pepping and others, 1983).

Retardation factors and reaction rates for the interconversion of the species of interest in HLW disposal are not generally available. The methodology described above, however, can be applied to available data as follows. If R_B is assumed to be 1.0, then species B is completely unretarded and migrates at a velocity equal to the ground-water velocity. Then, for a given value of R_A , the corresponding value of k^* [which can be obtained either from Equation (4.3) or Figure 5] is the lower limit for the reaction rate constant that needs to be considered for performance assessment studies. In this study, that value is denoted k_m . If the reaction rate were any lower than that value, the conversion of A to B could not cause a discharge of the radionuclide greater than its EPA release limit. This means that if a regulatory agency wished to use available sorption data to ensure compliance of a site with the EPA Standard, then it must be shown that the reaction rate constant is less than that minimum value, k_m .

As discussed in Siegel and Erickson (1984a,b), a conservative analysis (i.e., one that will overestimate radionuclide discharge) can be made assuming that measured sorption ratios can be used to calculate values of R_A . The actual integrated discharge of a multi-species system of ^{243}Am , for example, will be less than that of a two-species system in which R_B is zero and R_A is taken from the average measured sorption ratios for Am. The maximum permissible rate of conversion of the sorbing species to a nonsorbing species was also calculated for tuff, salt, and basalt. These were expressed as minimum chemical stability ($1/k_m$) that would ensure compliance with the release limits in the EPA Standard. Ranges for this parameter were obtained from curves like those in Figure 5 and the ranges of retardation factors, R_A , in Table 8. The ranges of $1/k_m$ are shown for tuff, salt, and basalt in Figure 6.

4.3 Application to Experimental Design

In this section, the minimum chemical stability values previously derived are applied to the analysis of data from batch sorption experiments. In typical batch sorption experiments, fluid-phase compositions are monitored until no statistically significant change appears to occur during some time period, (usually on the order of days). The experiment is then assumed to be at equilibrium. However, as discussed above, some chemical speciation reactions that convert strongly sorbing species to more weakly sorbing species might occur too slowly to be detected during the given time period, but would occur rapidly enough to seriously affect cumulative radionuclide discharges during a regulatory period, which is on the order of ten thousand years.

Figure 7a illustrates a hypothetical batch sorption experiment in which species A, the initially dominant, more strongly sorbing species, converts irreversibly to nonsorbing species B. As shown in Appendix B, if ρ_{ha} is

Table 8

Retardation Factors Assumed for Species A of ²⁴³Am

Medium	SNL*		WISP†	
	Minimum	Mean	Minimum	"Probable"
Basalt	58	16,000	60	500
Salt	110	24,300	300	1,000
Zeolitized				
Tuff	1,020	7,585	300	1,000
Vitric				
Tuff	300	1,220	300	1,000

*NUREG/CR-3235 (Pepping and others, 1983 and Siegel and Chu, 1983)

†Waste Isolation Systems Panel, (WISP, 1983)

the rate constant for sorption of species A and k is the rate constant for the irreversible conversion of species A to B, then Equation (4.4) describes the change in concentration of the radionuclide as a function of time.

$$\frac{C_A + C_B}{C_0} = 1 + \frac{1}{(b^2 - 4C)^{1/2}} \left[(\rho ha - b_1) (1 - k/b_1) e^{-b_1 t} - (\rho ha - b_2) (1 - k/b_2) e^{-b_2 t} \right] \quad (4.4)$$

where

$$b_1 = \frac{-b + (b^2 - 4C)^{1/2}}{2}$$

$$b_2 = \frac{-b - (b^2 - 4C)^{1/2}}{2}$$

$$b = \rho ha \left(1 + \frac{mRd_A}{v} \right) + k$$

$$C = \rho h a k$$

where

- m = mass of solid substrate
- v = solution volume
- q_A = concentration of A on solid

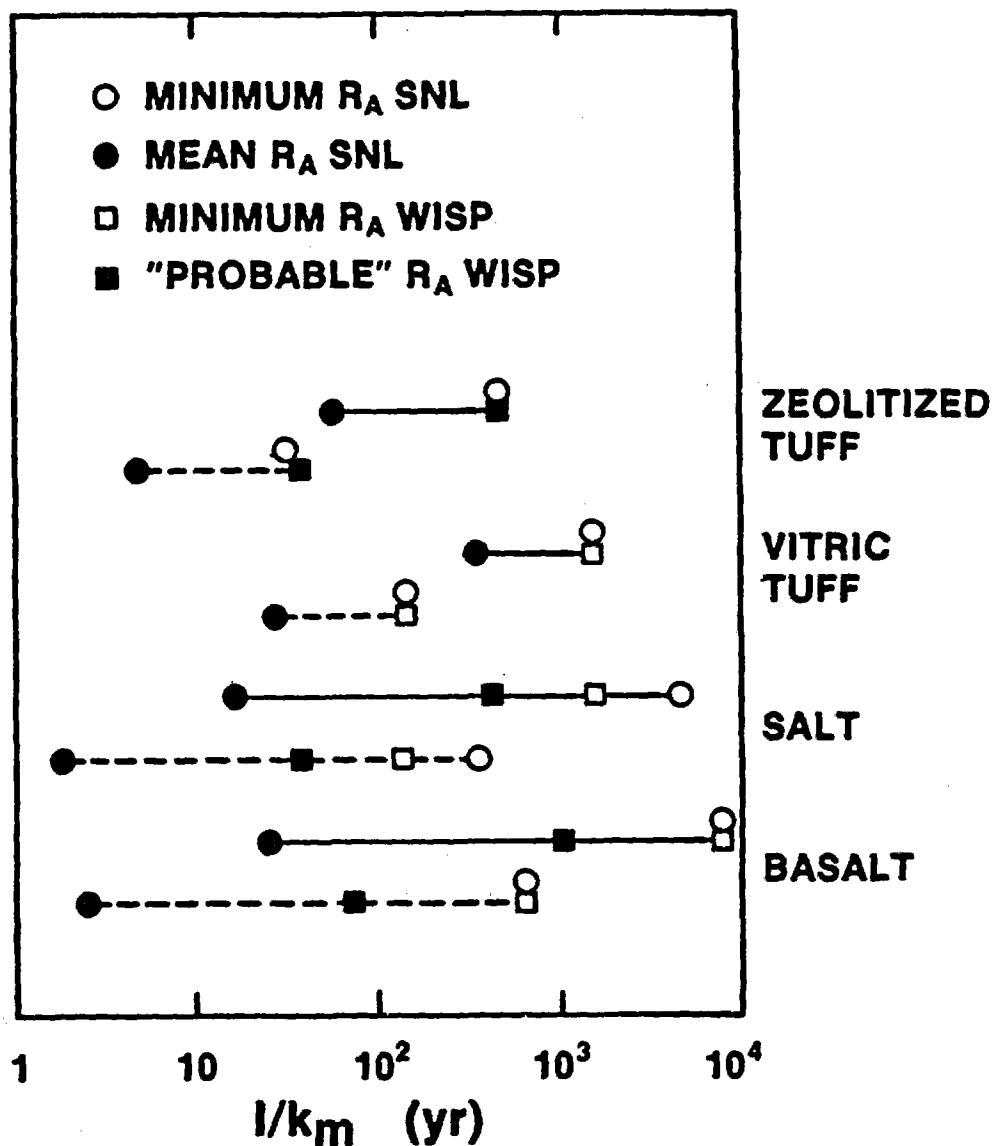


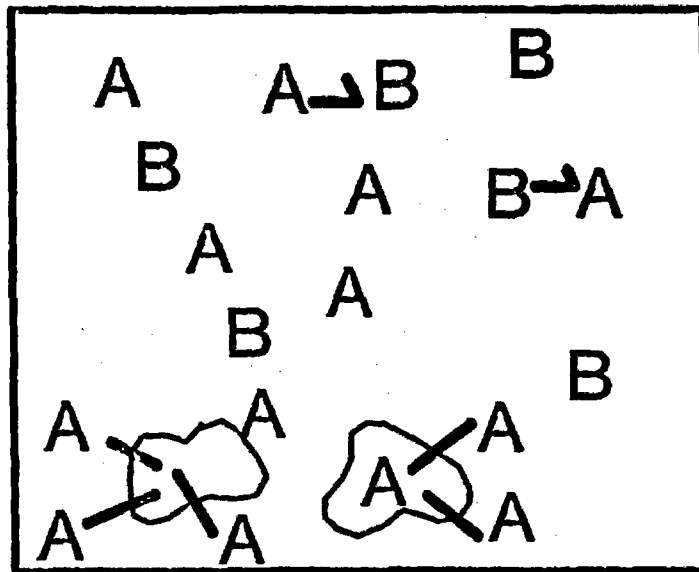
Figure 6. Media-Specific Chemical Stability l/k_m Required to Ensure that Integrated Discharge of ^{243}Am is Less than the EPA Release Limit ($t_0 = 0$ yr, $R_B = 1.0$; $x/v = 1000$ yr, Fractional release rate = $10^{-5}/\text{yr}$). Solid line corresponds to $C_B^0 = 8 \times 10^{-9}$ M; broken line corresponds to $C_B^0 = 1 \times 10^{-10}$ M, where C_B^0 is the initial concentration of the nonsorbing species B in the facility. Ranges of R_A values were taken from SNLA studies (Pepping and others, 1983 and Siegel and Chu, 1983) and the Waste Isolation Systems Panels (WISP) Study (WISP, 1983).

- C_0 - total initial concentration of radionuclide
- C_A - concentration of A in liquid
- C_B - concentration of B in liquid
- ρ - grain density
- h - mass transfer coefficient
- a - interfacial surface area per gram of solid
- k - reaction rate constant
- Rd_A - sorption ratio for species A
- t - time since start of experiments

Solutions to Equation (4.4) are derived and plotted in Appendix B for typical parameter values. A schematic plot of the solution of the equation is shown in Figure 7b.

The curve shows that if species A converts irreversibly to species B, then the concentration of the radionuclide in solution will initially decrease rapidly as species A is sorbed by the solid, reach an apparent steady state for several days, but then increase as significant amounts of species A convert to the poorly sorbed species B. Figure 7b also shows that the time needed for the solution concentration to rise detectably above the "steady-state" concentration depends on the experimental precision of the analytical techniques used to monitor the solution concentration. If the precision were equal to ϵ_1 , then after t_1 days it would be clear that the solution concentration had not reached steady state and that speciation reactions unaccounted for by a simple sorption model were occurring. An experimental technique with a poorer precision ϵ_2 would require a longer period t_2 to observe these effects.

Use of the methodology for geochemical sensitivity analysis as developed above can be illustrated as follows. A range of retardation factors for a radionuclide can be obtained from data from laboratory and/or field studies for a potential HLW repository site. Equations (4.2) and (4.3) can be used to calculate a corresponding range of chemical stabilities which ensure that discharges of the radionuclide will not exceed a given limit (see for example Figure 5). Pairs of values of R_A and k_m obtained in this way could be used in Equation (4.4) to produce graphs such as Figure 7b. From these graphs and from knowledge of ϵ , the analytical precision of the method used to monitor solution concentration in the batch test, it is possible to determine the duration of the experiment required to quantitatively observe speciation effects that could lead to unforeseen violations of the EPA Standard (or any other specified release limit). Applications of this methodology for several radionuclides are illustrated in Siegel and Erickson (1986).



BATCH EXPERIMENT

Figure 7a. Conversion of Hypothetical Sorbing Species A to a Nonsorbing Species During a Batch Sorption Experiment Considered in Equation (4.4).

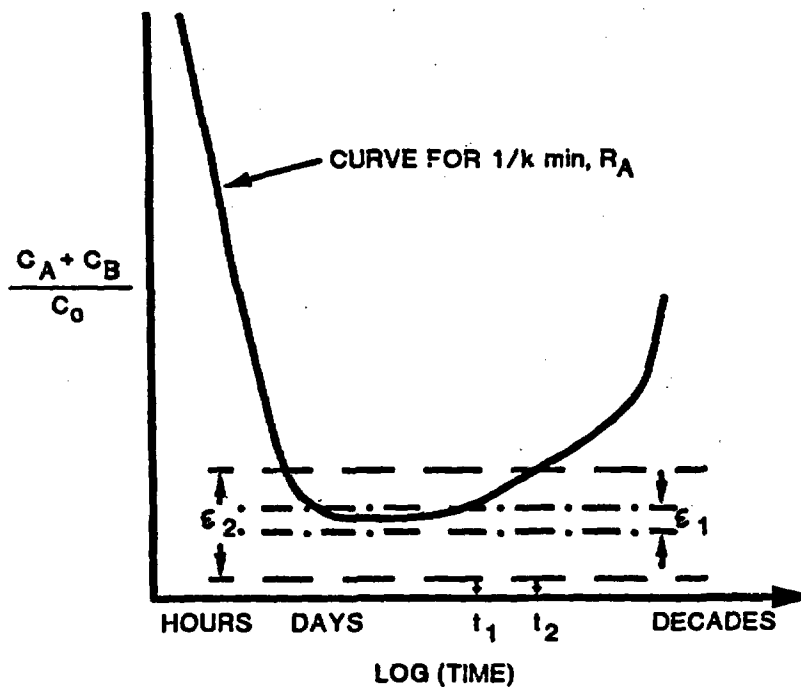


Figure 7b. Solution to Equation (4.4) and Relationship Between Analytical Precision ϵ_1 and Experimental Run Time t_1 Required to Observe Disequilibrium Due to Irreversible Conversion of A \rightarrow B.

5. COUPLED TRANSPORT AND CHEMICAL EFFECTS

Coupled reaction-transport codes that explicitly model geochemical reactions have been proposed as an alternative to currently available performance assessment codes (Muller and others, 1982). These codes are clearly useful in providing basic mechanistic insights and identifying key chemical parameters in radionuclide transport. The routine use of transport codes in performance assessment would require a large number of simulations over wide ranges of parameter values. The TRANQL code (Cederberg, 1985a,b) was evaluated to determine if it could be used in routine performance assessment calculations and in sensitivity studies designed to evaluate the potential errors caused by the neglect of coupled reaction-transport effects by existing performance assessment transport codes such as NWFT/DVM (Campbell and others, 1981) or NEFTRAN (Longsine and others, 1987).

5.1 Description of TRANQL

TRANQL is an equilibrium geochemical transport model that couples MICROQL (Westall, 1979) a subset of the speciation code MINEQL (Westall and others, 1976; Davis, 1977) with the transport model ISOQUAD (Pinder and Gray, 1977). The TRANQL code is described extensively in Cederberg (1985a,b) and Cederberg and Street (1985); the following description is summarized from these references.

In TRANQL, the chemical speciation equations for interactions among aqueous species and between solution species and surface-complexes are posed independently of the equations for mass transport. The one-dimensional transport equations are written in terms of C_T , the total (aqueous and sorbed) concentration, and of C_A , the total aqueous concentration of each chemical component:

$$\frac{\partial C_T}{\partial t} = D_L \frac{\partial^2 C_{AQ}}{\partial x^2} - v \frac{\partial C_{AQ}}{\partial x} \quad (5.1)$$

Here D_L and v are the longitudinal hydrodynamic dispersion coefficient and average ground-water velocity, respectively. Thus, the time derivative of the total component concentration is obtained from the total concentration of the aqueous species, ground-water velocity, and hydrodynamic dispersion. The set of transport equations is solved using the Galerkin finite element method with an implicit time-stepping scheme in the TRANSPORT module. The total aqueous concentration C_{AQ} of a component is obtained from solution of a set of algebraic equations relating concentrations of aqueous and sorbed species. This set of chemical-equilibrium equations is solved by iteration with the MICROQL module using the Newton-Raphson method.

The original version of TRANQL as described in Cederberg (1985a) is a prototype code which was designed for computer code research and development and not specifically for the multiple efficient runs needed in performance assessment analyses. This version of the code has been used to model one-dimensional and two-dimensional mass transport of cadmium and

ethylene-diamine tetraacetic acid (EDTA) in the presence of aqueous complexation, adsorption at the solid/solution interface and ion exchange. Precipitation/dissolution and radioactive decay/production were not simulated, however, in the chemical reaction submodel. The efficiency and accuracy of TRANQL have been compared to other models and it has been claimed that TRANQL is a relatively efficient model which can be extended to include all significant chemical processes and to simulate transport in two-dimensional and three-dimensional flow regimes (Cederberg, 1985a,b).

Previous studies using TRANQL have examined hydrologic and chemical systems that are much simpler than those expected at proposed HLW repository sites. For example, TRANQL has been used to simulate results of the Palo Alto Baylands Field Project (Valocchi and others, 1981; Cederberg, 1985a,b). Simulations involving transport over distances of tens of meters over 40 days with ground-water velocities on the order of 0.1 m/day have been carried out. It was necessary to determine if it is feasible to use the current version of TRANQL to model scenarios of interest in HLW disposal. These simulations would involve the behavior of complex chemical systems over $5 k_m$ distances for time periods in excess of 10,000 years. The bulk of this work was carried out at Stanford University by J. Leckie and V. Tripathi and is summarized below.

5.2 Feasibility of TRANQL Simulations in Performance Assessment

Three separate investigations were carried out in the evaluation of the use of TRANQL for long-term simulations. In the first study, the efficiency of TRANQL was evaluated as a function of simulation time and mean flow velocity. These calculations were for very simple geochemical and hydrological systems where no precipitation, dissolution, or changes in pH were allowed. A one-dimensional flow model was used, represented by 45 finite elements and 92 nodes. The results are summarized in Table 9. For grid scales (≈ 1 cm) and flow velocities (≈ 1 to 10 cm/day) similar to those used in TRANQL simulations in the references cited above, several years of CPU time would be required for geochemically simple, long-term simulations. Increasing the grid size to tens of meters (roughly equivalent to decreasing the flow velocity by five orders of magnitude) would decrease the CPU requirements to tens of months but may lead to numerical instabilities and loss of accuracy. This study showed that it would not be feasible to carry out long-term simulations with the present version of TRANQL on the VAX 11/750 or DEC 20 computers used at Stanford.

In the second investigation in this study, the CPU times obtained from the above calculations were scaled to obtain a rough estimate of run times required on the larger, faster computers available at SNLA. A short benchmarking code that mimics the most time-consuming operations of TRANQL was written at Stanford and is included in Tripathi and others (1987). Versions of the code were run on the SNLA CRAY-1 and CDC Cyber 180/855 main frame computers and on an IBM PC/AT computer (512 kilobytes RAM). The run times in these computers are compared to those of the Stanford computers in Table 10.

Table 9

Comparisons of TRANQL Simulation Run Times

<u>Computer</u>	<u>Flow Velocity (cm/day)</u>	<u>Simulated Time (yr)</u>	<u>Time Step (hr)</u>	<u>CPU Time (min)</u>
DEC 20	8	0.001	1	307
DEC 20	0.08	0.019	4	5.3
VAX 11/750	0.08	1	4	648.0
VAX 11/750	0.00008	1	84	25.5
CRAY-1*	0.00008	10,000	NA	2400*

*Rough estimate of CPU Time.

Table 10

Comparison of Benchmark Code Run Times

<u>Computer</u>	<u>Stanford University</u>		<u>SNLA</u>		
	<u>DEC 20</u>	<u>VAX 11/750</u>	<u>IBM PC/AT</u>	<u>CDC</u>	<u>CRAY-1</u>
CPU Time*	25	50	250	3.7	0.46

*Required CPU time (seconds) for 100 iterations (ILOOP = 100). Ratios of run times were same for ILOOP = 1, 10, 100, 1000.

These calculations suggest that the CPU times required for TRANQL on the CRAY-1 computer at SNLA will be less than one percent of the times reported for the VAX 11/750 at Stanford. This means that with the present form of TRANQL, a single simulation with a grid size of 10 meters for a geochemically simple system (14 complexes), would still require approximately 40 hours of CPU time in the SNLA CRAY-1. It is possible, since the benchmark code was very small and was not vectorized, that the CRAY's performance was seriously underestimated. For large programs and with proper implementation, TRANQL could run faster in the CRAY. However, substantial improvements in efficiency would be required before TRANQL could be used to run even simple long-term simulations at an affordable cost (1 hour of CPU time on the SNLA-CRAY-1 costs \$1,000).

About 88 to 99 percent of the CPU time spent in the simulations as described above was used in MICROQL, the chemical equilibrium calculation module of TRANQL. In the third part of the TRANQL evaluation, the effect of chemical complexity on the run-time of MINEQL (the superset of MICROQL) was evaluated by comparing calculations on the DEC 20 for a simple geochemical system (11 aqueous species) with those for a more complex, realistic system (183 aqueous species; 73 possible solids). A single calculation when pH and speciation were calculated required 2 seconds of CPU time for the simple system and 50 seconds of CPU time for the more complex problem. This suggests that for the complex system, 1.25 hours of CPU time would be required per time step for the 45 element/92 node grid model in the TRANQL calculations described above. A 10,000-year simulation would require several weeks of CPU time in the CRAY-1.

The Stanford staff suggested that improvements to the efficiency of MINEQL/MICROQL would be the key step in reducing the execution time of TRANQL. The degree of improved efficiency cannot be estimated a priori; however, and improvement of 1 to 2 orders of magnitude is not unreasonable.

Two different types of improvements appear feasible. First, the nonlinear equation solver built into the chemical-equilibrium submodel does not use state-of-the-art numerical techniques. Recent advances in solving nonlinear-equation sets like those found in TRANQL have shown significant improvements in computational speed. While it is impossible to quantify this improvement in general terms, claims of up to a 36-fold increase in solution speed have been made. Such improved algorithms are commonly used in the numerical simulation of combustion, a problem with a mathematical structure very similar to the ground-water transport problem. Thus, the prognosis for successful implementation seems quite good.

A second improvement in model performance might be achieved through careful mathematical analysis of the structure of the nonlinear-equation set. In particular, the solution to the equation set is probably dominated by a subset of the equations. A methodology to isolate the appropriate subset has not yet been identified, but analogous approaches are used in several other fields, so some general methodologies do exist. The magnitude of any performance improvement would clearly depend on the particular chemical system being simulated, therefore, it is impossible to provide quantitative estimates of performance improvement. Although it appears that it will not be feasible to use TRANQL to carry out full simulations of geochemically realistic systems for HLW performance assessment, it may be possible to use an improved version of the code in sensitivity studies.

6. APPROXIMATE METHODS FOR CALCULATION OF RADIONUCLIDE DISCHARGES IN FRACTURED ROCK

The studies described in previous sections of this report have all dealt with radionuclide transport in a porous medium. Many of the potential HLW repository sites are in fractured media where fluid flow is primarily in the fractures and the chemical concentrations in the rock matrix will depend on the rate of matrix diffusion. In these rocks, the time required for radionuclide diffusion into the rock matrix must be considered in transport calculations.

6.1 Derivation of Criteria for Application of Three Approximate Methods

Approximate methods for calculating radionuclide discharges in fractured, porous rock can be derived from a set of rigorous general transport equations (Erickson, 1983). Approximations to the general transport equations for a region of saturated porous rock containing a system of uniform, parallel flat plates have been obtained under the following conditions: (1) fluid flow occurs along the axis of the fractures (in the x-direction) and is negligible in the porous matrix; (2) effects due to hydrodynamic dispersion are negligible; (3) radionuclide concentrations in the fractures are uniform; (4) local chemical equilibrium exists at the fracture-matrix and matrix-pore-water interfaces; (5) bulk radionuclide diffusion in the pore water occurs normal to the fracture axis (in the z-direction); (6) surface diffusion of nuclides in the interfacial regions between the pore water and mineral phases negligibly affects transport in the porous matrix; (7) radionuclide sorption is reversible and can be represented by linear isotherms; (8) colloidal transport of nuclides is negligible; (9) radionuclides exist as a single species; (10) radioactive decay and production of the nuclide of interest are negligible; and (11) diffusion coefficients are constant. Under these conditions the general transport equation reduces to:

$$\frac{\partial C_f}{\partial t} + v \frac{\partial C_f}{\partial x} + m_f \frac{\partial M}{\partial t} = 0 \quad (6.1)$$

- C_f - the radionuclide concentration in the fracture fluid
- C_m - the radionuclide concentration in the matrix pore water
- v - mass-averaged fluid velocity
- m_f - volume of matrix/volume of fractures $(1 - \phi_f)/\phi_f$
- ϕ_f - fracture porosity
- t - time
- x - spatial coordinate in the direction of the bulk fluid motion

for the fracture fluid and:

$$\frac{\partial C_m}{\partial t} = D_e \frac{\partial^2 C_m}{\partial z^2} \quad (6.2)$$

- $D_e = D/\alpha^2 R_m$
- α - tortuosity/constrictivity factor for the porous matrix

R_m - radionuclide retardation factor for the porous matrix
 z - spatial coordinate in the direction of diffusion in the porous matrix for the pore fluid.

Three approximate methods for calculating radionuclide discharges in fractured, porous rock have been evaluated: (1) the porous-medium approximation where radionuclide diffusion rates into the matrix are proportional to depletion rates in the fracture fluids, (2) a linear-driving-force approximation where radionuclide diffusion rates into the matrix are proportional to the difference between bulk concentrations in the matrix and the fracture fluids, and (3) a semi-infinite-medium approximation where radionuclide diffusion rates into the matrix are calculated assuming a semi-infinite matrix. The above three methods are described, criteria for application of each given, and the respective uncertainties in calculated radionuclide discharges are assessed in Erickson and others (1986). The general form of criteria for application of each method was derived from a general consideration of fluid residence times in the fractures and relaxation times for radionuclide concentration gradients in the matrix. Numerical criteria were then obtained from the solution to the transport equations for specific cases involving radionuclide decay, chemical reaction, and varying matrix properties (Erickson and others, 1986). For example, if fluid flow in saturated rock is one-dimensional and primarily occurs in parallel fractures having relatively uniform aperture $2b$ and spacing $2B$, and if matrix porosity ϕ_m , grain density ρ_s , fracture porosity ϕ_f and sorption isotherms $F(C)$ in the matrix are relatively uniform, then the porous-medium approximation applies when

$$x/v > 50B^2 \alpha^2 \phi_f / [\phi_m D(1 - \phi_f)] \quad (6.3)$$

The linear-driving force applies when

$$x/v > 0.2 B^2 \alpha^2 \phi_f / [\phi_m D(1 - \phi_f)] \quad (6.4)$$

and the semi-infinite medium applies when

$$x/v < B^2 \alpha^2 \phi_f / [\phi_m D(1 - \phi_f)] \quad (6.5)$$

Here, D is the radionuclide diffusion coefficient in the pore water; v is the average fluid velocity in the fractures; x is the radionuclide transport path length, and α is a tortuosity/constrictivity factor for the matrix.

Site-specific data for tuff and granite (Siegel and Chu, 1983; Guzowski, and others, 1983; Tien and others, 1985; Neretnieks, 1980; Birgersson and Neretnieks, 1984; Carlson and others, 1984) were used with the above criteria. Results are shown in Figure 8. For tuff, the porous-medium approximation will be applicable even for relatively thin beds ($x = 30$ m). The linear-driving force or semi-infinite-medium approaches would be necessary for extreme cases involving relatively unrealistic porosities and fluid velocities. For granite, the semi-infinite-medium or linear-driving-force approaches may be generally required, while the porous medium approximation may be applicable only to relatively large granite bodies (Erickson and others, 1986).

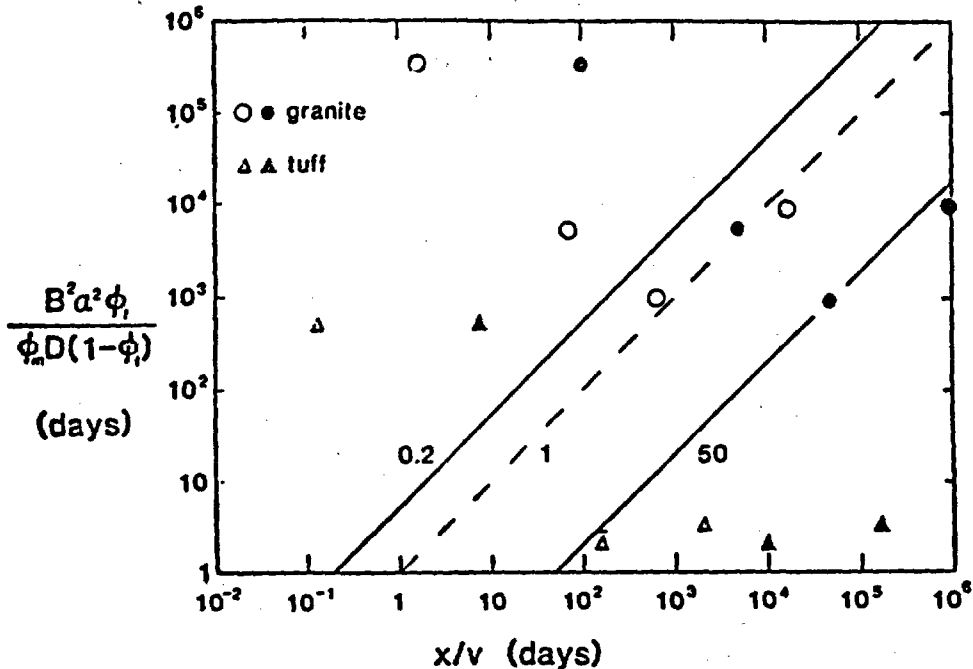


Figure 8. Application of Criteria to Representative Site-Specific Data for Granite and Tuff. Numbers on lines are ratios of $B^2\alpha^2\phi_i/\phi_m D(1-\phi_i)$ to x/v . Areas below lines marked '0.2' and '50' correspond to conditions under which linear-driving-force and porous-medium approximations, respectively, apply. The semi-infinite-medium approach applies in the area above the line marked '1'. Solid and open symbols refer to transport distances of $x = 2000$ meters and $x = 30$ meters respectively.

6.2 Semi-Infinite Medium Approximation Including Radioactive Decay

Theoretically, the transport of radionuclides whose relative concentrations (C/C_0) are close to zero at the center of a matrix block bound by parallel fractures should be described by a semi-infinite medium approximation. In the previous section, the effects of radioactive decay were not included in the derivation of the approximate transport equations for fractured porous rock. The concentrations of a decaying radionuclide in the matrix will be less than that predicted by Equation (6.2) for a stable isotope. It is useful to determine the conditions for which development of a semi-infinite medium approximation for decaying radionuclides is required for performance assessment calculations.

In this section, the effect of radioactive decay on transport was examined for the semi-infinite medium case. The concentration profiles and penetration depths of specific radionuclides in a semi-infinite basalt matrix were calculated using the equations described below and data listed in Table 11. The concentrations of the radionuclides in the matrix relative to the radionuclide concentration in the fracture (C/C_0) were calculated as a

Table 11

Results of Semi-Infinite Basalt Matrix Calculations Including
Radioactive Decay

Isotope	Half-life (Yr)	Retardation Factor	C/C ₀ [*]
Pu240	6.76E3	200	0.37
*Pu241	14.6	200	-0
Pu242	3.79E5	200	0.53
*Pu238	89.	200	-0
Pu239	2.44E4	200	0.48
U236	2.39E7	50	0.75
U233	1.62E5	50	0.75
U238	4.51E9	50	0.75
U234	2.47E5	50	0.75
U235	7.1E8	50	0.75
*Th232	1.41E10	5000	1.6E-3
*Th229	7.3E3	5000	7.3E-4
*Th230	8.0E4	5000	1.5E-3
Cm245	8.27E3	500	0.21
Cm246	8.0E3	500	0.16
*Am241	433.	500	3.6E-3
Am243	7.65E3	500	0.20
Np237	2.14E6	100	0.66
Sn126	1.0E5	1000	0.15
Tc99	2.14E5	5	0.92
I129	1.6E7	1	0.96

*Nuclides for which semi-infinite approximation might be used.

*At x = 0.5 meter and t = 10⁴ yrs.

function of distance, x, into the matrix at 10,000 years. If radioactive decay decreases radionuclide concentrations to near zero levels in the center of the matrix block within the 10,000-year EPA regulatory period, then a semi-infinite medium approximation may be applicable.

The equation describing the one-dimensional diffusion of a decaying radionuclide is

$$\frac{\partial C}{\partial t} = (D/R) \frac{\partial^2 C}{\partial x^2} - \lambda C \quad (6.6)$$

where D is the effective diffusivity, R is the retardation factor of the radionuclide, and λ is the decay constant of the radionuclide. Given that x = 0 at the surface, the initial and boundary conditions are C(0,x) = 0; C(t, x \rightarrow ∞) = 0; and C(t,0) = C₀, the fracture concentration. The solution is:

$$C(t,x) = \frac{C_0}{2} \left\{ e^{-x \sqrt{\frac{R\lambda}{D}}} \operatorname{erfc} \left[\frac{x}{2\sqrt{Dt/R}} - \sqrt{\lambda t} \right] + e^{\sqrt{\frac{R\lambda}{D}} x} \operatorname{erfc} \left[\frac{x}{2\sqrt{Dt/R}} + \sqrt{\lambda t} \right] \right\} \quad (6.7)$$

The results of parametric calculations using the above equation are presented in Figure 9. Concentration profiles in the rock matrix at $t = 10,000$ years are plotted for nuclides with several different half lives ($t_{1/2}$) and for several different retardation factors (R). These plots may be used to assess the need for a semi-infinite approximation for discrete combinations of matrix block width, radionuclide half-lives and retardation factors. For example, Equation (6.7) was also used to calculate $C(x,t)/C_0$ for the twenty-one radionuclides listed in Table 11. The retardation factors used were taken from the WISP study (WISP, 1983). The relative concentration C/C_0 for each radionuclide at $x = 0.5$ m (typical half-spacing between fractures in Columbia Plateau basalts) was calculated. The C/C_0 values listed in Table 11 indicate the concentration level of each radionuclide at $x = 0.5$ m, assuming that the matrix extends to infinity. For a finite matrix where $x = 0.5$ m is the true half-spacing, C/C_0 could be much higher than that shown in the table. Data from the Basalt Waste Isolation Project (BWIP) site (Long, 1978) indicate that spacing between fractures in basalt flows at Hanford ranges from 0.2 m to 3 m and is generally < 1 m. This means that, in general, concentrations in the centers of the blocks will be higher than those shown in Table 11. The results of this scoping calculation, therefore, overestimate the need for a semi-infinite approximation to model radionuclide transport. The values of relative concentration listed in Table 11 show that, except for the very short-lived (^{241}Pu , ^{238}Pu and ^{241}Am) and the highly retarded (Th isotopes) radionuclides, concentrations in the matrix are significantly higher than zero. The semi-infinite approximation may not be required for fractured basaltic rock for the values of retardation factors listed in Table 11. The same kind of analysis could be applied to other fractured media such as tuff.

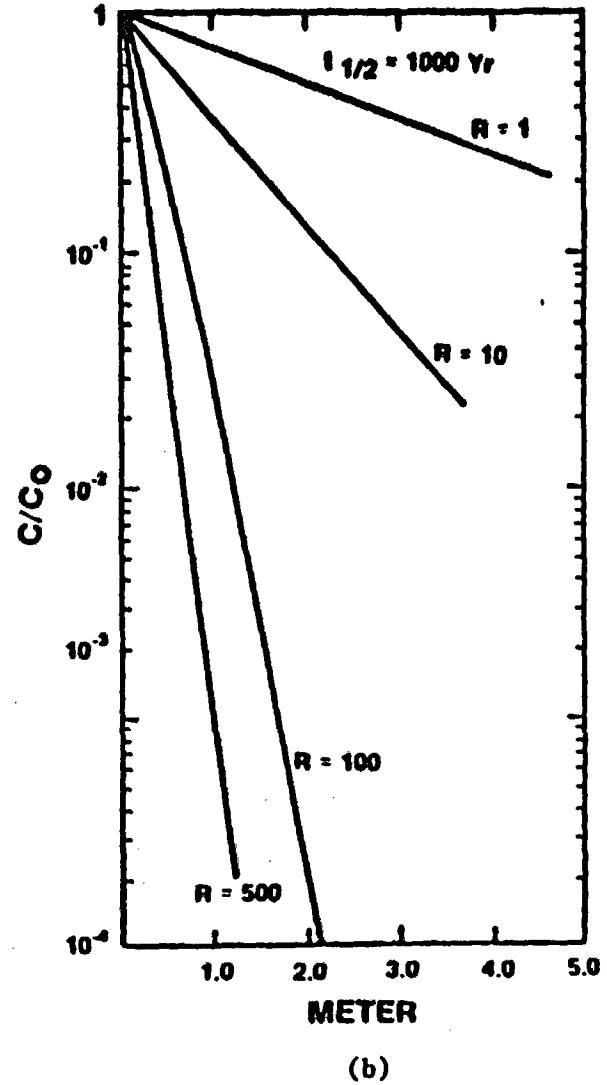
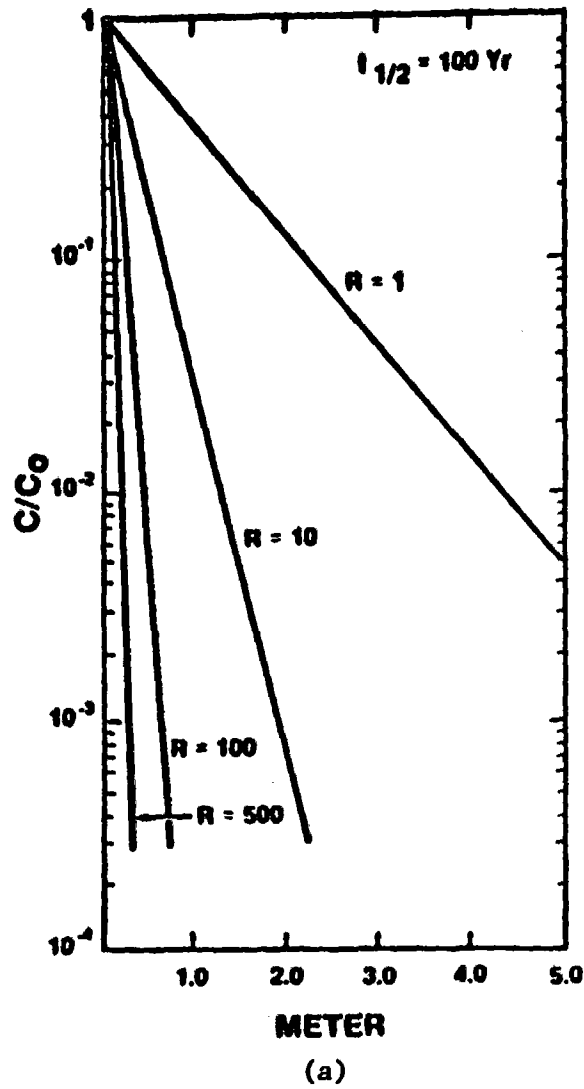


Figure 9. Concentration Profile of Diffusion of Radionuclides into a Semi-Infinite Rock Matrix Adjoining a Fracture After 10,000 Years for Different Radionuclide Retardation Factors (R_s). (a) Radionuclide Half-Life = 100 yr. (b) Half-Life = 1,000 yr.

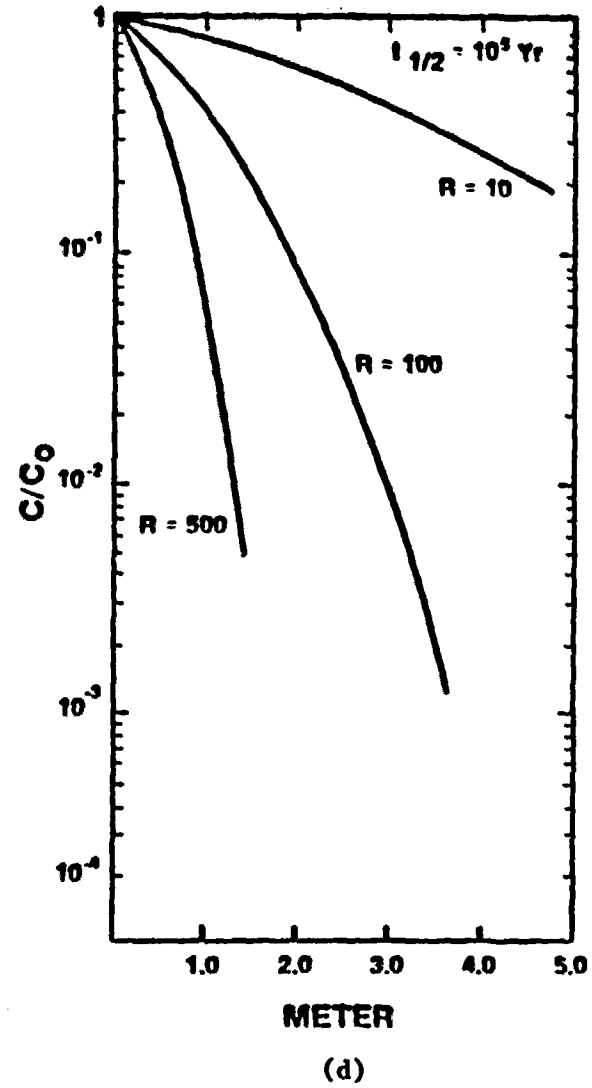
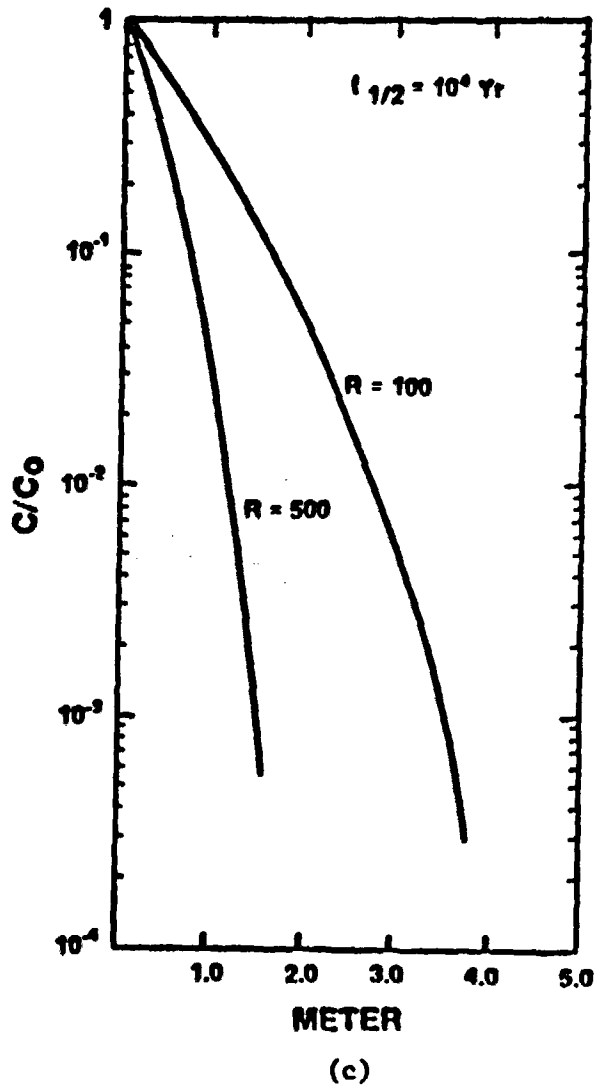


Figure 9. (concluded). (c) Half-Life = 10,000 yr. (d) Half-Life = 100,000 yr.

7. POTENTIAL TRANSPORT OF RADIONUCLIDES BY COLLOIDS

The release rate of radionuclides from a high-level waste repository to the accessible environment may be increased as a result of colloidal transport (Champ and others, 1982; cf. Bonano and others, 1984). As part of this work, several bounding calculations designed to assess the potential importance of the transport of radionuclides by colloids and particulates from HLW repositories were carried out. The calculations were performed for the "scenario" illustrated in Figure 10. It is important to note that no assessment of the probability or completeness of this "scenario" was made. This "scenario" was used solely to illustrate the relationships among potential processes.

The sequence of processes that are illustrated in Figure 10 can be summarized as follows:

1. Aqueous radionuclides are released from the waste and diffuse through the backfill;
2. Natural colloids flow by and are ready to adsorb radionuclides;
3. Radionuclides sorb onto natural colloids (e.g., phyllosilicate or zeolite particles) and form pseudocolloids;
4. Outside the backfill the radionuclides precipitate due to supersaturation;
5. Some of the particles are retained by the walls of the fracture; or
6. The particles are transported by fluid flow through a fracture in the rock to the accessible environment.

The scope of the calculations performed is sharply focused on three significant aspects of the scenario: (1) migration and retention of colloids and particulates in a single fracture, (2) adsorption of radionuclides by natural colloids in ground water (pseudocolloids), and (3) production of radiocolloids by homogeneous nucleation.

7.1 Migration and Retention of Colloids in a Single Fracture

Bonano and Beyeler (1985), determined the transport and capture rates of colloidal particles in terms of dimensionless parameters for a parallel-plate channel simulating a single fracture. The particle velocity normal to the walls of the channel was related to the sum of external forces acting on the particle. The forces considered were the gravitational, London-Van der Waals, and electric-double-layer forces. A single fracture geometry was chosen because the lower porosity and permeability of a porous matrix tend to increase the capture of particles. Therefore, by considering a system with high porosity and high permeability, such as a fracture, a lower bound for retardation of the particles will be established.

It was assumed that the particles are very small and the suspension very dilute so that the presence of the particles does not alter the flow field. This assumption implies a lower bound for the retardation of the particles,

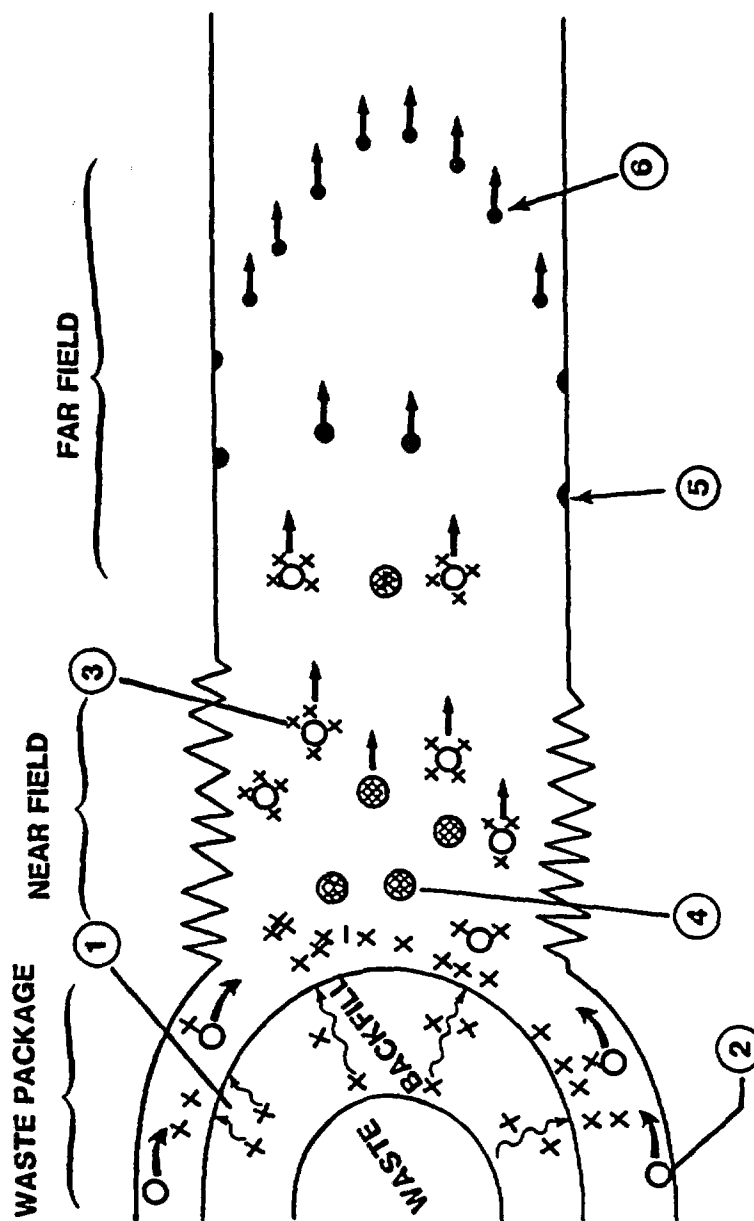


Figure 10. Colloid Release Scenario

Key: (1) Aqueous radionuclide species diffuse through backfill. (2) Natural ground-water colloids flow past waste package. (3) Radionuclides released from backfill are sorbed by natural ground-water colloids to form "pseudocolloids" and are carried to far field. (4) Sharp temperature gradient in vicinity of waste package causes supersaturation with respect to radioelement solid phases and true colloids precipitate. (5,6) Particles (both true colloids and pseudocolloids) are carried through far field by fluid flow through a fracture; some particles are retained on walls of fracture.

since fundamentally, the particle front trails the hydrodynamic front. With the undisturbed flow field, only the governing equation for the particle concentration,

$$\frac{\partial \phi}{\partial t} = \nabla \cdot [\lambda \nabla \phi] - \nabla \cdot (\underline{v} \phi) \quad (7.1)$$

needs to be solved (ϕ = particle concentration, t = time, λ = Brownian diffusivity, and \underline{v} = particle velocity vector). The velocity vector \underline{v} has two components, one along the axis of the channel, which depends on the fluid velocity, and the other, normal to the walls of the channel, given by

$$v_n = F_{ext} / \mu a \quad (7.2)$$

where F_{ext} is the sum of external forces acting on a particle of radius a in a fluid of viscosity μ . The external forces include London-van der Waals, electrokinetic and gravitational forces, the forms of which have been discussed by other workers (Guzy and others, 1983; Adamczyk and van de Ven, 1981). The effects of different inlet particle source rates and parameters (such as particle size, fluid velocity, surface charges for the particle, and the channel walls) on capture and, hence, migration of the particles were examined. Average velocities for both the fluid and the particles were also obtained.

A computer program (Bonano and Beyeler, 1984) was written to solve the steady-state convective diffusion equation as a function of dimensionless separation, concentration, position and capture efficiency. The results are expressed in terms of the Sherwood number, Sh , normalized colloid concentration and the velocity of the particle front relative to the average fluid velocity. The Sherwood number is a measure of the rate of particle capture, due to the external forces, relative to parametric analysis is given in Figure 11. The graph shows the colloid concentration profile (normalized to maximum colloid concentration) as a function of separation from the fracture wall (normalized to both the fracture half-width and particle radius) and the distance x that an ensemble of particles has traveled (normalized to the average fluid velocity, fracture width and Brownian diffusivity). As the particles move along the fracture, the concentration decreases due to capture (note that desorption of colloids from the fracture wall is not considered here). Figure 12 shows the Sherwood number as a function of normalized position along the flow path for different particle sizes.

The results of these calculations showed that the dynamic balance between the particle production rate and the rate of capture has a significant effect on the concentration of particles leaving the fracture. This effect arises because the rate of particle capture is directly proportional to the number of particles in suspension. If more particles are produced near the inlet of the fracture, then capture rates are higher at the same location. When higher number of particles are produced near the outlet, then the capture rate is higher at that location. If the particle production rate is uniform along the length of the fracture, so is the capture rate.

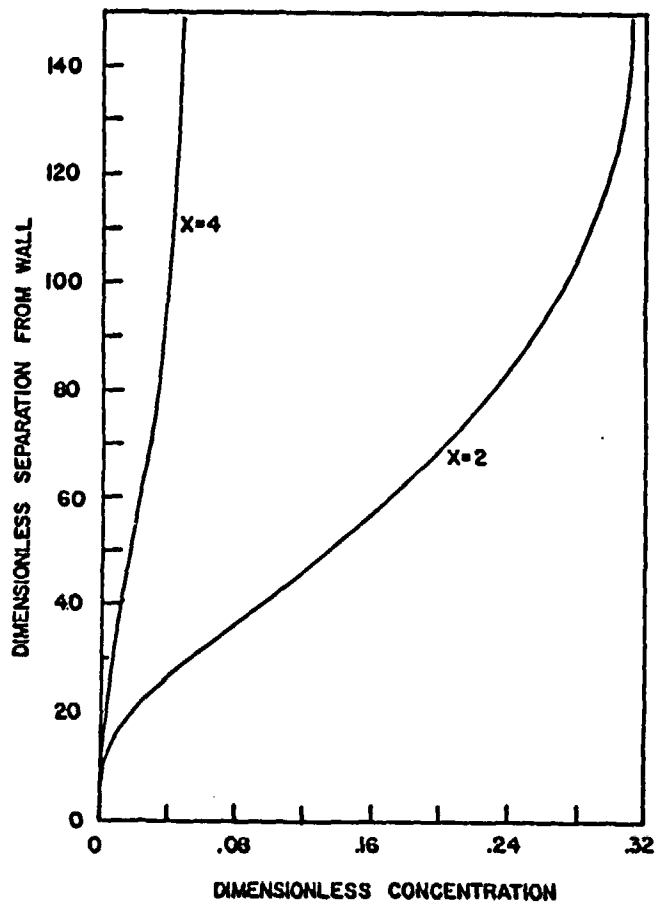


Figure 11. Colloid Concentration Profiles for Single Fractures as a Function of Position Along Channel

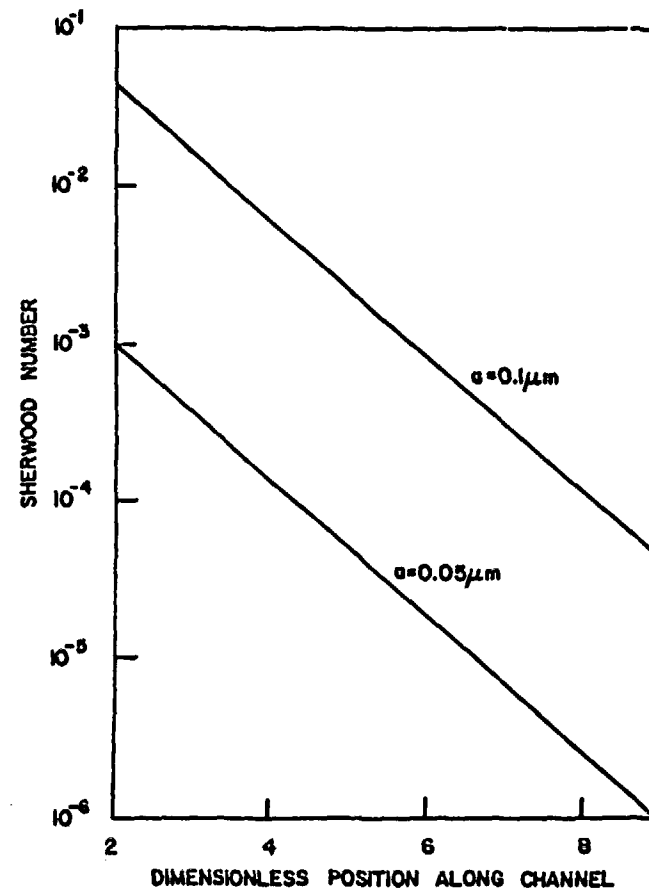


Figure 12. Sherwood Number as a Function of Position for Different Sizes

In addition, Figure 12 shows that the larger the particle radius, a , the higher the rate of capture. Doubling (0.05 to 0.1 μm) the particle size results in an increase in the capture rate of an order of magnitude. Over the range of average velocities considered (0.5 to 2 cm/s) no significant changes were detected in the capture rate when the former was varied. Because the particles preferentially travel near the center of the fracture, the average velocity of the particle front is higher than the average fluid velocity. The calculations and results are described in more detail in Bonano and Beyeler (1985).

The physical parameter values assumed in the calculations described by Figures 11 and 12 were not chosen to represent conditions expected at HLW repositories. Instead, values in these preliminary studies were chosen to allow comparison of this method of analysis with other studies in the literature. Future applications could involve calculations for conditions representative of geological environments surrounding HLW facilities. In addition, the effects of particle size distribution, particle growth rates, fluid velocity and source functions and desorption and resuspension of colloids could be examined.

7.2 Adsorption of Radionuclides by Natural Ground-Water Colloids (Pseudocolloids)

The purpose of these calculations was to estimate an upper bound for the ability of pseudocolloids to transport radionuclides. In this study, the size distribution and concentrations of natural colloids in ground water were considered; their maximum capacity for adsorption of radionuclides was estimated, and the resultant amount of radioactivity that could be transported was compared to NRC Regulation 10 CFR 20 (NRC, 1982).

7.2.1 Properties of Pseudocolloids

Pseudocolloids range in size from 1 nm to 1000 nm. They are composed primarily of phyllosilicates, zeolites, amorphous silica, ferromanganese oxyhydroxides, metal oxides, and organic materials (Stumm and Morgan, 1971, Yariv and Cross, 1979; Drever, 1982; Bonano and others, 1984). The size distribution and concentration of pseudocolloids in ground water is difficult to estimate at the present time. Few measurements of colloid size distributions have been attempted under natural conditions because of the theoretical and experimental difficulties in obtaining representative samples and observing low concentrations of particulates and interpreting results in a meaningful way. Measurements have been made of colloid size distributions in laboratory studies. Champ and others (1982) measured colloid size distributions using filtration and ultrafiltration in experiments with Pu-spiked soil columns. Distributions were measured after elution of 85 void volumes and after 250 to 350 void volumes. The reported size distributions were:

	A (85 Void Volumes)	B (250-350 Void Volumes)
Particulate (>450 nm)	21%	46%
Colloidal (50-450 nm)	23%	8%
(2.8-50 nm)		15%
(500-10,000 mol wt)	48%	27%
(<500 mol wt)	8%	4%

Eicholz and others (1981, 1982) studied the adsorption characteristics and transport of kaolinite colloids in small laboratory columns. These particulates were prepared by prolonged ball milling of kaolin. The size distribution estimated from their data is:

>200 nm	11%	
100-200 nm	51%	Median = 125 nm
50-100 nm	25%	
0-50 nm	13%	

measured concentrations of natural colloids in ground water range from about 1 ppb as reported by Apps and others (1983) for undisturbed ground water to 200 ppb for clear sea water (Yariv and Cross, 1979). Average concentrations of humic colloidal material are estimated to range from 3 to 45 ppb in major rivers in the United States (Yariv and Cross, 1979).

7.2.2 External Surface Adsorption

An upper bound to the adsorption capacity of monodisperse pseudocolloid suspensions for radionuclides was estimated by simple external surface-adsorption calculations and by consideration of the cation exchange capacity (CEC) of clay minerals. In the surface-adsorption calculations, the maximum adsorption of radionuclides with 1 Angstrom diameter was calculated for spherical particles. The number of radionuclide atoms per sphere was calculated for a variety of colloid sizes and the total concentration of radionuclide per cubic centimeter of ground water was calculated for a range of colloid concentrations. The results are presented in Figure 13. A detailed description of the calculations, the raw data, and the computer code used in the calculations are found in Appendix C.

The radionuclides considered are: ^{241}Am , ^{237}Np , ^{239}Pu , ^{226}Ra , ^{99}Tc , and ^{235}U . The estimated colloid concentrations in these parametric calculations ranged from 1 to 500 ppb and particle sizes were 10, 100, and 1000 nm. Radionuclide concentrations are expressed as Ci/m³ and are compared to the NRC Maximum Permissible Concentration (MPC) limits for soluble radionuclides (NRC, 1988) which have also been converted to units of Ci/m³. The NRC Rule 10CFR20 does not classify colloids as either "soluble" or "insoluble." Material that passes through a filter with a nominal opening of 450 nm is often classified as "dissolved" or "soluble." Thus, the colloid size range considered here spans the range for both dissolved and particulate matter. The conclusions reached in this section are conservative because the radionuclide concentrations associated with the

colloids have been compared to the more restrictive limit for "soluble" radionuclides. The comparison of the radionuclide concentration to the MPC in drinking water gave the following results. ^{237}Np , ^{99}Tc , and ^{235}U show the least hazard. For a colloid diameter of 1000 nm, the radionuclide concentration does not exceed the MPC. For a colloid diameter of 10 nm, the MPC is exceeded for colloid concentrations of 25 ppb and above. For a colloid diameter of 100 nm, each radionuclide exceeds the MPC at some colloid concentration but that concentration differs for the different radionuclides. ^{230}Th and ^{238}Pu concentrations exceed the MPC for colloid diameters of 10 and 100 nm and for 1000 nm if the colloid concentration is 25 ppb or higher. ^{241}Am and ^{226}Ra concentrations exceed the MPC for all colloid diameters and concentrations. Thus, naturally occurring colloids cannot be easily ruled out as a transport factor in geologic repositories.

Table 12 shows the relationships between colloid size, concentration and other physical properties. At a given concentration of colloids (mass/mass), the surface area of a collection of small particles will be larger than that of a collection of larger particles. Figure 13 shows that particle surface area plays an important role while colloid concentration is not quite as sensitive over the parameter ranges studied. It is important to note the actual surface area of a swelling clay would be larger than that calculated for these idealized spheres in Table 12 and the Figure 13.

7.2.3 Adsorption by Cation Exchange

In the second set of calculations, the maximum radioactivity that could be carried by colloids was estimated from the cation exchange capacity (CEC) of secondary minerals. In soil science and geology, CEC is measured by the uptake and release of ammonium ions from 1 M ammonium acetate at pH 7.0. Reported CECs for representative clay minerals and zeolites are listed in Table 13. The calculations of maximum radionuclide capacity are described below.

Calculation:

^{239}Pu radiation level on zeolite with maximum CEC.

Zeolite: Assume 530 meq/100#g = 5.3×10^{-3} eq/g = 5.3×10^{-3} g mole
 (CEC atoms/g) $5.3 \times 10^{-3} \times 6.023 \times 10^{23} = 3.2 \times 10^{21}$ atoms/g

Assuming a mononuclear singly charged cation, 3.2×10^{21} atoms/g is the concentration of a radionuclide in atoms/gram of colloid. For multivalent cations, we divide by the total charge to determine the number of nuclei or atoms/gram of colloid. For tetravalent ^{239}Pu the CEC is reduced to 0.8×10^{21} atoms/gram. Next, the mass concentration is converted to atoms/cc of solution using an assumed concentration for the colloids. For a solution concentration of 100 ppb, equivalent concentrations of 8×10^{23} atoms/cc and 2.3×10^{-3} Ci/m³ can be calculated for ^{239}Pu ($t_{1/2} = 2.4 \times 10^4$ yr). The MPC for soluble ^{239}Pu is 5×10^{-6} Ci/m³ which is more than 2 orders of magnitude lower than the maximum colloid capacity calculated with this method.

Table 12

Colloid Concentrations and Size Effects*

Colloid Size Colloid Concentration	1 nm 50×10^{-9} g/ml	10 nm 50×10^{-9} g/ml	1000 nm 50×10^{-9} g/ml	10 nm 1×10^{-9} g/ml	10 nm 10×10^{-9} g/ml
Total Colloid Surface Area (cm^2/ml)	1.3	0.13	0.0013	0.0026	0.026
Conc. of Nuclei (moles/ml)	6.9×10^{-9}	4.6×10^{-10}	4.6×10^{-12}	9.1×10^{-12}	9.1×10^{-11}
Number of Colloids No./ml	4.2×10^{13}	4.2×10^{10}	4.2×10^4	8.3×10^9	8.3×10^8
Size Dependent Effects (Single Colloid)					
Mass of a Colloid (g)	1.2×10^{-21}	1.2×10^{-18}	1.2×10^{-12}		
Surface Area cm^2	3.1×10^{-14}	3.1×10^{-12}	3.1×10^{-8}		
No. of Nuclei/ Colloid	67	6700	6.7×10^7		

*Assumed colloid density = 2.3 g/cc; diameter of radionuclides = 0.2 nm.

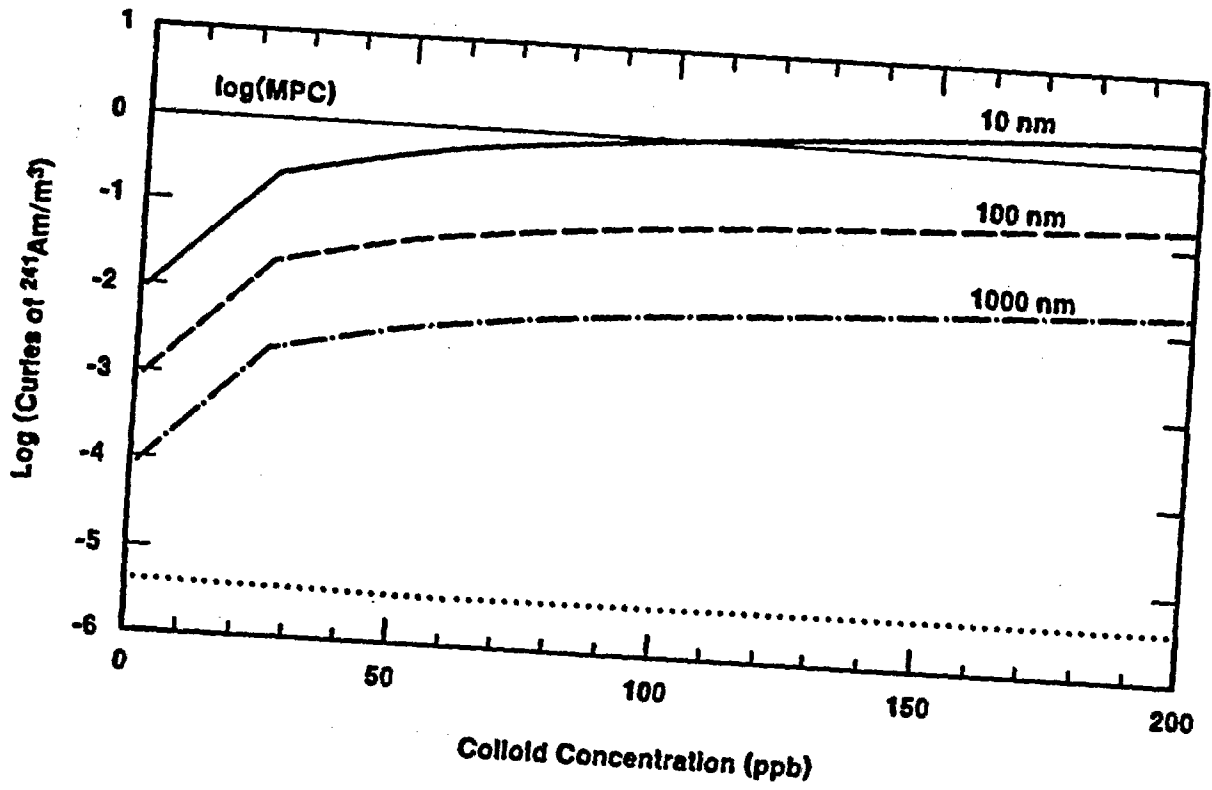


Figure 13a. Colloid Radiation Levels for ^{241}Am

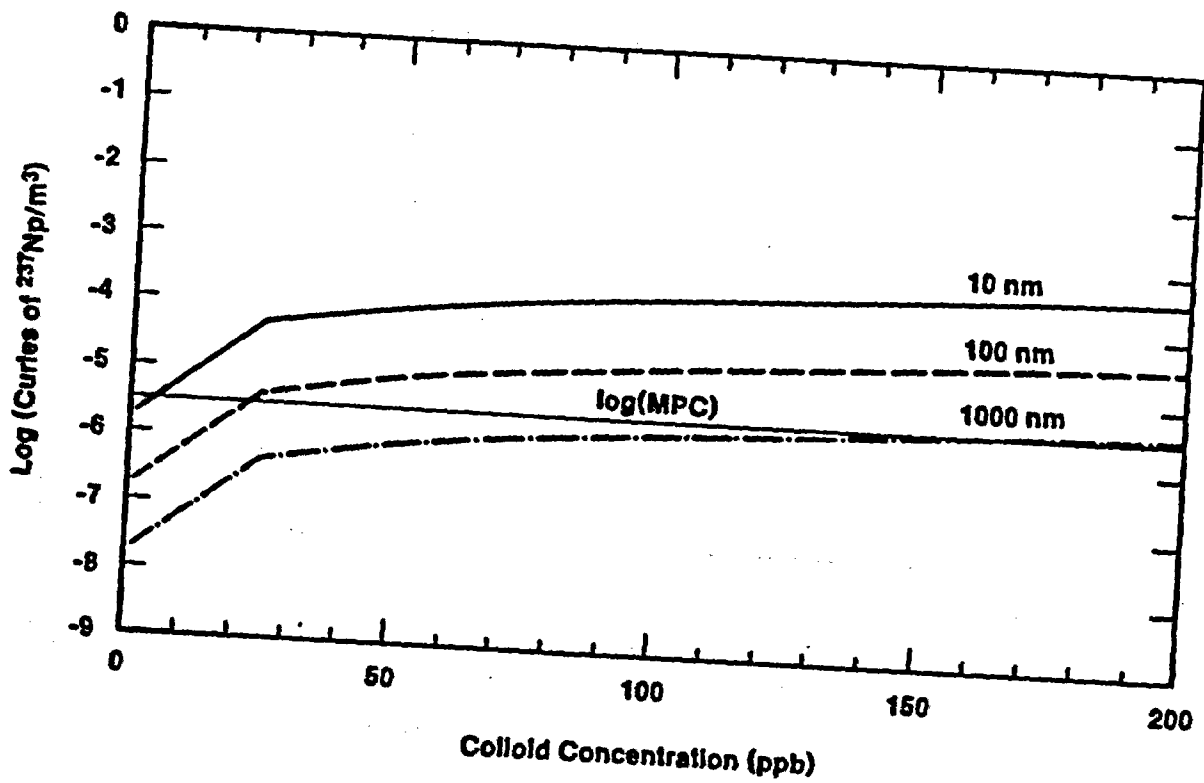


Figure 13b. Colloid Radiation Levels for ^{237}Np

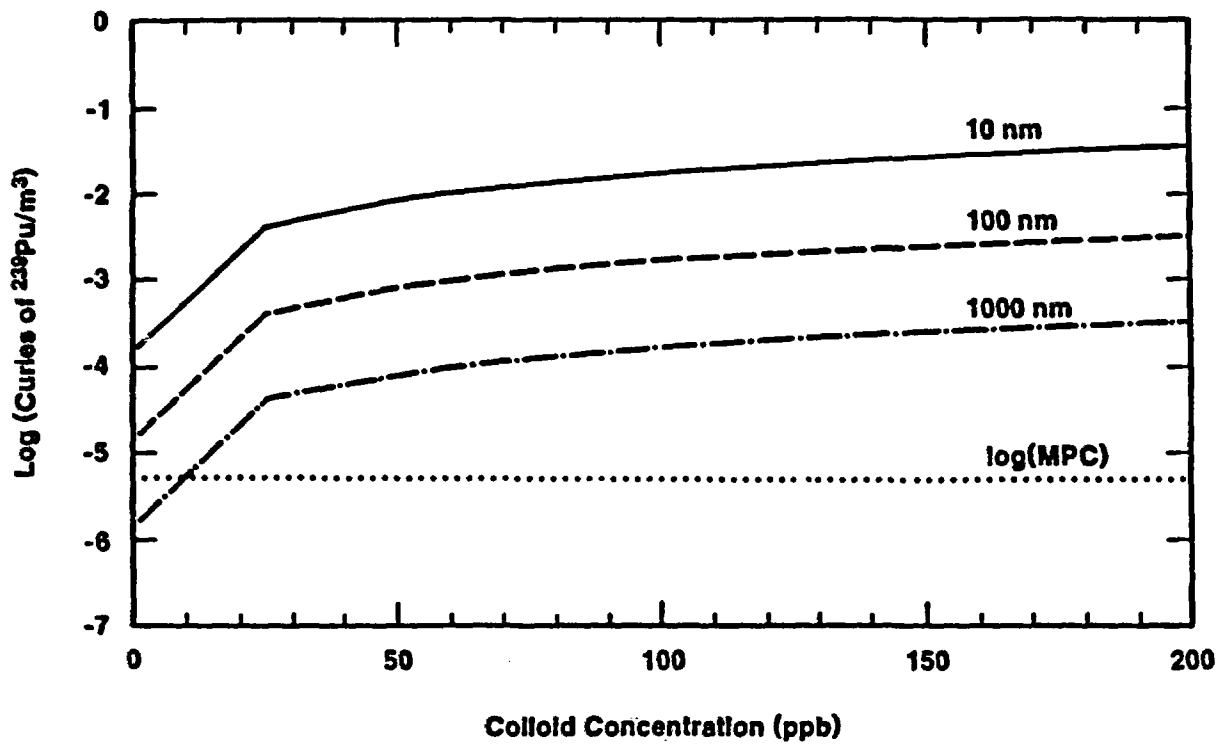


Figure 13c. Colloid Radiation Levels for ^{239}Pu

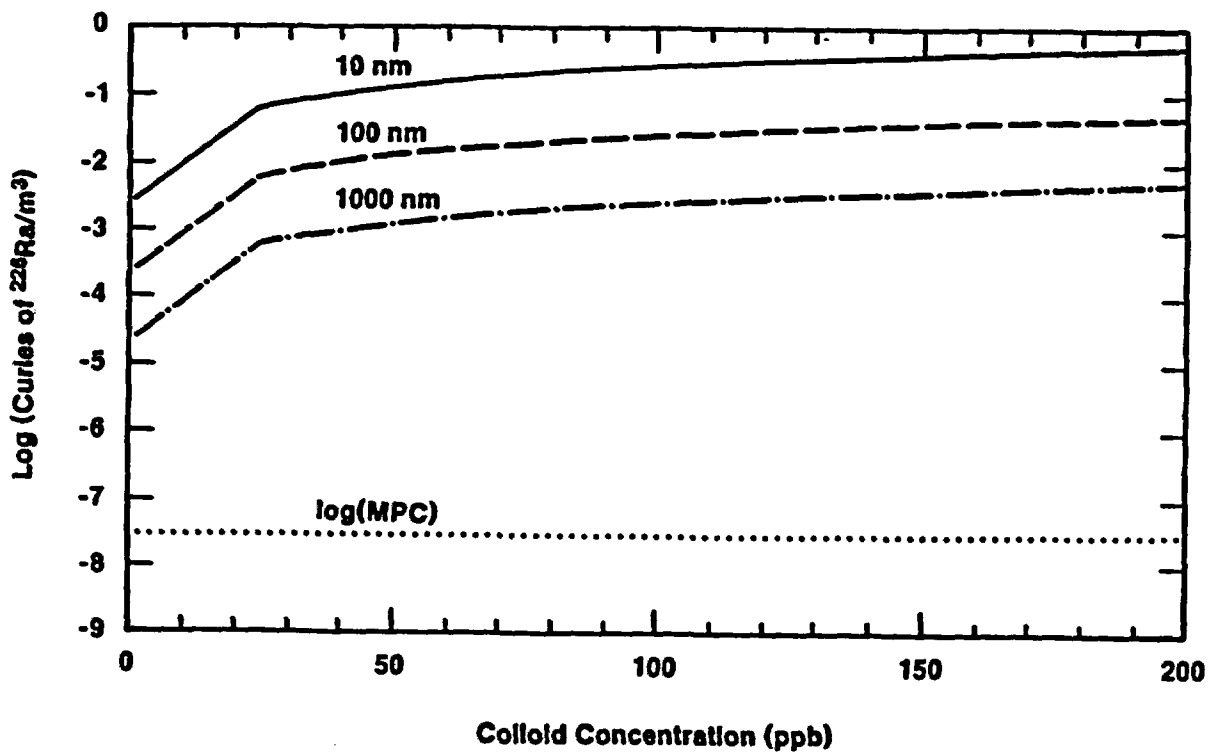


Figure 13d. Colloid Radiation Levels for ^{226}Ra

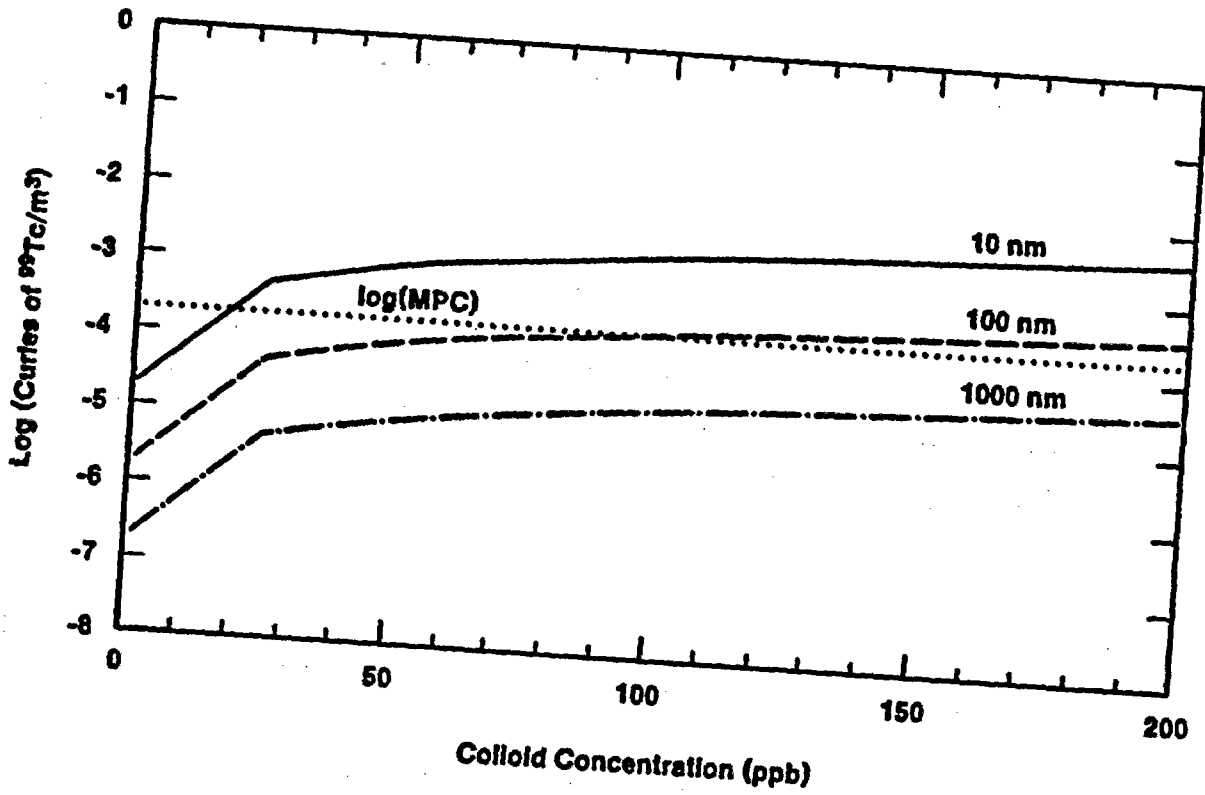


Figure 13e. Colloid Radiation Levels for ^{99}Tc

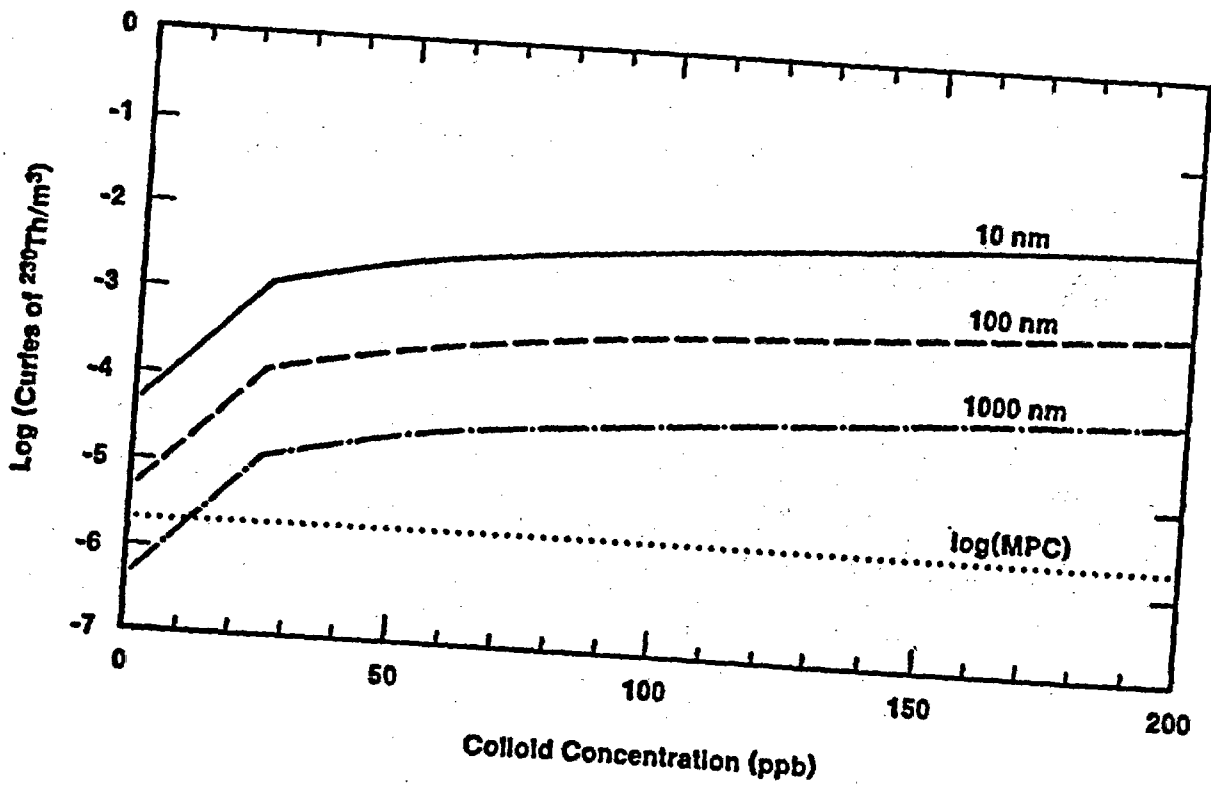


Figure 13f. Colloid Radiation Levels for ^{230}Th

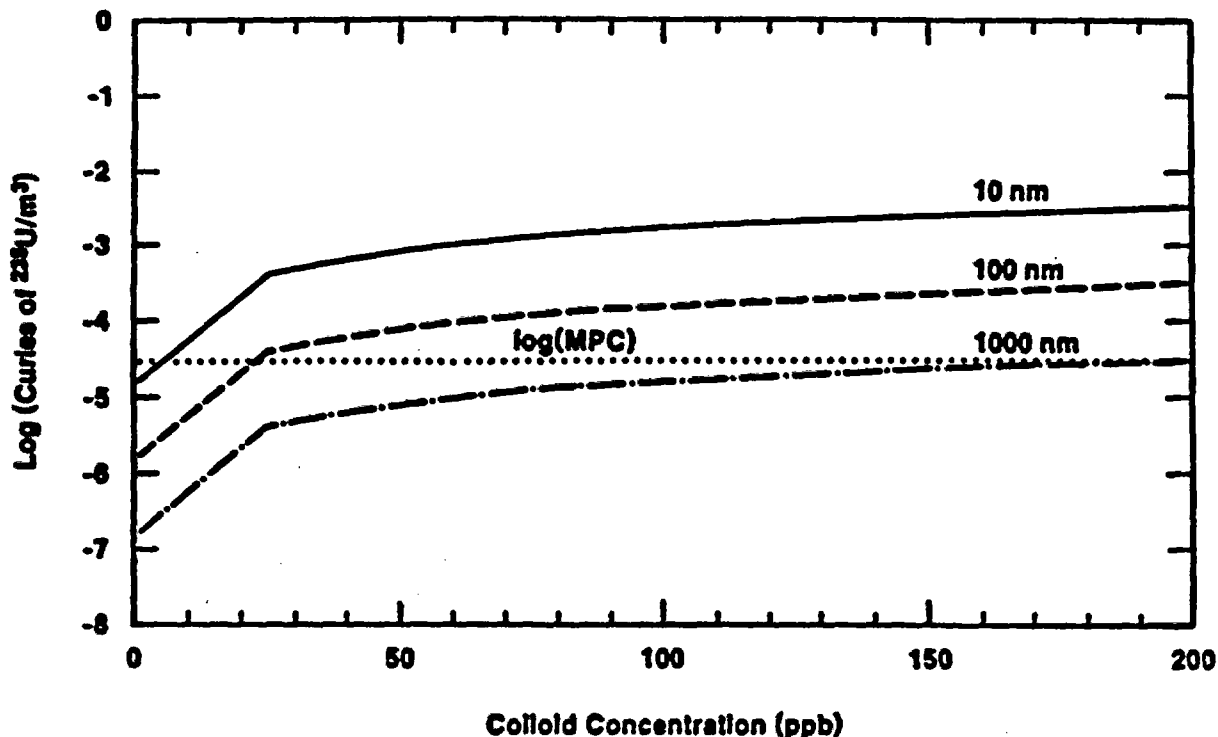


Figure 13g. Colloid Radiation Levels for ^{235}U

The value $2 \times 10^{-3} \text{ Ci/m}^3$ is nearly equal to that calculated by the surface area method ($1.2 \times 10^{-3} \text{ Ci/m}^3$) for 100-nm colloids at 100 ppb concentration. Thus, both sets of worst-case calculations indicate that natural colloids in moderate concentrations could carry significant concentrations of radionuclides if they are not retained by interactions with the rock matrix.

It must be emphasized that these calculations are preliminary and it should not be inferred that the results represent the actual capacity of colloids to transport radionuclides. The results show an attempt to estimate a worst-case upper bound for the radionuclide-carrying capacity of pseudocolloids. Future work in this area would best be focused on an examination of the relationship between the calculated radionuclide concentration and integrated radionuclide discharge. Attempts to calculate more realistic radionuclide capacities for natural materials under site-specific conditions would also be of benefit. Both empirical radionuclide-specific conditions sorption ratios (K_d or R_d) and theoretical models could be used in support of the latter objective. Although reliable data on colloid concentration and size distribution in waters at potential HLW repository sites are currently unavailable, such information should be incorporated into the analysis as they are obtained.

7.3 Production of Radiocolloids by Homogeneous and Heterogeneous Nucleation

One of the processes included in the colloid release scenario depicted in Figure 10 is the production of colloids by precipitation. This mechanism

Table 13

Cation Exchange Capacities for Clays and Zeolites

<u>Mineral</u>	<u>CEC meq/100g</u>	<u>Source</u>
Smectite	80-150	Drever (1982)
Vermiculite	120-200	Drever (1982)
Illite	10-40	Drever (1982)
Kaolinite	1-10	Drever (1982)
Chlorite	10	Drever (1981)
Zeolite	170-530	Daniels and others (1982)
Clinoptilolite	230	Daniels and others (1982)
Mordenite	230	Daniels and others (1982)
Analcime	450	Daniels and others (1982)
Montmorillonite	117	Daniels and others (1982)
Heulandite	330	Daniels and others (1982)

may be important if ground water becomes locally supersaturated with respect to a radionuclide-bearing solid phase due to sharp changes in flow rate, temperature, or fluid composition. An attempt was made to estimate an upper bound for this type of colloid formation through a review of experimental data describing nucleation and growth rates measured in crystallizers. The methods used to analyze available data are summarized below.

Nucleation and growth-rate data can be obtained from Crystal Size Distribution (CSD) diagrams. A CSD is a plot of crystal population, n (no./ μ -cc), versus crystal size, L (microns). At steady state, the CSD is a straight line which is extrapolated to zero size to find the nuclei population, n_0 , and a slope $1/TG$, where T is the residence time and G is the size independent growth rate (Mullin, 1972).

Data for CSD diagrams can be obtained from Continuous Mixed Suspension Product Removal Crystallizers (CMSMPR) (Larson and Randolph, 1969; Randolph and Larson, 1971). In these experiments, a cool solution of constant composition is fed into a warmer, well-stirred vessel and crystallization occurs due to supersaturation. The effect of temperature, agitation rate, solids concentration, seed size and geometry, and degree of supersaturation can be examined in these experiments.

The solution to the steady-state population balance for a CMSMPR crystallizer can be described by:

$$n = n_0 \exp(-L/TG) \quad (7.3)$$

where

- L - particle size (microns)
- T - (V/Q) residence time (s)
- Q - volumetric flow rate (cm³/s)
- V - suspension volume (cm³)
- G - (dL/dt) size-independent growth rate (micron/s)
- N - number of crystals
- n - crystal population (no./micron-cm³)
- n_o - (dN/dL)|_{L=0} nuclei population (no./cm³).

The nucleation rate B_o (no./cm³-s) is:

$$B_o = \left. \frac{dN}{dL} \right|_{L=0} \frac{dL}{dt} = n_o G \quad (7.4)$$

No data for radionuclide-bearing solids have been found in the literature. A preliminary analysis of experimental data has been carried out for studies of potassium sulfate (Cise, 1971), aluminum trihydroxide (Misra and White, 1971) ammonium alum, sodium chloride and ammonium sulfate (Randolph and Larson, 1971). Nucleation rates ranging from 300 to 30,000 particles/cc-min were obtained. Growth rates of 15 to 80 nm/s were calculated from the same data.

These rates should be higher than those expected in HLW repositories for several reasons. The crystallization experiments were performed at agitation rates much higher than those expected in geologic media. Cise's data (1971) show that increasing the impeller stirring rate increases the nucleation rate. Secondary nucleation occurs when the impeller breaks crystals, and this is not expected in geologic media. In addition, crystallizer agitation decreases the film thickness of the nucleus and increases the diffusion rate to the surface of the nucleus. Therefore, crystals should grow faster in a crystallizer than in geologic media.

At present, it cannot be rigorously established that these data are upper bounds for colloid formation rates at HLW repositories. Nucleation and growth rates are dependent upon the degree of supersaturation, residence time, temperature, and flow rate in a complex manner, (Misra and White, 1971; Koros and others, 1972; Randolph and Larson, 1971, Larson and Randolph, 1969; Cise, 1971). Crystallizer data which can be extrapolated to conditions similar to those anticipated in geologic media would be necessary to substantiate these rate data as upper bounds for performance assessment calculations.

8. CONCLUSIONS

Performance assessment requires calculating radionuclide discharge for many sets of conditions and scenarios. In general, such calculations use empirical retardation factors that describe the combined effect of all radionuclide/fluid/rock interactions. This method, however, may underestimate radionuclide discharges and disguise potential violations of regulatory standards. An alternative approach, coupled reaction-transport models, can be used to obtain a detailed understanding of physiochemical phenomena but the general application of such rigorous models may be impractical in risk assessment. In the Geochemical Sensitivity Analysis project, methods are being developed to identify conditions where chemical-speciation reactions, nonlinear or irreversible sorption, and colloidal transport can significantly affect calculated radionuclide discharges. The results of this study can be used to determine when complex phenomenological models (chemical-transport simulators) are truly required for risk assessments.

Critical reviews of data for use with mathematical models of chemical equilibrium, sorption and transport were described in this report. The results of these reviews are found in two computerized data management systems: the Aqueous Solutions Database (ASD) and the Sandia Sorption Data Management System (SSDMS). The ASD contains basic thermochemical data that can be used to calculate the chemical speciation and the extent of sorption in model systems. It uses the DATATRIEVE system and is accessible via telephone on the VAX cluster at Lawrence Berkeley Laboratories. Two computer codes, MINEQL and PHREEQE, were identified as candidates for calculating equilibrium speciations for the systems that are expected at HLW sites. It is intended that interfaces between these codes and the data management systems described above will be developed.

The SSDMS contains descriptions of batch sorption (K_d) experiments. It uses the dBASE III data base system for personal computers and is available in floppy disks from the Nuclear Regulatory Commission. The process of maintaining, updating and developing these databases is continuing both at SNLA and at LBL.

The possibility of including coupled transport and chemical effects in performance assessment calculations was examined using the TRANQL code. The computational efficiency of TRANQL was examined in this study. It was concluded that although rigorous coupled calculations can be used to provide insight into the mechanisms and key chemical parameters involved in radionuclide transport, use of the TRANQL code will not be practical in performance assessments. Future work should be directed toward the development of retardation factors that bound the coupled transport-speciation effects and improve the efficiency of codes like TRANQL.

Parametric calculations designed to examine the effect of homogeneous reaction rates on radionuclide discharge were presented. A case where a sorbing species A is converted to a nonsorbing species B was studied. Assuming that the reaction from A to B involves first-order kinetics and that the transport rate of each species can be calculated from a retardation factor multiplied by the water velocity, equations for the integrated

radionuclide discharge were presented. By setting the integrated radionuclide discharge equal to the release limits in the EPA Standard 40 Part CFR 191, and varying the retardation factors for the radionuclides, the radionuclide source term, and hydrological data, a minimum chemical stability needed for radionuclide species to comply with the EPA Standard can be identified and compared to the radionuclide chemical stability observed in laboratory studies. The analysis could be used to determine the criteria for experiments designed to quantitatively observe the effect of important chemical speciation reactions. The results can be used by regulatory agencies to prioritize research needs and to evaluate published or ongoing radionuclide transport studies.

Criteria for the application of three approximate models for radionuclide transport in fractured porous rock were presented. The three models considered are the equivalent porous-medium approximation, the linear-driving-force approximation, and the semi-infinite-medium approximation. These numerical criteria are calculated from measureable geochemical and hydrological parameters. Site-specific data for tuff and granite were used with the above criteria. Results indicate that for tuff, the porous-medium approximation usually should be valid even for relatively thin beds ($x = 30$ m), and that the linear-driving-force or semi-infinite medium approaches are necessary only for extreme parameter values. For granite, the semi-infinite-medium or linear-driving-force approaches may be required, while the porous-medium approximation may be applicable only to relatively large granitic bodies.

The effect of the presence of colloids in natural ground waters on radionuclide transport was investigated as part of this study. Results of calculations of the movement of colloids along a fracture, the potential for colloidal suspensions to transport adsorbed radionuclides, and the formation of colloids by nucleation were presented. Radionuclide concentrations adsorbed to hypothetical colloidal suspensions were compared to the Maximum Permissible Concentration (MPC) in drinking water. The parametric calculations gave the following results: ^{237}Np , ^{99}Tc , and ^{235}U show the least hazard while ^{241}Am and ^{226}Ra concentrations exceed the MPC for all colloid diameters and concentrations. For a colloid diameter of 100 nm, each radionuclide examined exceeds the MPC at a unique suspension concentration. ^{230}Th and ^{239}Pu concentrations exceed the MPC for colloid diameters of 10 and 100 nm and for 1000 nm if the colloid concentration is 25 ppb or higher. Thus, sorption of radionuclides on naturally occurring colloids cannot be easily ruled out as a transport factor in geologic repositories.

References

- Adamczyk, A., and van de Ven, T. G. M., 1981, "Deposition of Particles Under External Forces in Laminar Flow Through Parallel-Plate and Cylindrical Channels," J. Colloid Interface Sci., Vol. 80, 340-356 (1981).
- Apps, J. A., Carnahan, C. L., Lichtner, P. C., Michael, M. C., Perry, D., Silva, R. J., Weres, O., and White, A. F., Status of Geochemical Problems Relating to the Burial of High-Level Radioactive Waste, Lawrence Berkeley Laboratory, Berkeley, CA, NUREG/CR-3062, LBL-15103, 1983.
- Ashton-Tate, dBASE III User Manual, Ashton-Tate, 1984.
- Baes, C. F., and Mesmer, R. E., The Hydrolysis of Cations, (NY: John Wiley & Sons, Inc., 1976).
- Birgersson, L., and Neretnieks, I., Diffusion in the Matrix of Granitic Rock: Field Test in the Stripa Mine, Part 2, The Scientific Basis for Nuclear Waste Management, Vol. 6. G. McVay, ed., (NY: Elsevier, 1984), pp. 247-254.
- Bonano, E. J., and Beyeler, W., "Computer Program to Implement Solution of Conservation Equation for Colloids in Single Fractures," in Geochemical Sensitivity Analysis, Letter Report to the U.S. Nuclear Regulatory Commission, FIN A-1756, Progress Report for Fiscal Year 1984.
- Bonano, E. J., Davis, P. A., Shippers, L. R., Brinster, K. F., Beyeler, W. B., Updegraff, C. D., Shepard, E. R., Tilton, L. M., Wahi, K. K., 1988, Demonstration of a Performance Assessment Methodology for High-Level Radioactive Waste Disposal in Basalt Formations, Sandia National Laboratories, Albuquerque, NM, SAND86-2325, NUREG/CR-4759, June 1989.
- Bonano, E. J., Nuttall, H. E., and Siegel, M. D., 1984, Review of the Physical Phenomena and Population Balance for Radioactive Colloid Transport, Letter Report, Sandia National Laboratories, Albuquerque, NM.
- Bonano, E. J., and Beyeler, W. E., 1985, "Transport and Capture of Colloidal Particles in Single Fractures," Scientific Basis for Waste Management, Vol. 8, C. M. Jantzen and others, ed., Materials Research Society, PN, pp. 385-394.
- Bryant, E. A., and Vaniman, D. T., Research and Development Related to the Nevada Nuclear Waste Storage Investigations, July 1 - September 30, 1983, Los Alamos National Laboratory, Los Alamos, NM, LA-100006-PR, 1984.
- Carlsson, L., Winberg, A., and Rosander, B., Investigations of Hydraulic Properties in Crystalline Rock, The Scientific Basis for Nuclear Waste Management, Vol. 6, G. McVay, ed., (NY: Elsevier, 1984), pp. 255-267.

Campbell, J. E., Longsine, D. E., and Cranwell, R. M., Risk Methodology for Geologic Disposal of Radioactive Waste: The NWFT/DVM Computer Code Users Manual, Sandia National Laboratories, SAND81-0886, NUREG/CR-2081, November 1981.

Cederberg, G. A., and Street, R. L., "A General Numerical Algorithm for Modeling the Transport of Solutes in a Multicomponent System," Amer. Geophys. Union Trans., Vol. 66, p. 172 (1985).

Cederberg, G. A., TRANQL: A Ground-Water Mass-Transport and Equilibrium Chemistry Model for Multicomponent Systems, Ph.D. Dissertation, Stanford University, 1985a.

Cederberg, G. A., "The Effects of Geochemical Processes on the Transport of Contaminants in Multicomponent Systems: A Modeling Perspective," International Symposium on Coupled Processes Affecting the Performance of a Nuclear Waste Repository, Lawrence Berkeley Laboratory, Berkeley, CA, 1985b.

Champ, D. R., Merritt, W. E., and Young, J. L., "Potential for the Rapid Transport of Plutonium in Groundwater as Demonstrated by Core Column Studies," Scientific Basis for Nuclear Waste Management, Vol. 5, W. Lutze, ed., (North-Holland, 1982) pp. 745-754.

Cise, M. D., Crystal Growth and Nucleation Kinetics of the Potassium Sulfate System in a Continuous-Flow, Seeded Crystallizer, Ph.D. Dissertation, University of Arizona, 1971.

CODATA Task Group on Key Values for Thermodynamics: CODATA Recommended Key Values for Thermodynamics 1977, CODATA Bulletin 28, CODATA Secretariat, 51 Boulevard de Montmorency, 75016 Paris France (April 1978).

Daniels, W. R., et al., Summary Report on the Geochemistry of Yucca Mountain and Environs, Los Alamos National Laboratory, Los Alamos, NM, LA-9328-MS, 1982.

Davis, J. A., Adsorption of Trace Metals and Complexing Ligands at the Oxide/Water Interface, Ph.D. Dissertation, Stanford University, 1977.

DEC, VAX DATATRIEVE Handbook, (Maynard, Massachusetts: Digital Equipment Corporation, September 1984), Order No. AA-W675A-TE.

DOE, Draft Environmental Assessment Reference Repository Location, Hanford Site, Washington, U.S. Department of Energy, Office of Civilian Radioactive Waste Management, DOE/RW-0017, 1984.

Drever, James I., The Geochemistry of Natural Waters, (NJ: Prentice Hall, 1982) pp. 79-82.

Eicholz, G. G., Wahlig, B., Powell, G., and Craft, T. F., "Subsurface Migration of Radioactive Waste Materials by Particulate Transport," Nuclear Technology, Vol. 58, pp. 511-520 (1982).

Eicholz, G. G., and Craft, T. F., Role of Particulates in Subsurface Migration of Wastes, IAEA Symp. Knoxville, SM257/73, 1981, pp. 541-555.

Erickson, K. L., "Approximations for Adapting Porous Media Radionuclide Transport Models to Analyses of Transport in Jointed, Porous Rock," The Scientific Basis for Nuclear Waste Management, Vol. 5, D. Brookins, ed., (NY: Elsevier, 1983) pp. 473-480.

Erickson, K. L., Chu, M. S. Y., Siegel, M. D., and Beyler, W., "Approximate Methods to Calculate Radionuclide Discharges for Performance Assessment of HLW Repositories in Fractured Rock," in Waste Management 86, ol. 2, R. G. Post ed., (Tucson, AZ: University of Arizona, 1986) pp. 377-386.

Guzowski, R. V., Nimick, F. B., Siegel, M. D., and Finley, N. C., Repository Site Data Report for Tuff: Yucca Mountain Nevada, Sandia National Laboratories, Albuquerque, NM, NUREG/CR-2937, SAND82-2105, 1983.

Guzy, C. J., Bonano, E. J., and E. J. Davis, "The Analysis of Flow and Colloidal Particle Retention in Fibrous Porous Media," J. Colloid Interface Sci., Vol. 95, 523, (1983).

JANAF Thermochemical Tables 2 ed., National Technical Information Services, 1971.

Kent, D., Tripathi, V. J., and Lecki, J. O., Surface Complexation Modeling of Radionuclide Adsorption in Subsurface Environments, Sandia National Laboratories, SAND86-7175, NUREG/CR-4807, March 1988.

Koros, W. J., et al., American Institute of Chemical Engineers. Symposium Series, Vol. 68 (121), 1972.

Larson, M. A., and Randolph, A. D., Chemical Engineering Progress Symposium Series, Vol. 65 (95), 1969.

Lemire, R. J., An Assessment of the Thermodynamic Behavior of Neptunium in Water and Model Groundwaters from 25 to 150 C, Atomic Energy of Canada, Ltd., Pinawa, Manitoba, Canada, AECL-7817, 1984.

Lemire, R. J., and Tremaine, P. R., "Uranium and Plutonium Equilibrium in Aqueous Solutions to 200 C," Jour. Chem. Engin. Data, Vol. 25, pp. 361-370, (1980).

Long, P. E., Characterization and Recognition of Interflow Structure, Grande Rhonde Basalt, Rockwell Hanford Operations, RHO-BWI-LD-10, 1978.

Longsine, D. E., Bonano, E. J., and Harlan, C. P., 1987, User's Manual for the NEFTRAN Computer Code, Sandia National Laboratories, SAND86-2405, NUREG/CR-4766, September 1987.

Misra, C., and White, E. T., Chemical Engineering Progress Symposium Series, Vol. 67 (110), 1971.

- Muller, A. B., and Duda, L. E., 1982, "The Influence and Modeling of Waste Nuclide Aqueous Speciation on Geosphere Retardation Processes Relevant to Risk Assessment," Waste Management '82, Vol. 1, R. G. Post ed., Am. Nuc. Soc. Symposium on Waste Management, Tucson, 1982.
- Mullin, J. W., Crystallization, (Butterworth & Co., 1972).
- Naumov, G. B., Rhzhenko, B. N., and Khodakovsky, I. L., 1974, Handbook of Thermodynamic Data, Translated by G. J. Soleimani, U.S. Geological Survey, Menlo Park, CA 94025, PB-226-722, National Technical Information Service, Springfield, VA.
- Neretnieks, I., "Diffusion in the Rock Matrix: An Important Factor in Radionuclide Retardation?" Jour. Geophys. Res., Vol. 85, pp. 4379-4397, (1980).
- NRC, "Standards for Protection Against Radiation," U.S. Nuclear Regulatory Commission, Washington, DC, 10 CFR, Part 20, Title 10, Code of Federal Regulations, 1988, p.264.
- Parker, V. B., Thermal Properties of Aqueous Uni-univalent Electrolytes, National Bureau of Standards, Gaithersburg, MD, NSRDS-NBS 2, 1965.
- Parkhurst, D. L., Thorenstenson, D. C., Plummer, L. N., 1980, PHREEQE-a Computer Program for Geochemical Calculations, 80-96, U.S. Geological Survey, Reston, VA 22092.
- Pepping, R. E., Chu, M. S., and Siegel, M. D., 1983, Technical Assistance for Regulatory Development: Review and Evaluation of the Draft EPA Standard 40CFR191 for Disposal of High-Level Waste, Volume 4. A Simplified Analysis of a Hypothetical Repository in a Bedded Salt Formation, Sandia National Laboratories, NUREG/CR-3235, (April 1983).
- Pinder, G. F., and Gray, W. G., Finite Element Simulation in Surface and Subsurface Hydrology, (NY: Academic Press, 1977).
- Phillips, S. L., Thermodynamic Data for Nuclear Waste Disposal: Overview of Available Data and Criteria for Selection of Data, Lawrence Berkeley Laboratory, Berkeley, CA, LBID-977, 1984.
- Phillips, S. L., Phillips, C. A., and Skeen, J., Hydrolysis, Formation and Ionization Constants at 25° C and at High Temperature-High Ionic Strength, Lawrence Berkeley Laboratory, Berkeley, CA, LBL-14996, 1985.
- Phillips, S. L., Hale, F. V., Silvester, L. F., and Siegel, M. D., Thermodynamic Tables for Nuclear Waste Isolation, Vol. I. Aqueous Solutions Database, Lawrence Berkeley Laboratory, Berkeley, CA, SAND87-0323, NUREG/CR-4864, LBL-22860, 1988.
- Pytkowicz, R. M., ed., Activity Coefficients in Electrolyte Solutions: Volumes 1 and 2, (CRC Press, Inc., 1979).

Randolph, A. D., and Larson, M. A., Theory of Particulate Processes, (NY: Academic Press, 1971).

Salter, P. F., and Jacob, G. K., BWIP Data Package for Reference Solubility and Kd Values, Rockwell Hanford Operations Rept., SD-BWI-DP-001, 1983.

Siegel, M. D., and Chu, M. S., Technical Assistance for Regulatory Development. Review and Evaluation of the Draft EPA Standard 40CFR191 for Disposal of High-Level Waste. Volume 3: Simplified Analysis of a Hypothetical Repository in a Tuff Formation, Sandia National Laboratories, Albuquerque, NM, NUREG/CR-3230, 1983.

Siegel, M. D., Erickson, K. L., and Vopicka, D. A., 1984a, Letter Report on "Geochemical Sensitivity Analysis: I. Radioelement Speciation; Identification of Conditions and Criteria for Design of Transport Experiments When Radioelement Speciation Must Be Considered in High-Level Waste Repository Risk Assessment," Sandia National Laboratories, December 1984.

Siegel, M. D., and Erickson, K. L., "Radionuclide Releases From a Hypothetical Nuclear Waste Repository: Potential Violations of the Proposed EPA Standard by Radionuclides with Multiple Aqueous Species," Waste Management 84, Vol. 1, R. G. Post, ed., (Tucson, AZ: University of Arizona, 1984b).

Siegel, M. D., and Erickson, K. L., 1986, "Geochemical Sensitivity Analysis for Performance Assessment of HLW Repositories: Effects of Speciation and Matrix Diffusion," in Proceedings of the Symposium on Groundwater Flow and Transport Modeling for Performance Assessment of Deep Geologic Disposal of Radioactive Waste: A Critical Evaluation of the State of the Art, NUREG/CP-0079, PNL-SA-13796, pp. 467-490.

Smith, R. M., and Martell, A. E., Critical Stability Constants, Vol. 4: Inorganic Complexes, (NY: Plenum Press, 1976).

Stumm, W., and Morgan, J. J., Aquatic Chemistry, (NY: Wiley-Interscience, 1981).

Tien, P., Siegel, M. D., Guzowski, R., and others, Repository Site Data for Unsaturated Tuff, Yucca Mountain, Sandia National Laboratories, Albuquerque, NM, SAND85-2668, NUREG/CR-4110, 1985.

Tripathi, V. W., Yeh, G. T., and Siegel, M. D., "A Benchmark in Portable Fortran: Speeds of CPU and In-Memory Data Transfer Operations for Hydrogeochemical Models," Computers in the Geosciences, Vol. 13, No. 4, pp. 405-408, (1987).

Valocchi, A. J., Street, R. L., and Roberts, P. V., "Transport of Ion-Exchanging Solutes in Groundwater: Chromatographic Theory and Field Simulation," Water Resour. Res., 17(5), pp. 1517-1527, (1981).

Westall, J. C., Zachary, J. L., and Morel, F. M. M., MINEOL--A Computer Program for the Calculations of Chemical Equilibrium Composition of Aqueous Systems, Tech. Note 18, Water Qual. Lab., R. M. Parsons Lab. Water Resour. Environ. Eng., Dep. Civil Eng., Mass. Inst. Technol., Cambridge, MA, 1976.

Westall, J., MICROOL: I. A Chemical Equilibrium Program in BASIC, EAWAG, Swiss Federal Institute of Technology, Duebendorf, Switzerland, 1979.

WISP, Waste Isolation Systems Panel, A Study of the Isolation System for Geologic Disposal of Radioactive Wastes, National Research Council, (National Academy Press, 1983).

Wolfsberg, K., Vaniman, D. T., and Ogard, A. E., Research and Development Related to the Nevada Nuclear Waste Storage Investigations, January 1 - March 31, 1983, LANL 9793-PR, Los Alamos National Laboratory, Los Alamos, NM, 1983.

Yariv, S., and Cross, H., Geochemistry of Colloid Systems for Earth Scientists, (NY: Springer-Verlag, 1979).

APPENDIX A

Annotated Bibliography of Available Compilations of Thermochemical Data for Actinides and Fission Products

Compilations described in this section are those having critically evaluated data. To a large extent, these compilations contain new data; they are rich in references to the research literature, thereby giving direct links to the sources of their data; and, they are authoritative. Each compilation is referenced in research publications and other reports, attesting to significant use by scientists and engineers. Finally, publication of the compilation represents a major effort on the part of the professional staff involved in the work.

References to publications of the compilations are found in the Literature Cited section, appended to the end of this appendix. Note that the original nomenclature used in the cited reference has been used in each review. Thus, for example, the equivalent terms $H^\circ(T)-H^\circ(298)$ and $H^\circ-H^\circ_{298}$ are used in References 6 and 7 respectively.

CODATA Recommended Key Values for Thermodynamics, 1977

Reference 1

These key values were selected by a Task Group chaired by J. D. Cox, National Physical Laboratory, Teddington, England. Values for enthalpy of formation, entropy, and $H^\circ(298.15)-H^\circ(0)$ are tabulated for over 100 substances at 25°C and zero ionic strength. Included are data on tin, lead, thorium, and cesium. Only a few substances for each metal are covered; for example, $Pb(cr)$, $Pb(g)$, Pb^{2+} , and $PbSO_4(cr)$. The majority of substances important to nuclear waste disposal such as carbonate, sulfate, fluoride, and chloride complexes of the metal ions are not included. The elements selenium, curium, and radium are also not covered.

The NBS Tables of Chemical Thermodynamic Properties

Reference 2

This widely used compilation tabulates enthalpy of formation, Gibbs energy of formation, entropy, heat capacity, enthalpy of formation at 0°K and $H^\circ(298.15)-H^\circ(0)$ values at 25°C, and mostly zero ionic strength. For each element in the publication, values are given for crystalline and amorphous solids, gases, liquids, and aqueous forms for hundreds of substances. It is comprehensive in coverage for the elements; only americium, curium, neptunium, plutonium, lawrencium,

fermium, californium, berkelium, nobelium, mendelevium, and einsteinium are not included. Data for tin were prepared in 1965; for lead, in 1965; thorium in 1980; cesium in 1979.

The Chemical Thermodynamics of Actinide Elements and Compounds. Part 1. The Actinide Elements

Reference 3

Tabulated are recommended values for Gibbs energy of formation, enthalpy of formation, entropy, heat capacity, $H^\circ(T) - H^\circ(298)$, $- [G^\circ(T) - H^\circ(298)]/T$ from 0°K up to 6000°K for the crystalline, gaseous, and liquid forms of the following actinides: thorium, protactinium, uranium, neptunium, plutonium, americium, and curium.

Included also are summary tables which contain temperatures and enthalpies of transformation for solid phases of the elements. Examples are $\text{Th}(\alpha) \rightarrow \text{Th}(\beta)$ at 2023°K, accompanied by an enthalpy change of 860 cal mol⁻¹. Other tables list entropy and heat capacity of actinide metals at 25°C, for example $S^\circ(\text{Am}(s)) = 13.02 \pm 0.65$ cal mol⁻¹ K⁻¹, $C_p^\circ[\text{Pu}(s)] = 7.85 \pm 0.08$ cal mol⁻¹ K⁻¹; coefficients of heat capacity equations for various phases of actinide metals; C_p° , S° and $\Delta_f H^\circ$ of actinide gases; and Gibbs energy of formation of the gaseous phase from the condensed phases.

The Chemical Thermodynamics of Actinide Elements and Compounds. Part 2. The Actinide Aqueous Ions

Reference 4

This is a widely referenced compilation of enthalpy of formation, Gibbs energy of formation and entropy for the actinide ions at 25°C. Covered are the MO_2^{2+} ions for U, Np, Pu, Am; MO_2^+ ions of Pa, U, Np, Pu, and Am; M^{4+} ions for Th, Pa, U, Np, Pu, Am, and Bk; and M^{3+} ions of Ac, U, Np, Pu, Am, Cm, Bk. Data are also included for californium, einsteinium, fermium, mendelevium, nobelium, and lawrencium.

The Chemical Thermodynamics of Actinide Elements and Compounds. Part 3. Miscellaneous Actinide Compounds

Reference 5

This is a comprehensive summary of Gibbs energy of formation, enthalpy of formation, and entropy for mainly crystalline hydroxides, sulfates, acetates, nitrates, oxalates, sulfites, tungstates, carbonates, chromates, formates, hydrates, selenates, uranates at 25°C. More data are tabulated for $\Delta_f H^\circ$. Some aqueous species are included; most of the species covered are uranium species. Values of thermodynamic properties tabulated over the temperature range 0-1000°K for

certain substances such as thorium sulfate, uranyl sulfate, and uranium tetraoxide.

The Chemical Thermodynamics of Actinide Elements and Compounds. Part 8. The Actinide Halides

Reference 6

This recent publication contains comprehensive thermodynamic data on gaseous and solid actinide halides. Tables of C_p^0 , S^0 , $\Delta_f H^0$, $\Delta_f G^0$, $\log K_p^0$, $-[G^0(T)-H^0(298)]/T$ and $[H^0(T)-H^0(298)]$ are given over the temperature interval 298-2500°K for F, Cl, Br, and I substances. Examples are $PuF_6(g)$, $NpBr_3(c)$, and $UO_2Br_2(c)$. Most information is given for uranium halides. The narrative portion includes tabulation of other data such as enthalpies of solution and formation of UO_2Cl_2 in HCl solution.

JANAF Thermodynamic Tables

Reference 7

An authoritative tabulation of Gibbs energy of formation, enthalpy of formation, entropy, heat capacity, $-(G^0-H^0_{298})/T$, $(H^0-H^0_{298})$, and $\log K_p$ values for hundreds of substances mainly in the solid state, but including also liquids and gaseous ions. This is a highly reliable source of data on oxides, halides, sulfates, carbonates, and other solids such as silicates. Values of these properties are tabulated over an extended temperature range, e.g., 0°K to 2000°K for elements such as tin, lead, cesium, and strontium.

Handbook of Thermodynamic Data

Reference 8

Thermodynamic properties are given for a large number of substances in the solid, liquid, gaseous, and aqueous solution states. For actinides and other elements such as uranium, strontium, cesium, tin, lead, selenium and thorium are covered. By far the data covered are most complete for $\Delta_f G^0$ values, in terms of aqueous species such as ThF_2^{2+} and $UO_2SO_4(aq)$. Equilibrium quotients are given up to 350°C as mathematical equations for over 50 chemical reactions, e.g., $HS^- = S^- + H^+$; $HF = F^- + H^+$. Over 1500 references are given to research and other publications covering the time up to the 1960's.

Thermodynamic Properties of Minerals and Related Substances at 298.15°K and 1 Bar (100,000 Pascals) Pressure and at Higher Temperatures

Reference 9

The U.S. Geological Survey Bulletin 1452 is a reliable source of thermodynamic properties for minerals and related substances to over 1000°K. Values of Gibbs energy of formation, enthalpy of formation, heat capacity, and entropy are listed for a number of minerals, solids, metal ions, and complexing ligands relevant to nuclear waste storage such as U^{4+} , Ni^{2+} , CO_3^{2-} , and SO_4^{2-} .

Critical Stability Constants, Vol. 4, Inorganic Complexes

Reference 10

This is a widely referenced compilation of formation constants up to about 1974-1975. It is a rich source of formation constants mainly at 25°C, and ionic strengths from zero to 3.0. Stability constants tabulated are often the average of an unspecified number of published values, rather than selection of a single value considered the most reliable.

Handbook of Thermochemical Data for Compounds and Aqueous Species

Reference 11

Values are given for $\Delta_f G$, $\Delta_f H$, and S from 25 to 300°C for over 500 solid, gaseous, and aqueous substances. Data are included for Th, U, Pu^{3+} , and Pu(c).

The Hydrolysis of Cations

Reference 12

Critically evaluated data with assigned uncertainties on hydrolysis constants up to 1974-1975 are found in the widely referenced book The Hydrolysis of Cations. The authors include detailed discussions on experimental procedures, data handling, and interpretation, uncertainties and effect of ionic strength together with a substantial number of references to original publications. Summary tables permit use of an extended Debye-Huckel equation to calculate hydrolysis constants from tabulated coefficients at 25°C and mainly at specific ionic strengths, e.g., 0.3, 1.0, and 3.0, and molalities. Actinides covered are U, Pu, Np, Am, Th, Cm, in their various oxidation states.

A Computer-Assisted Evaluation of the Thermochemical Data of the Compounds of Thorium

Reference 13

An excellent tabulation of values at 25°C for Gibbs energy of formation, enthalpy of formation, entropy, heat capacity, and $(H-H_{298})$, $(H-H_0)$, $(G-H_{298})/T$ for solid, gaseous, and liquid compounds of thorium. These compounds are oxides, fluorides, chlorides, bromides, and iodides of thorium over the temperature range 0°K to 2500°K.

Selected Values of Chemical Thermodynamic Properties. Compounds of Uranium, Protactinium, Thorium, Actinides, and the Alkali Metals

Reference 14

This publication from National Bureau of Standards has tables of recommended values for enthalpy of formation, Gibbs energy of formation, entropy, and heat capacity at 25°C for crystalline and amorphous solids, gases, and aqueous substances. Several hundred compounds of the elements are covered; however, most data are for enthalpy of formation. Compounds of cesium are extensively covered (about 200 substances).

The Thermochemical Properties of the Uranium-Halogen Containing Compounds

Reference 15

A critical evaluation resulting in tables of values for Gibbs energy of formation, enthalpy, of formation, entropy and heat capacity of uranium-halogen compounds. Details are given of the procedure and rationale for selection of recommended values. Covered are fluoride, chloride, bromide, iodide compounds in the solid, gaseous, and solution states. Extensive data are given of Gibbs energy and enthalpy changes for several hundred reactions, including experimental values.

Hydrolysis and Formation Constants at 25°C

Reference 16

This is a critical compilation consisting of hydrolysis and formation constants at 25°C for about 20 metals in their oxidation states expected in natural waters. Complexing ligands include OH^- , F^- , Cl^- , SO_4^{2-} , CO_3^{2-} , PO_4^{2-} . Coefficients for an extended Debye-Huckel equation are included to permit estimating values of $\log K(I)$ up to 3 ionic strengths.

Thermochemical Data for Uranium, Plutonium, and Neptunium

Reference 17

Hydrolysis and formation values have also been calculated at zero ionic strength for about 20 species of plutonium and uranium by Lemire and Tremaine; these log K values were calculated from Gibbs energies of formation, which were calculated by a modified Criss-Cobble entropy extrapolation. The work is an excellent source of tabulated values for Gibbs energy and entropy of: solids, liquids and gases; ligands; aqueous plutonium and uranium species; and, estimated selected stability constants up to 200°C. Lemire extended the work to include neptunium in 1984.

LITERATURE CITED

1. CODATA Task Group On Key Values for Thermodynamics: CODATA Recommended Key Values for Thermodynamics 1977, CODATA Bulletin 28, CODATA Secretariat, 51 Boulevard de Montmorency, 75016 Paris, France (April 1978).
2. D. D. Wagman, W. H. Evans, V. B. Parker, R. H. Schumm, I. Halow, S. M. Bailey, K. L. Churney, and R. L. Nuttall, "The NBS Tables of Chemical Thermodynamic Properties," J. Phys. Chem. Ref. Data 1982, V. 11, Suppl No. 2.
3. F. L. Oetting, M. H. Rand, and R. J. Ackermann, The Chemical Thermodynamics of Actinide Elements and Compounds. Part 1. The Actinide Elements, International Atomic Energy Agency, Karntver Ring, 11, P.O. Box 590, A-1011 Vienna, Austria (March 1976).
4. J. Fuger, and F. L. Oetting, The Chemical Thermodynamics of Actinide Elements and Compounds. Part 2. The Actinide Aqueous Ions, International Atomic Energy Agency, Karntver Ring 11, P.O. Box 590, A-1011 Vienna, Austria (July 1976).
5. E. H. P. Cordfunke, and P. A. G. O'Hare, The Chemical Thermodynamics of Actinide Elements and Compounds. Part 3. Miscellaneous Actinide Compounds, International Atomic Energy Agency, Karntver Ring 11, P.O. Box 590, A-1011 Vienna, Austria (January 1978).
6. J. Fuger, V. B. Parker, W. N. Hubbard, and F. L. Oetting, The Chemical Thermodynamics of Actinide Elements and Compounds. Part 8. The Actinide Halides, International Atomic Energy Agency, Karntver Ring 11, P.O. Box 590, A-1011 Vienna, Austria (December 1983).
7. D. R. Stull, H. Prophet, JANAF Thermochemical Tables, 2nd ed., Nat. Std. Ref. Data Ser., Nat. Bur. Stand., 1971, 37. M. W. Chase, J. L. Curnutt, A. T. Hu, H. Prophet, A. N. Syverud, L. C. Walker: J. Phys. Chem. Ref. Data 1974, v. 3, 311. M. W. Chase, J. L. Curnutt, H. Prophet, R. A. McDonald, A. N. Syverud: Ibid. 1975, v. 4, 1. M. W. Chase, J. L. Curnutt, R. A. McDonald, A. N. Syverud: Ibid., 1978, v. 7, 793. M. W. Chase, J. L. Curnutt, J. R. Downey, R. A. McDonald, A. N. Syverud, E. A. Valenzuela: Ibid., 1982, v. 11, 695.
8. G. B. Naumov, B. N. Rhzhenko, and I. L. Khodakovsky, Handbook of Thermodynamic Data, Translated by G. J. Soleimani, U.S. Geological Survey, Menlo Park, CA 94025 (January 1974). PB-226-722, National Technical Information Service, Springfield, Virginia 22161.

9. R. A. Robie, B. S. Hemingway, and J. R. Fisher, Thermodynamic Properties of Minerals and Related Substances at 298.15 K and 1 Bar (100,000 Pascals) Pressure and at Higher Temperatures, Geol. Surv. Bull. 1452, U.S. Government Printing Office, Washington, D.C. 20402 (1978).
10. R. M. Smith, and A. E. Martell, Critical Stability Constants. Vol. 4: Inorganic Complexes, Plenum Press, New York 10011 (1976).
11. H. E. Barner, and R. V. Scheuerman, Handbook of Thermochemical Data for Compounds and Aqueous Species, John Wiley & Sons, Inc., New York (1978).
12. C. F. Baes, and R. E. Mesmer, The Hydrolysis of Cations, John Wiley & Sons, Inc., New York (1976).
13. D. D. Wagman, R. H. Schumm, and V. B. Parker, A Computer-Assisted Evaluation of the Thermochemical Data of the Compounds of Thorium, NBSIR-77-1300, National Bureau of Standards, Washington, D.C. 20234 (August 1977).
14. D. D. Wagman, W. H. Evans, V. B. Parker, R. H. Schumm, and R. L. Nuttall, Selected Values of Chemical Thermodynamic Properties. Compounds of Uranium, Protactinium, Thorium, Actinium, and the Alkali Metals, NBS Technical Note 270-8, National Bureau of Standards, Washington, D.C. 20234 (May 1981).
15. V. B. Parker, The Thermochemical Properties of the Uranium-Halogen Containing Compounds, NBSIR-80-2029, National Bureau of Standards, Washington, D.C. 20234 (July 1980).
16. S. L. Phillips, Hydrolysis and Formation Constants at 25°C, LBL-14313, Lawrence Berkeley Laboratory, Berkeley, California 94720 (May 1982).
17. R. J. Lemire, and P. R. Tremaine, J. Chem. Eng. Data 1980, v. 25, 361. R. J. Lemire, AECL-7818, At. Energy Canada, Ltd. [Rep.], AECL, 1984.

APPENDIX B

Analysis of Data From Batch Sorption Experiments When Radionuclides Undergo Chemical Speciation Reactions

K. L. Erickson

Introduction

In typical batch sorption experiments fluid-phase compositions are monitored until no statistically significant change appears to occur during some time period, which is usually on the order of several days. The system is then assumed to be at equilibrium. However, some chemical speciation reactions which convert strongly sorbing species to more weakly sorbing species might occur too slowly to be detected during the given time period, but would occur rapidly enough to seriously affect cumulative radionuclide discharges during a regulatory period which is on the order of ten thousand years. A numerical example illustrating these effects is given below, and some basic considerations for designing or evaluating data from batch sorption experiments are described.

Theory

Consider a batch sorption experiment in which a fluid phase containing a given radionuclide N_j of element N is contacted with a solid phase. In the fluid phase, let the radionuclide exist as two chemical species, A_1 and A_2 , which undergo the chemical speciation reaction



where L denotes some other fluid-phase constituent, and α and ρ are stoichiometric coefficients. The corresponding reaction rate expression is

$$r_{A_1} = -\frac{dC_{A_1}}{dt} = k_1 C_{A_1}^{n_1} C_L^{n_L} - k_2 C_{A_2}^{n_2} \quad (1)$$

where C_{A_1} , C_{A_2} , and C_L are the fluid-phase molar concentrations of species A_1 , A_2 , and L , respectively; k_1 and k_2 are the forward and reverse reaction rate constants.

respectively; the exponents n_1 , n_2 , and n_L are greater than zero; r_{A_1} denotes the rate of depletion of species A_1 , and t denotes time. In most cases, the exponent n_1 in Equation (1) will be unity or greater; C_{A_1} will be less than 1 molar, and the expression

$$r_{A_1} \approx k^* C_{A_1} \quad (2)$$

will give reaction rates equal to or greater than those obtained from Equation (1). In Equation (2),

$$k^* = k_1 C_{L_{\max}}^{n_L}, \text{ and } C_{L_{\max}}^{n_L} \text{ is the maximum anticipated value of } C_L^{n_L}.$$

Let \bar{C}_{A_1} and \bar{C}_{A_2} denote the solid-phase concentrations (mole/kg) due to sorption of species A_1 and A_2 , respectively, and let the sorption equilibria for species A_1 be more favorable than those for species A_2 . For purposes of illustration, assume that the sorption isotherms can be considered at least approximately linear. Also, since sorption rates, particularly those for physical adsorption and ion exchange, are diffusion-limited, either in the fluid and/or solid phase, a reasonable expression for sorption rates would be of the form

$$\frac{d\bar{C}_{A_i}}{dt} = \rho h s \left(\Gamma_{A_i} C_{A_i} - \bar{C}_{A_i} \right) \quad (3)$$

where h = mass transfer coefficient, cm/day

s = surface area of the solid per unit mass, cm^2/gm

t = time, day

Γ_{A_i} = sorption equilibrium distribution function for species A_i (taken as at least approximately constant), cm^3/gm

ρ = grain density of the solid, gm/cm^3 .

Typical half-lives for sorption reactions in laboratory batch experiments are on the order of hours to days. Note that for

the case in which sorption rates are limited by diffusion in the solid-phase, \bar{C}_{A_1} is the average solid-phase concentration at any given time, and the quantity $\Gamma_{A_1} C_{A_1}$ is the equilibrium solid phase concentration defined by the isotherm.

If Equation (2) is used to give an upper bound for the rate of depletion of A_1 due to the speciation reaction, then the material balances for species A_1 are

$$V \frac{dC_{A_1}}{dt} = -m \frac{d\bar{C}_{A_1}}{dt} - V k^* C_{A_1} \quad (4)$$

with

$$C_{A_1}(0) = C_{A_1}^0 \quad (5)$$

and

$$\frac{d\bar{C}_{A_1}}{dt} = \rho h s (\Gamma_{A_1} C_{A_1} - \bar{C}_{A_1}) \quad (6)$$

with

$$\bar{C}_{A_1}(0) = 0 \quad (7)$$

where m = mass of solid

V = volume of solution.

The material balances for species A_2 are

$$V \frac{dC_{A_2}}{dt} = -m \frac{d\bar{C}_{A_2}}{dt} + V a k^* C_{A_1} \quad (8)$$

with

$$C_{A_2}(0) = 0 \quad (9)$$

and

$$\frac{d\bar{C}_{A_2}}{dt} = \rho h s \left(\Gamma_{A_2} C_{A_2} - \bar{C}_{A_2} \right) \quad (10)$$

with

$$\bar{C}_{A_2}(0) = 0 \quad (11)$$

The solutions to Equations (4) and (6) with initial conditions given by Equations (5) and (7) can be obtained using Laplace transforms (see Addendum) and are

$$\frac{C_{A_1}}{C_{A_1}^0} = \frac{(b_1 + \rho h s)}{\sqrt{b^2 - 4d}} e^{b_1 t} - \frac{(b_2 + \rho h s)}{\sqrt{b^2 - 4d}} e^{b_2 t} \quad (12)$$

and

$$\bar{C}_{A_1} = \frac{C_{A_1}^0 \rho h s \Gamma_{A_1}}{\sqrt{b^2 - 4d}} \left(e^{b_1 t} - e^{b_2 t} \right) \quad (13)$$

where

$$b = \rho h s \left(1 + \frac{m \Gamma_{A_1}}{V} \right) + k^*$$

$$b_1 = \frac{-b + \sqrt{b^2 - 4d}}{2}$$

$$b_2 = \frac{-b - \sqrt{b^2 - 4d}}{2}$$

$$d = \rho h s k^*$$

Again, for purposes of illustration, let the sorption equilibrium distribution function Γ_{A_2} for species $A_2 = 0$, and let the stoichiometric coefficient $a = 1$. Then the material balances for species A_2 are

$$\frac{dC_{A_2}}{dt} = k^* C_{A_1} \quad (14)$$

with

$$C_{A_2}(0) = 0$$

and

$$\bar{C}_{A_2} = 0$$

The solution to Equation (14) with initial condition given by Equation (9) is (see Addendum)

$$C_{A_2} = \frac{k^* C_{A_1}^0}{\sqrt{b^2 - 4d}} \left[\left(\frac{b_1 + \rho h s}{b_1} \right) e^{b_1 t} - \left(\frac{b_2 + \rho h s}{b_2} \right) e^{b_2 t} - \rho h s \left(\frac{1}{b_1} - \frac{1}{b_2} \right) \right] \quad (15)$$

Batch Sorption Experiments

Generally, in batch sorption experiments a known volume V of a solution containing the nuclide of interest is contacted with a known mass m of solid. The initial radioactivity A_0 of the nuclide per unit volume of solution is known. The subsequent radioactivity A of the solution is monitored as a function of time, and when A appears to remain constant, the system is assumed to be at equilibrium. The amount of the nuclide sorbed by the solid is then calculated from V , values of A/A_0 , and the respective sample volumes. For the case

where $C_{A_2}(0) = 0$, $\Gamma_{A_2} = 0$, and the stoichiometric coefficient $a = 1$,

$$\frac{A}{A_0} = \frac{C_{A_1} + C_{A_2}}{C_{A_1}^0} \quad (16)$$

and from Equations (12) and (15),

$$\frac{A}{A_0} = \frac{C_{A_1} + C_{A_2}}{C_{A_1}^0} = 1 - B e^{-b_1 t} \left(1 - e^{-\sqrt{b^2 - 4d} t} \right) \quad (17)$$

where

$$B = \frac{m\Gamma_{A_1}}{V \sqrt{\left[1 + \frac{m\Gamma_{A_1}}{V} + \frac{k^*}{\rho h s} \right]^2 - \frac{4k^*}{\rho h s}}}$$

As an example, consider a case in which $\Gamma_{A_1} \approx$ a constant = 300 cm³/gm. Assume that results from geochemical sensitivity analyses indicate that if a chemical speciation reaction occurs, the value of k^* must be less than 2/3 yr⁻¹ (0.0018 day⁻¹) if cumulative radionuclide discharges are to comply with the EPA standard. In typical laboratory batch experiments, reasonable values for m , V , and $\rho h s$ would be 1 gm, 100 cm³, and 0.17 day⁻¹ (sorption reaction half-life of about 1 day), respectively. If Γ_{A_1} and k^* are taken as 300 cm³/gm and 0.0018 day⁻¹, respectively, then Equation (17) becomes

$$\frac{A}{A_0} = 1 - 0.75 e^{-0.0005t} \left(1 - e^{-0.68t} \right) \quad (18)$$

Values of A/A_0 versus t for a hypothetical experiment described by Equation (18) are given on Figure 1 for $2 \leq t \leq 40$ days, and on Figure 2 for $1 \leq t \leq 2000$ days. From Figure 1, it can be seen that unless the precision in experimentally determined values of A/A_0 were very high, the experiment would appear to reach equilibrium during the interval between about 8 and 40 days. To detect the effects of the chemical speciation reaction, data for a much longer time interval would be required, as indicated on Figure 2. The time interval required to detect effects would depend on the precision in the experimental data.

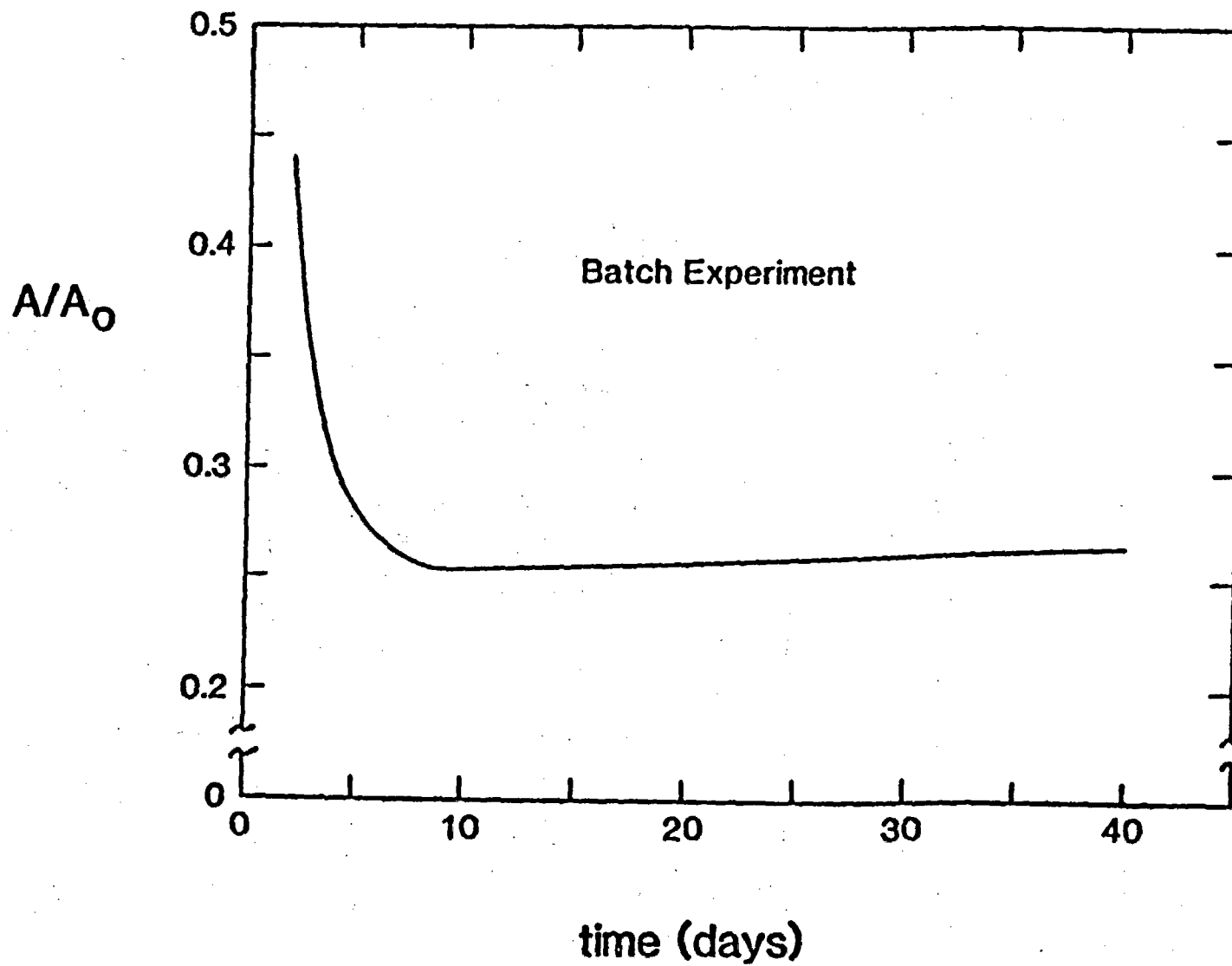


Figure 1. Values of A/A_0 Versus Time t for a Hypothetical Batch Sorption Experiment
($m = 1$ gm, $V = 100$ cm³, $\Gamma_{A_1} = 300$ cm³/gm, $\rho_{hs} = 0.17$ day⁻¹,
 $k^* = 0.0018$ day⁻¹)

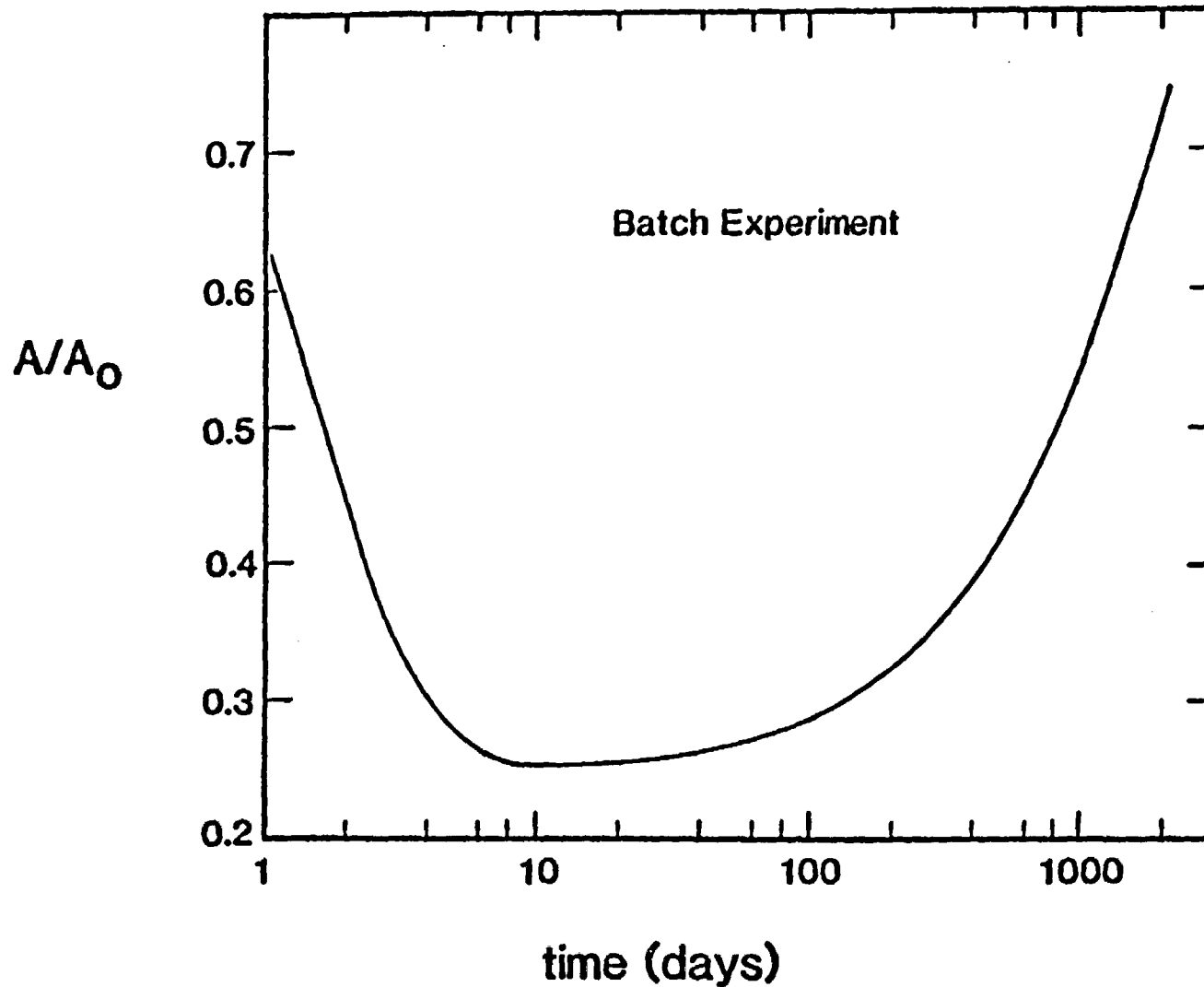


Figure 2. Values of A/A_0 Versus Time t for a Hypothetical Batch Sorption Experiment
($m = 1$ gm, $V = 100$ cm³, $\Gamma_{A_1} = 300$ cm³/gm, $\rho_{hs} = 0.17$ day⁻¹,
 $k^* = 0.0018$ day⁻¹)

In general, sensitivity analyses can identify the combinations of values of Γ and k^* which could result in cumulative radionuclide discharges which violate the EPA standard. Knowing those values and the expected precision in experimental data, analyses similar to the above example could be used to define criteria for:

- (1) Designing batch sorption experiments which will be of sufficient duration to detect the effects of any chemical speciation reactions which might result in violations of the EPA standard; and
- (2) Evaluating data from previous experiments to determine if the effects of speciation reactions which could cause violation of the EPA standard would have been detected.

Conclusions

Batch sorption experiments should be examined closely to determine if chemical speciation reactions which may significantly affect cumulative radionuclide discharges could be detected. Criteria for evaluating data and designing experiments can be developed using analyses similar to those discussed above.

Addendum

Let $\tilde{C}_{A_1}(p)$ denote the Laplace transform of $C_{A_1}(t)$ with respect to t , and similarly define $\tilde{C}_{A_2}(p)$. Then from Equations (4) through (7)

$$\tilde{C}_{A_1} = \frac{C_A^0(p+\rho hs)}{p^2 + [\rho hs(1+m\Gamma_{A_1}/V)+k^*]p + \rho hsk^*}$$

or

$$\tilde{C}_{A_1} = \frac{C_A^0(p+\rho hs)}{(p-b_1)(p-b_2)}$$

where b_1 and b_2 are defined above. Also,

$$\bar{C}_{A_1} = \frac{\rho h s \Gamma_{A_1} \bar{C}_{A_1}^0}{p + \rho h s}$$

Using the residue theorem (see J. Crank, The Mathematics of Diffusion, Clarendon Press, Oxford, 1975, pp. 26-27),

$$C_{A_1} = \frac{C_{A_1}^0}{\sqrt{b^2 - 4d}} \left[(b_1 + \rho h s) e^{b_1 t} - (b_2 + \rho h s) e^{b_2 t} \right] \quad (12)$$

and

$$\bar{C}_{A_1} = \frac{C_{A_1}^0 \rho h s \Gamma_{A_1}}{\sqrt{b^2 - 4d}} \left[e^{b_1 t} - e^{b_2 t} \right]$$

where b and d are defined above. Now, from Equation (14),

$$C_{A_2} = k^* \int_0^t C_{A_1} dt$$

or

$$C_{A_2} = \frac{k^* C_{A_1}^0}{\sqrt{b^2 - 4d}} \left[\left(\frac{b_1 + \rho h s}{b_1} \right) e^{b_1 t} - \left(\frac{b_2 + \rho h s}{b_2} \right) e^{b_2 t} - \rho h s \left(\frac{1}{b_1} - \frac{1}{b_2} \right) \right] \quad (15)$$

Then from Equations (12), (15), and (16)

$$\frac{A}{A_0} = \frac{C_{A_1} + C_{A_2}}{C_{A_1}^0} = 1 - B e^{-b_1 t} \left(1 - e^{-\sqrt{b^2 - 4d} t} \right) \quad (17)$$

where B is defined above.

Appendix C

COLCAP: A Computer Code for the Calculation of Radionuclide Adsorption by Naturally Occurring Ground-Water Colloids

C.1 Introduction

Naturally occurring colloids arise primarily from the partial dissolution of clays in the rock matrix. These clay colloids are able to adsorb radionuclides which in turn prevent the radionuclides from adsorbing to the rock matrix. The mobile radionuclide-colloid species travel at the same velocity as the ground water. The code COLCAP has been developed to give a preliminary view of the role colloids may play in radionuclide transport. Using a surface adsorption approach, the code calculates the number of radionuclides that may adsorb to a monodisperse colloid suspension for a given particle size and concentration. Using the radionuclide half life, the number of radionuclides adsorbed is converted to the curies adsorbed per cubic meter and then compared with the maximum permissible concentration of the radionuclide in drinking water in the NRC regulation 10CFR20.

C.2 Surface Adsorption Calculations

A surface area approach is used to model the radionuclide adsorption in COLCAP. This is reasonable for non-swelling clays such as kaolinite but underestimates the surface available for binding in swelling clays such as montmorillonite. The colloids are assumed to be spherical. In the code, the radionuclide ions are assumed to have a 1 Angstrom diameter and to form an adsorption monolayer on the colloid. The colloid particle density is fixed at a constant value of 2.59 g/cm^3 . The input to the code requires the half life of the radionuclides (years) and the MPC (maximum permissible concentration) of the radionuclides (Ci/m^3).

The calculation in the code involves first converting the half life of the radionuclide from years to seconds. Then for a colloid concentration of 1 ppb and colloid diameters of 10, 100, and 1000 nm, the radionuclide carrying capacity of the colloidal suspension is calculated as follows. The mass of a single colloid in grams is calculated as:

$$m_c = \rho_c V_c = \frac{4}{3} \pi r_c^3 \rho_c \quad (\text{g}) \quad (1)$$

where ρ_c is the density of the colloid (2.59 g/ml), V_c is the volume of the colloid and r_c is the radius of the colloid (cm). The number of colloids per ml is calculated by converting N , the concentration in ppb, ($\text{g colloids} / 10^9 \text{ gm}$

solution) to g/ml (g colloid/ ml solution) and dividing by the mass of a single colloid or:

$$n_c = (N \times 10^{-9}) / m_c \quad (\text{colloids/ml}) \quad (2)$$

where n_c is the number of colloids per milliliter of solution and it is assumed that the density of the solution is 1 g/ml. The number of radionuclide atoms per milliliter of solution assuming a monolayer of radionuclides adsorbed to the colloid is estimated as:

$$n_r = S_c / \pi r_r^2 \quad (3)$$

where r_r is the radius of the radionuclide ions and S_c is the area through the centerline of the spheres as shown in Figure C-1 and calculated by the following:

$$S_c = 4 \pi (r_c + r_r)^2 n_c \quad (\text{cm}^2/\text{ml}) \quad (4)$$

The radius of the radionuclides, r_r , assumed in the program is 1 Angstrom or 1×10^{-8} cm. The decay constant is calculated as:

$$\lambda = 0.639/t^{1/2} \quad (\text{sec}^{-1}) \quad (5)$$

where $t^{1/2}$ is the half life in seconds. Finally, the curies per cubic meter of suspension are calculated by:

$$\text{Ci}/\text{m}^3 = n_r \lambda (1 \times 10^6) / (3.7 \times 10^{10}) \quad (6)$$

In COLCAP, Equation 6 is solved for the curies per cubic meter transported in a colloidal suspension of 1 ppb. Multiplying Equation 6 by the colloid concentration (ppb) then gives the curies per cubic meter transported by colloidal suspensions of other concentrations. The final form of the equation for Ci/m^3 in terms of colloid radius, r_c , expressed in nm, colloid concentration, N , expressed in ppb and radionuclide half life, $t^{1/2}$, expressed in years is

$$\text{Ci}/\text{m}^3 = \frac{2.02 \times 10^{15} N (r_c \times 10^{-7} + 1 \times 10^{-8})^2}{r_c^3 t^{1/2}} \quad (7)$$

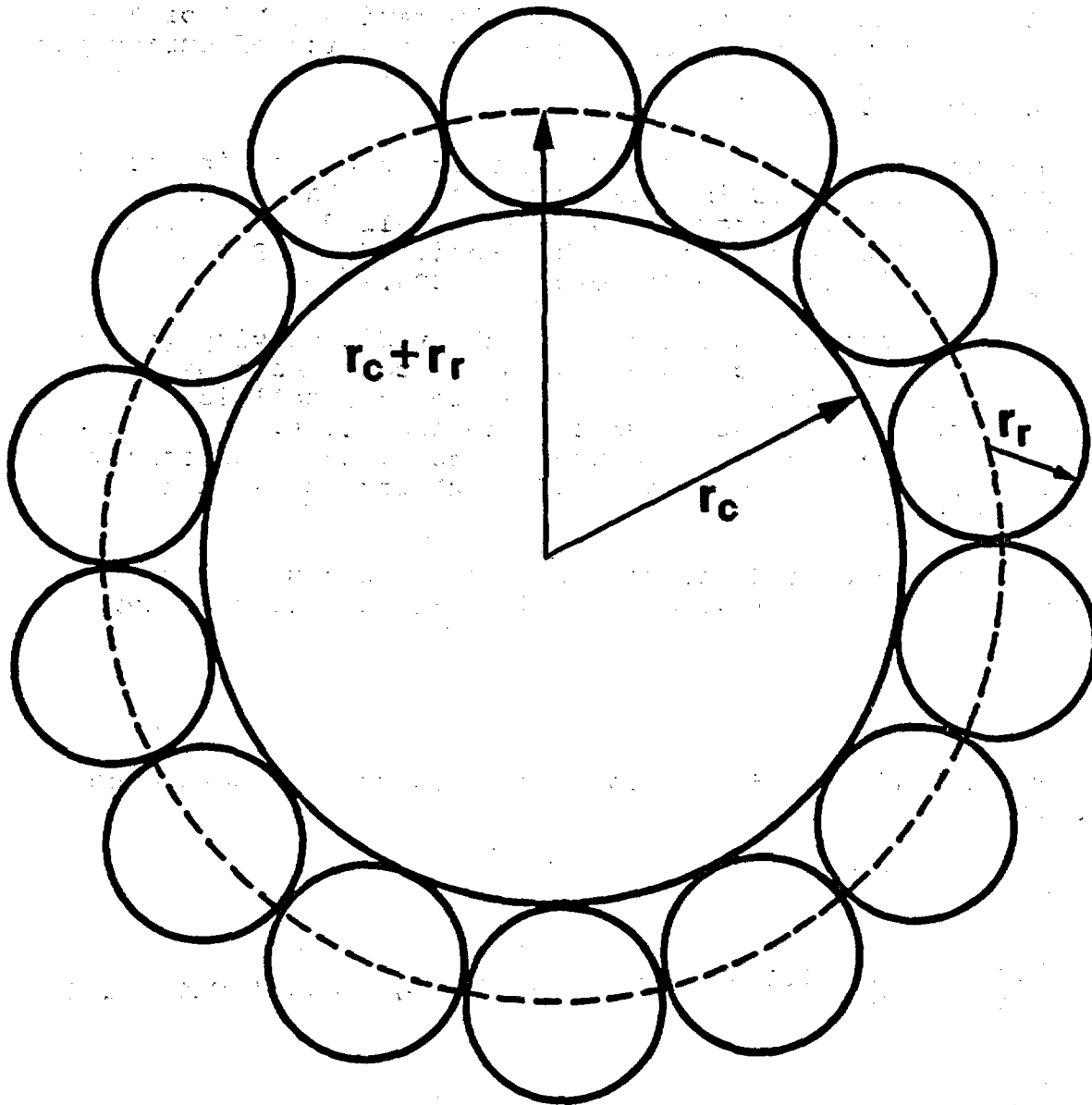


Figure C-1 Configuration Assumed for Calculation of the Number of Radionuclide Sorbed onto Colloid. The Dashed Line Represents the Sphere Whose Surface Area is Calculated in Equation 4.

C.3 Using COLCAP:

The following input is required in order to run COLCAP:

1. A radionuclide name
2. The half life of the radionuclide expressed in years
3. The maximum permissible concentration (MPC) of the radionuclide in drinking water in units of curies per cubic meter
4. Two output file names.

The code runs with IBM-PC BASIC. The user should be in the disk directory in which BASIC is located or set a path to that directory. The COLCAP program must be installed in the same directory as BASIC or a path must be specified. BASIC is generally found in the same directory as DOS.

The output consists of an estimate of the radioactivity (curies per cubic meter) that a colloid suspension could be expected to transport as a function of colloid diameter and colloid concentration. The output is written to two files. One keeps a record of the data produced and appends new data as necessary, and another formats the data as ASCII text for use with a plotting routine.

Once COLCAP is installed and the paths have been set, running COLCAP involves the following commands. First, the user types:

BASIC

This command loads the BASIC programming language. Next, the user types:

LOAD"COLCAP

Another "ok" prompt will appear. The user types RUN"COLCAP and will be prompted by:

Radionuclide = ?

The radionuclide name of interest should be entered followed by a return. For example,

Radionuclide = ? Np-237

The user is then prompted for the half-life in years. It should

be entered in a similar manner.

Half life in Years = ?

Next the MPC, maximum permissible concentration, of the radionuclide in ground water is asked for and should be supplied.

MPC, Maximum Permissible Concentration, in Curies/Cubic Meter = ?

Now the user must specify the output files. Two output files are created by this program. One serves as a running account of multiple data sets. Output to this file is in the form of a chart and if the same file name is entered for each radionuclide studied, the new chart is appended to the list of old charts. This file name is prompted by the following statement:

Enter File Name to Which Data (in Chart Form) is to be Stored.
If the File Already Exists, the New Data Will be Appended.?

The user now enters the file name followed by a return.

The second file is formatted to be read into plotting routines such as Slidewrite. Minor editing is required to remove identifying text from the beginning of the file. Note: if the file the user designates is already in existence, its contents are ERASED. The prompt should be followed by a file name and carriage return:

File Name for Formatted Data to be Used with Plotting Programs = ?

Three carriage returns are be required to run the program and return the "ok" prompt which signals the program's completion.

C.4 Program Listing

A listing of the COLCAP program in BASIC follows:

```

10 'COLCAP
20 '
30 'ORIGINAL PROGRAM WRITTEN BY H.E. NUTTALL      APRIL, 1984
40 'PROGRAM MODIFIED BY S.E. BAYLEY             APRIL, 1988
50 '
60 'DEFINITIONS: 1 CURIE = 3.7E10 /SEC
70 'MPC = MAXIMUM PERMISSIBLE CONCENTRATION (CURIES/CU M)
80 '
90 '*****
100 '
101 DIM DP(3), MP(3), NC(3), SURF(3), NA(3), CC(3), P2(3), LP2(3)
110 INPUT "RADIONUCLIDE = ";N$
120 INPUT "HALF LIFE IN YEARS = ";THALF
130 INPUT "MPC, MAXIMUM PERMISSIBLE CONCENTRATION, IN CURIES/CUBIC METER = ";MPC
132 PRINT
133 PRINT "ENTER FILE NAME TO WHICH DATA (IN CHART FORM) IS TO BE STORED."
134 INPUT "IF THE FILE ALREADY EXISTS, THE NEW DATA WILL BE APPENDED. ";FILEA$
135 PRINT
136 INPUT "FILE NAME FOR FORMATTED DATA TO BE USED WITH PLOTTING PROGRAMS = ";FI
140 IF INKEY$="" THEN GOTO 140
145 OPEN FILEA$ FOR APPEND AS 1
146 OPEN FILEB$ FOR OUTPUT AS 2
150 PRINT #1,:PRINT #1,: PRINT #1, " COLLOID CALCULATIONS FOR ";N$:PRINT
160 PRINT #1,:PRINT #1, "PARAMETERS":PRINT #1,:PRINT #1, "RADIONUCLIDE = ";N$
170 PRINT #1, "HALF LIFE IN YEARS = ";:PRINT #1, USING "##.##^";THALF
180 PRINT #1, "MPC IN CURIES/CUBIC METER = ";:PRINT #1, USING "##.##^";MPC:PR
190 PRINT #1, "*****"
200 PRINT #1, "COLLOID CONC., ppb";TAB(20);"CURIES/CU M";TAB(35);"LOG(CONC)";TAB
210 PRINT #1,
220 '*****
230 ' SET PARAMETERS
240 CONC=9.999999E-10                'CONVERT CONCENTRATION FROM 1 ppb TO gm/ml
250 '
260 PI=3.1459
270 DENSITY=2.59
280 '*****
285 THALFS=THALF*365!*24!*3600!      'CONVERTS YEARS TO SECONDS
290 FOR EDP = 1 TO 3
300 DP(EDP)=.0000001 * 10!^EDP      'PARTICLE DIAMETER IN cm
310 'CALCULATIONS
320 'CALCULATE THE NUMBER OF PARTICLES PER ml OF SOLUTION
330 MP(EDP)=4!/3!*PI*(DP(EDP)/2!)^3*DENSITY 'MASS OF A SINGLE COLLOID, gm
340 NC(EDP)=CONC/MP(EDP)              'NUMBER OF COLLOIDS PER ml
350 SURF(EDP)=4!*PI*((DP(EDP)/2!)+1E-08)^2*NC(EDP) 'SURFACE AREA OF COLLOIDS PER
360 NA(EDP)=SURF(EDP)/(PI*1E-16)
370 '
390 LAMBDA=.639/THALFS                'DECAY CONSTANT
400 CC(EDP)=NA(EDP)*LAMBDA*1000000!/3.7E+10 'CURIES/CUBIC METER
410 '
420 '
430 '
440 '
450 '*****

```

```

460 FOR MCONC = 1 TO 200 STEP 25
470 'OUTPUT OF DATA IN CHART FORM
480 IF MCONC = 26 THEN MCONC=MCONC-1
490 P1=CINT(MCONC*CONC*1E+09):P2(EDP)=MCONC*CC(EDP):P3=CINT(DP(EDP)*1E+07)
500 PRINT #1, P1;TAB(20)::PRINT #1, USING "##.##^"      "##.##";P2(EDP);
510 '
520 NEXT MCONC
521 NEXT EDP
522 '*****
523 PRINT #2, "PARAMETERS:  RADIONUCLIDE = ";N$
524 PRINT #2, TAB(16);"HALF LIFE IN YEARS = ";;PRINT #2, USING "##.##^";THALF
525 PRINT #2, "*****"
526 PRINT #2, "COLLOID CONC. (ppb)";TAB(22);"LOG(CONC OF RADIOACTIVITY) FOR COLL
527 PRINT #2, TAB(22);"10nm";TAB(35);"100nm";TAB(48);"1000nm"
531 FOR MCONC = 1 TO 200 STEP 25
532 'FORMATTED OUTPUT INTENDED FOR PLOTTING ROUTINE SUCH AS SLIDEWRITE
533 IF MCONC = 26 THEN MCONC = MCONC-1
534 P1=CINT(MCONC*CONC*1E+09)
535 FOR EDP = 1 TO 3
536 LP2(EDP) =.43429*LOG(MCONC*CC(EDP))      'LOG OF THE CONC OF RADIOACTIVITY
537 NEXT EDP
538 PRINT #2, P1;TAB(20)::PRINT #2, USING "###.##";LP2(1)::PRINT #2, TAB(34)::PR
539 NEXT MCONC
540 IF INKEY$="" THEN GOTO 540
550 END
OK

```

C.5 Sample Calculations

The following is a listing of the results from the calculations for Am-241. The output in chart format for use with SLIDEWRITE has the following form:

COLLOID CALCULATIONS FOR Am-241

PARAMETERS

```

RADIONUCLIDE = Am-241
HALF LIFE IN YEARS = 4.58E+02
MPC IN CURIES/CUBIC METER = 4.00E-06

```

```

*****
COLLOID CONC., ppb  CURIES/CU M      LOG(CONC)      COLLOID SIZE, nm

```

COLLOID CONC., ppb	CURIES/CU M	LOG(CONC)	COLLOID SIZE, nm
1	9.16E-03	-2.04	10
25	2.29E-01	-0.64	10
50	4.58E-01	-0.34	10
75	6.87E-01	-0.16	10
100	9.16E-01	-0.04	10
125	1.15E+00	0.06	10
150	1.37E+00	0.14	10
175	1.60E+00	0.20	10
200	1.83E+00	0.26	10
1	8.84E-04	-3.05	100

25	2.21E-02	-1.66	100
50	4.42E-02	-1.35	100
75	6.63E-02	-1.18	100
100	8.84E-02	-1.05	100
125	1.11E-01	-0.96	100
150	1.33E-01	-0.88	100
175	1.55E-01	-0.81	100
200	1.77E-01	-0.75	100
1	8.81E-05	-4.06	1000
25	2.20E-03	-2.66	1000
50	4.40E-03	-2.36	1000
75	6.61E-03	-2.18	1000
100	8.81E-03	-2.06	1000
125	1.10E-02	-1.96	1000
150	1.32E-02	-1.88	1000
175	1.54E-02	-1.81	1000
200	1.76E-02	-1.75	1000

COLLOID CALCULATIONS FOR Np-237

PARAMETERS

RADIONUCLIDE = Np-237
 HALF LIFE IN YEARS = 2.14E+06
 MPC IN CURIES/CUBIC METER = 3.00E-06

COLLOID CONC., ppb	CURIES/CU M	LOG (CONC)	COLLOID SIZE, nm
1	1.96E-06	-5.71	10
25	4.90E-05	-4.31	10
50	9.80E-05	-4.01	10
75	1.47E-04	-3.83	10
100	1.96E-04	-3.71	10
125	2.45E-04	-3.61	10
150	2.94E-04	-3.53	10
175	3.43E-04	-3.46	10
200	3.92E-04	-3.41	10
1	1.89E-07	-6.72	100
25	4.73E-06	-5.33	100
50	9.46E-06	-5.02	100
75	1.42E-05	-4.85	100
100	1.89E-05	-4.72	100
125	2.36E-05	-4.63	100
150	2.84E-05	-4.55	100
175	3.31E-05	-4.48	100
200	3.78E-05	-4.42	100
1	1.89E-08	-7.72	1000
25	4.71E-07	-6.33	1000
50	9.43E-07	-6.03	1000
75	1.41E-06	-5.85	1000
100	1.89E-06	-5.72	1000
125	2.36E-06	-5.63	1000
150	2.83E-06	-5.55	1000
175	3.30E-06	-5.48	1000
200	3.77E-06	-5.42	1000

COLLOID CALCULATIONS FOR Pu-239

PARAMETERS

RADIONUCLIDE = Pu-239
 HALF LIFE IN YEARS = 2.44E+04
 MPC IN CURIES/CUBIC METER = 5.00E-06

 COLLOID CONC., ppb CURIES/CU M LOG(CONC) COLLOID SIZE, nm

1	1.72E-04	-3.76	10
25	4.30E-03	-2.37	10
50	8.60E-03	-2.07	10
75	1.29E-02	-1.89	10
100	1.72E-02	-1.76	10
125	2.15E-02	-1.67	10
150	2.58E-02	-1.59	10
175	3.01E-02	-1.52	10
200	3.44E-02	-1.46	10
1	1.66E-05	-4.78	100
25	4.15E-04	-3.38	100
50	8.30E-04	-3.08	100
75	1.24E-03	-2.90	100
100	1.66E-03	-2.78	100
125	2.07E-03	-2.68	100
150	2.49E-03	-2.60	100
175	2.90E-03	-2.54	100
200	3.32E-03	-2.48	100
1	1.65E-06	-5.78	1000
25	4.13E-05	-4.38	1000
50	8.27E-05	-4.08	1000
75	1.24E-04	-3.91	1000
100	1.65E-04	-3.78	1000
125	2.07E-04	-3.68	1000
150	2.48E-04	-3.61	1000
175	2.89E-04	-3.54	1000
200	3.31E-04	-3.48	1000

DISTRIBUTION

**U.S. Nuclear Regulatory Commission
Division of High-Level Waste
Management
Document Control Center
Washington, DC 20555
Attn: R. Browning**

**U.S. Nuclear Regulatory Commission
Geosciences and Systems Performance
Branch
Division of High-Level Waste
Management
Mail Stop 4H3
Washington, DC 20555 (10)
Attn: D. J. Brooks
P. P. Brooks
R. L. Ballard
J. W. Bradbury
D. L. Chery
R. Codell
S. Coplan
N. Eisenberg
P. S. Justus
T. Mo**

**U.S. Nuclear Regulatory Commission
Technical Branch
Division of Low-Level Waste
and Decommissioning
Mail Stop 5E4
Washington, DC 20555
Attn: M. R. Knapp
R. J. Starmer**

**U.S. Nuclear Regulatory Commission
Office of Nuclear Regulatory
Research
Mail Stop NL-005
Washington, DC 20555 (6)
Attn: G. F. Birchard
L. A. Kovach
T. J. Nicholson
J. D. Randall
M. Silberberg**

**Los Alamos National Laboratory
P.O. Box 1663
Los Alamos, NM 87545 (8)
Attn: D. L. Bish
B. Carlos
W. R. Daniels
B. R. Erdal
J. F. Kerrisk
A. E. Ogard
D. T. Vaniman
K. Wolfsberg**

**Lawrence Livermore National
Laboratory
P.O. Box 808 L-104
Livermore, CA 94550 (5)
Attn: W. Bourcier
D. Isherwood
K. G. Knauss
V. M. Oversby
T. J. Wolery**

**Department of Environmental Sciences
University of Virginia
Charlottesville, VA 22903
Attn: W. R. Kelly**

**Lawrence Berkeley Laboratory
University of California
Berkeley, CA 94720
Attn: J. Apps
C. L. Carnahan
F. Hale
S. L. Phillips**

**Brookhaven National Laboratory
Nuclear Waste Management Division
Upton, NY 11973 (3)
Attn: E. P. Bause
D. G. Schweitzer
P. Soo**

**Savannah River Laboratory
Chemical Technology Division
Aiken, SC 29808
Attn: C. M. Jantzen**

Oak Ridge National Laboratory
P.O. Box X
Oak Ridge, TN 37831 (13)
Attn: W. D. Arnold
J. T. Bell
J. E. Blencoe
N. H. Cutshall
T. O. Early
L. M. Ferris
R. M. Gove
G. K. Jacobs
A. D. Kelmers
D. C. Kocher
S. Y. Lee
R. E. Meyer
V. S. Tripathi

Westinghouse Hanford Operations
P.O. Box 800
Richland, WA 99352 (7)
Attn: S. M. Baker
G. S. Barney
J. H. LaRue
J. Myers
P. F. Salter
G. Solomon
M. I. Wood

Battelle Pacific Northwest
Laboratory
P. O. Box 999
Richland, WA 99352 (9)
Attn: L. L. Ames
M. J. Apter
D. G. Coles
W. J. Gray
E. A. Jenne
K. Krupka
G. L. McVay
D. Rai
J. Serne

U.S. Department of Energy
Waste Management Project Office
Nevada Operations Office
Las Vegas, NV 89104
Attn: J. S. Szymanski

Dept. of Geology and Institute of
Meteoritics
University of New Mexico
Albuquerque, NM 87131 (4)
Attn: D. Brookins
L. Crossey
R. Ewing
K. Keil

Environmental Engineering and
Science
Department of Civil Engineering
Stanford University
Stanford, CA 94305 (2)
Attn: J. O. Leckie
D. Freyberg

National Science Foundation
Division of Earth Sciences
Washington, DC 20555
Attn: R. Buden

Ecology and Environment, Inc.
Buffalo Corporate Center
368 Pleasantview Drive
Lancaster, NY 14086
Attn: P. J. Bembia (1)

Center for Nuclear Waste
Regulatory Analysis
Southwest Research Institute
6220 Culebra Road
San Antonio, TX 78284
Attn: J. L. Russell (3)
W. Murphy
R. Pabalan
Library (1)

Sandia National Laboratories

1512 K. L. Erickson
3141 S. A Landenberger (5)
3151 W. I. Klein
6230 W. C. Luth
6233 T. R. Gerlach
6233 W. H. Casey
6233 J. L. Krumhansl
6300 R. W. Lynch
6330 W. D. Weart
6331 A. R. Lappin
6331 M. Siegel (10)
6332 L. D. Tyler
6332 E. J. Nowak
6334 D. R. Anderson
6334 L. H. Brush
6400 D. J. McCloskey
6410 D. A. Dahlgren
6415 R. M. Cranwell
6416 E. J. Bonano
6416 P. A. Davis
6416 C. P. Harlan
6416 C. D. Leigh (10)
8524 J. A. Wackerly

BIBLIOGRAPHIC DATA SHEET

(See instructions on the reverse)

1. REPORT NUMBER
*(Assigned by NRC, Add Vol., Supp., Rev.,
and Addendum Numbers, if any.)*

NUREG/CR-5085
SAND85-1644

2. TITLE AND SUBTITLE

Progress in Development of a Methodology for Geochemical
Sensitivity Analysis for Performance Assessment

Parametric Calculations, Preliminary Databases, and
Computer Code Evaluation

3. DATE REPORT PUBLISHED

MONTH | YEAR
August | 1989

4. FIN OR GRANT NUMBER

A1756

5. AUTHOR(S)

M.D. Siegel, C.D. Leigh, Editors

6. TYPE OF REPORT

7. PERIOD COVERED *(Inclusive Dates)*

8. PERFORMING ORGANIZATION - NAME AND ADDRESS *(If NRC, provide Division, Office or Region, U.S. Nuclear Regulatory Commission, and mailing address; if contractor, provide name and mailing address.)*

Sandia National Laboratories
Albuquerque, NM 87185

9. SPONSORING ORGANIZATION - NAME AND ADDRESS *(If NRC, type "Same as above"; if contractor, provide NRC Division, Office or Region, U.S. Nuclear Regulatory Commission, and mailing address.)*

Division of High-Level Waste Management
Office of Nuclear Material Safety and Safeguards
U.S. Nuclear Regulatory Commission
Washington, DC 20555

10. SUPPLEMENTARY NOTES

11. ABSTRACT *(200 words or less)*

The purpose of the Geochemical Sensitivity Analysis Project is to develop a methodology to identify physicochemical and hydrogeological conditions wherein use of a simple retardation factor will lead to underestimation or overly conservative estimation of the cumulative radionuclide discharge over the 10,000-year regulatory period. This report describes activities from the initiation of the Geochemical Sensitivity Analysis Project in April 1984 to September 30, 1985. During this first phase of the project, compilation of necessary geochemical data was started, radionuclide transport codes were evaluated and parametric methods to assess the significance of matrix diffusion, colloidal transport and reaction kinetics on integrated radionuclide discharge from high-level waste repositories were developed. Although available data are inadequate to support final conclusions for site specific conditions, the method of sensitivity analysis being developed in this project can be used to guide future data collection.

12. KEY WORDS/DESCRIPTORS *(List words or phrases that will assist researchers in locating the report.)*

high-level waste repositories
radionuclide discharge/transport computer codes
data base
geochemical sensitivity analysis
matrix diffusion
colloidal transport
reaction kinetics

13. AVAILABILITY STATEMENT

unlimited

14. SECURITY CLASSIFICATION

(This Page)

unclassified

(This Report)

unclassified

15. NUMBER OF PAGES

16. PRICE

**UNITED STATES
NUCLEAR REGULATORY COMMISSION
WASHINGTON, D.C. 20555**

**OFFICIAL BUSINESS
PENALTY FOR PRIVATE USE, \$300**

**SPECIAL FOURTH-CLASS RATE
POSTAGE & FEES PAID
USNRC
PERMIT No. G-67**